DISSERTATIONES SCHOLAE DOCTORALIS AD SANITATEM INVESTIGANDAM
UNIVERSITATIS HELSINKIENSIS

46/2018

PANU LUUKKONEN

Heterogeneity of Non-Alcoholic Fatty Liver Disease — Genetic and Nutritional Modulation of Hepatic Lipid Metabolism

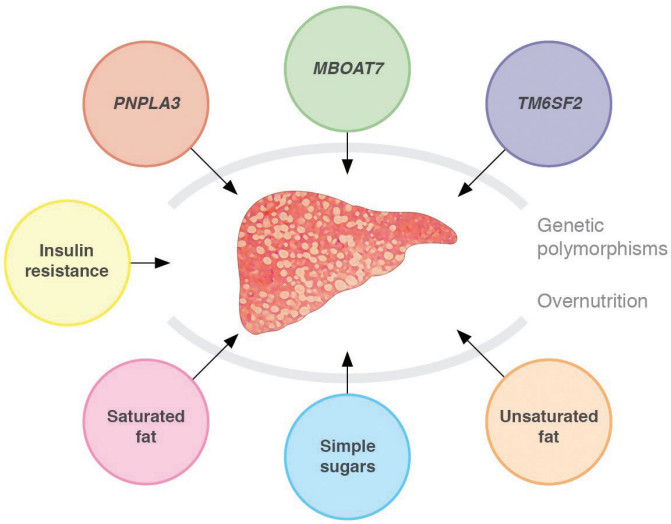

CLINICUM
DEPARTMENT OF MEDICINE
FACULTY OF MEDICINE
DOCTORAL PROGRAMME IN CLINICAL RESEARCH
UNIVERSITY OF HELSINKI

Department of Medicine
Clinicum
Faculty of Medicine
University of Helsinki
Helsinki, Finland

Doctoral Programme in
Clinical Research
University of Helsinki
Helsinki, Finland

Minerva Foundation
Institute for
Medical Research
Helsinki, Finland

HETEROGENEITY OF NON-ALCOHOLIC FATTY LIVER DISEASE

Genetic and Nutritional Modulation of Hepatic Lipid Metabolism

Panu Luukkonen

ACADEMIC DISSERTATION

To be presented, with the permission of the Faculty of Medicine of the University of Helsinki, for public examination in the Lecture Hall 2 at the Haartman Institute, Haartmaninkatu 3, Helsinki, on September 7th 2018, at 12 o'clock noon.

Helsinki 2018

SUPERVISOR
Professor Hannele Yki-Järvinen, MD, FRCP
Department of Medicine
Clinicum
Faculty of Medicine
University of Helsinki
Helsinki, Finland

REVIEWERS
Professor (emeritus) Tapani Rönnemaa, MD
Department of Medicine
Faculty of Medicine
University of Turku
Turku, Finland

Adjunct professor Fredrik Åberg, MD
Transplantation and Liver Surgery Clinic
Helsinki University Hospital
Helsinki, Finland

OPPONENT
Professor Rosalind Coleman, MD
Department of Nutrition and Department of Pediatrics
School of Public Health
University of North Carolina
Chapel Hill, North Carolina, USA

The Faculty of Medicine uses the Urkund system (plagiarism recognition) to examine all doctoral dissertations.

ISBN: 978-951-51-4372-3 (paperback)
ISBN: 978-951-51-4373-0 (PDF)
ISSN: 2342-3161 (print)
ISSN: 2342-317X (online)

Dissertationes Scholae Doctoralis Ad Sanitatem Investigandam Universitatis Helsinkiensis

Hansaprint Oy, Turenki 2018

ABSTRACT

Non-alcoholic fatty liver disease (NAFLD) is characterized by excess hepatic triglyceride (TG) accumulation that can originate from the dietary fat, adipose tissue lipolysis or hepatic *de novo* lipogenesis. NAFLD is strongly associated with insulin resistance and increased risk of type 2 diabetes, cardiovascular disease and advanced liver disease.

However, several single nucleotide polymorphisms in genes such as PNPLA3, MBOAT7 and TM6SF2 have been found to increase the risk of NAFLD and associated liver injury in the absence of insulin resistance. TGs themselves are metabolically inert lipids, while bioactive lipids such as ceramides and diacylglycerols have been suggested to mediate insulin resistance. Phospholipids are important for hepatic TG export. Whether the dissociation between hepatic steatosis and insulin resistance can be attributed to differences in the molecular lipid profile in the human liver is unknown.

In study I, we profiled the lipidome of liver biopsies from 125 obese subjects undergoing bariatric surgery using ultra-high performance liquid chromatography and gas chromatography combined with mass spectrometry. The subjects were divided based on median HOMA-IR, a marker of insulin resistance, to 'High HOMA-IR' and 'Low HOMA-IR'. 'High HOMA-IR' was used as a model of 'Metabolic NAFLD'. The same subjects were also divided into groups based on their PNPLA3 genotype to carriers and non-carriers of the I148M variant. Variant allele carriers were used as a model of 'PNPLA3 NAFLD'.

Steatosis and prevalence of NASH were similarly increased in 'Metabolic NAFLD' and 'PNPLA3 NAFLD'. The liver lipidome in 'Metabolic NAFLD' was characterized by saturated and monounsaturated TGs and free fatty acids, diacylglycerols and ceramides. Markers of the *de novo* ceramide synthetic pathway were increased in 'Metabolic NAFLD'. In contrast, in 'PNPLA3 NAFLD' the increase in liver fat was due to polyunsaturated TGs while other lipids were unchanged.

In study II, we investigated the effects of the MBOAT7 variant at rs641738 on liver histology and lipidome in biopsies from 115 bariatric surgery patients. The variant allele was associated with increased prevalence of liver fibrosis and altered concentrations of several polyunsaturated phosphatidylinositols, but not other lipids or markers of insulin resistance.

In study III, we examined the pathogenesis of the 'TM6SF2 NAFLD' by comparing the human liver and serum lipidome and liver transcriptome in 10 carriers and 80 non-carriers of the TM6SF2 E167K variant, and by determining the effects of TM6SF2 knockdown on fatty acid metabolism *in vitro*. In variant allele carriers, liver TG and cholesteryl-ester content was higher while that of phosphatidylcholines was lower as compared to non-carriers. Polyunsaturated fatty acids were deficient in liver and serum TGs and phosphatidylcholines but enriched in hepatic free fatty acids. The incorporation of polyunsaturated fatty acids into triglycerides and phosphatidylcholines (PCs) was decreased in TM6SF2 deficient cells. Hepatic gene expression of TM6SF2 was decreased in carriers, and correlated

with those genes regulated by PUFAs. Thus, hepatic lipid synthesis from PUFAs was impaired which could contribute to deficiency of PCs and increased hepatic TGs in TM6SF2 E167K variant carriers compared to non-carriers.

In study IV, we examined whether the dietary macronutrient composition influences the pathways, mediators and magnitude of overfeeding-induced changes in intrahepatic triglycerides and insulin resistance in 38 overweight subjects. We used a combination of state-of-the-art *in vivo* (imaging, stable isotope tracers and hyperinsulinemic-euglycemic clamp) and *ex vivo* (plasma lipidome, adipose tissue transcriptome and gut microbiome) techniques. Three weeks of overfeeding of saturated fat increased hepatic TGs more than that of unsaturated fat by increasing adipose tissue lipolysis. Moreover, the saturated fat-enriched diet increased insulin resistance, circulating ceramides and gram-negative gut bacteria. Simple sugars increased hepatic TGs by stimulating hepatic *de novo* lipogenesis. Each diet had distinct effects on the adipose tissue transcriptome. These results showed that the effect of overfeeding on hepatic metabolism depends on the dietary macronutrient composition. Saturated fat may be metabolically more harmful than unsaturated fat or simple sugars.

In summary, the present series of studies show that human NAFLD is a heterogenous disease. Both genetic factors and the macronutrient composition of the diet have distinct effect on hepatic lipid metabolism and the resulting phenotype.

TABLE OF CONTENTS

ABSTRACT 3

LIST OF ORIGINAL PUBLICATIONS 7

ABBREVIATIONS 8

1. INTRODUCTION 11

2. REVIEW OF THE LITERATURE 14

2.1 INTRODUCTION TO NAFLD 14

2.1.1. Definitions 14

2.1.2. Diagnosis 14

2.1.3. Prevalence and significance 14

2.1.3.1. Type 2 diabetes and the metabolic syndrome 15

2.1.3.2. Cardiovascular disease 15

2.1.3.3. Advanced liver disease and hepatocellular carcinoma 15

2.1.4. Risk factors for NAFLD 16

2.2. PATHOGENESIS OF NAFLD 16

2.2.1. 'Metabolic NAFLD' 16

2.2.1.1. Sources of hepatic fatty acids 16

2.2.1.1.1. Adipose tissue lipolysis *16*

2.2.1.1.2. Dietary fat *18*

2.2.1.1.3. De novo lipogenesis *19*

2.2.1.2. Fates of hepatic fatty acids 19

2.2.1.2.1. Triacylglycerols *20*

2.2.1.2.2. Diacylglycerols *21*

2.2.1.2.3. Ceramides *22*

2.2.1.2.4. Phospholipids *24*

2.2.1.3. Hepatocellular injury and fibrosis 26

2.2.1.4. Role of the gut in the pathogenesis of NAFLD 27

2.2.2. 'Genetic NAFLD' 28

2.2.2.1. The PNPLA3 I148M variant 28

2.2.2.2. The MBOAT7 rs641738 C>T variant 31

2.2.2.3. The TM6SF2 E167K variant 32

2.3. NUTRITIONAL MODULATION OF NAFLD 34

2.3.1. Energy intake 34

2.3.2. Macronutrient composition of the diet 34

3. AIMS OF THE STUDY 36

4. SUBJECTS AND METHODS 37

4.1. SUBJECTS AND STUDY DESIGNS 37

4.1.1. Studies I-III 37

4.1.4. Study IV 37

4.2. METHODS 38

4.2.1. Liver fat content (I-IV) 38

4.2.2. Lipidomics (I-IV) 39

4.2.3. Hepatic gene expression (III) 43

4.2.4. Adipose tissue gene expression (IV) 43

4.2.5. Adipose tissue lipolysis (IV) 44

4.2.6. *De novo* lipogenesis (IV) 45

4.2.7. Body composition (I-IV) 45

4.2.8. Energy expenditure and substrate oxidation (IV) 45

4.2.9. Intestinal microbiota (IV) ... 45
4.2.10. Genotyping (I-IV) ... 46
4.2.11. Other analytical procedures (I-IV) ... 46
4.2.12. *In vitro* experiments (III) ... 47
4.2.13. Statistical analyses (I-IV) ... 48

5. RESULTS ... 50
5.1. SUBJECT CHARACTERISTICS (I–IV) ... 50
5.2. HUMAN LIVER LIPIDOME (I-III) ... 53
5.2.1. 'Metabolic NAFLD' (I) ... 53
5.2.2. 'PNPLA3 NAFLD' (I) ... 57
5.2.3. 'MBOAT7 NAFLD' (II) ... 58
5.2.4. 'TM6SF2 NAFLD' (III) ... 58
5.3. *IN VITRO* EXPERIMENTS (III) ... 59
5.4. HEPATIC GENE EXPRESSION (III) ... 60
5.5. METABOLIC EFFECTS OF DIFFERENT OVERFEEDING DIETS (IV) ... 60
5.5.1. Macronutrient composition of the diet ... 60
5.5.2. Fatty acid composition of VLDL-TG ... 60
5.5.3. Body composition and energy expenditure ... 61
5.5.4. Liver fat content ... 62
5.5.5. *De novo* lipogenesis and adipose tissue lipolysis ... 62
5.5.6. Insulin resistance ... 62
5.5.7. Ceramides and endotoxemia ... 62
5.5.8. Adipose tissue gene expression ... 65

6. DISCUSSION ... 66
6.1. 'METABOLIC NAFLD' ... 66
6.2. 'GENETIC NAFLD' ... 68
6.2.1. 'PNPLA3 NAFLD' ... 68
6.2.2. 'MBOAT7 NAFLD' ... 70
6.2.3. 'TM6SF2 NAFLD' ... 71
6.3. METABOLIC EFFECTS OF DIFFERENT OVERFEEDING DIETS ... 74
6.3.1 Effects on sources of hepatic fatty acids ... 75
6.3.2 Effects on insulin resistance ... 76
6.4. 'DOUBLE TROUBLE' AND 'TRIPLE TROUBLE' ... 78

7. SUMMARY AND CONCLUSIONS ... 81

8. ACKNOWLEDGEMENTS ... 83

9. REFERENCES ... 85

LIST OF ORIGINAL PUBLICATIONS

This thesis is based on the following original publications referred to in the text by their Roman numerals.

I. **Luukkonen PK***, Zhou Y*, Sädevirta S, Leivonen M, Arola J, Orešič M, Hyötyläinen T, Yki-Järvinen H. Hepatic ceramides dissociate steatosis and insulin resistance in patients with non-alcoholic fatty liver disease. *Journal of Hepatology*. 2016; 64:1167-75.

II. **Luukkonen PK**, Zhou Y, Hyötyläinen T, Leivonen M, Arola J, Orho-Melander M, Orešič M, Yki-Järvinen H. The MBOAT7 variant rs641738 alters hepatic phosphatidylinositols and increases severity of non-alcoholic fatty liver disease in humans. *Journal of Hepatology*. 2016; 65:1263-1265.

III. **Luukkonen PK**, Zhou Y, Nidhina Haridas PA, Dwivedi OP, Hyötyläinen T, Ali A, Juuti A, Leivonen M, Tukiainen T, Ahonen L, Scott E, Palmer JM, Arola J, Orho-Melander M, Vikman P, Anstee QM, Olkkonen VM, Orešič M, Groop L, Yki-Järvinen H. Impaired hepatic lipid synthesis from polyunsaturated fatty acids in TM6SF2 E167K variant carriers with NAFLD. *Journal of Hepatology*. 2017; 67:128-136.

IV. **Luukkonen PK**, Sädevirta S, Zhou Y, Kayser B, Ali A, Ahonen L, Lallukka S, Pelloux V, Gaggini M, Jian C, Hakkarainen A, Lundbom N, Gylling H, Salonen A, Orešič M, Hyötyläinen T, Orho-Melander M, Rissanen A, Gastaldelli A, Clément K, Hodson L, Yki-Järvinen H. Saturated Fat is More Metabolically Harmful for the Human Liver than Unsaturated Fat or Simple Sugars. *Diabetes Care. In press.*

* Designates co-first authorship.

ABBREVIATIONS

^{1}H-MRS	proton magnetic resonance spectroscopy
ACACB	acetyl-CoA carboxylase beta
ACC	acetyl-CoA carboxylase
ACLY	ATP citrate lyase
ACS	acyl-CoA synthetase
ACSL3	acyl-CoA synthetase long-chain family member 3
Akt	protein kinase B
ALOX5	arachidonate 5-lipoxygenase
ALP	alkaline phosphatase
ALT	alanine aminotransferase
AST	aspartate aminotransferase
APOC3	apolipoprotein C-III
AST	aspartate aminotransferase
ATGL	adipose triglyceride lipase
ATP	adenosine triphosphate
BMI	body mass index
CARB	simple sugar
CD14	cluster of differentiation 14
CD36	cluster of differentiation 36, fatty acid translocase
CE	cholesteryl ester
CerS	ceramide synthase
ChREBP	carbohydrate-responsive element-binding protein
CI	confidence interval
CL	cardiolipin
CoA	coenzyme A
CPT1	carnitine palmitoyltransferase 1
CTα	CTP:phosphocholine cytidylyltransferase alpha
CVD	cardiovascular disease
DAG	diacylglycerol
DGAT	diacylglycerol acyltransferase
DNL	*de novo* lipogenesis
DNA	deoxyribonucleic acid
ELISA	enzyme-linked immunosorbent assay
ELOVL6	fatty acid elongase 6
FA	fatty acid
FAME	fatty acid methyl ester
FAS	fatty acid synthase
FFA	free fatty acid
fP	fasting plasma
fS	fasting serum
G3P	glycerol 3-phosphate
GC	gas chromatography
GGT	gamma-glutamyltransferase
GPAT	glycerol phosphate acyltransferase
GPR120	G-protein coupled receptor 120
HbA_{1C}	glycated haemoglobin A_{1C}
HCC	hepatocellular carcinoma
HDL	high-density lipoprotein

HOMA-IR	homeostasis model assessment of insulin resistance
IHTG	intrahepatic triglyceride
KEGG	Kyoto Encyclopedia of Genes and Genomes
LBP	lipopolysaccharide-binding protein
LC	liquid chromatography
LCFA	long-chain fatty acid
LD	lipid droplet
LDL	low-density lipoprotein
LPA	lysophosphatidic acid
LPAAT	lysophosphatidic acid acyltransferase
LPCAT3	lysophosphatidylcholine acyltransferase 3
LPIAT1	lysophosphatidylinositol acyltransferase 1
LPLAT	lysophospholipid acyltransferase
LPS	lipopolysaccharide
MBOAT7	membrane bound-O-acyltransferase domain-containing 7
MetS	metabolic syndrome
MGL	monoacylglycerol lipase
MRI	magnetic resonance imaging
mRNA	messenger RNA
MRS	magnetic resonance spectroscopy
MS	mass spectrometry
MUFA	monounsaturated fatty acid
NAFL	non-alcoholic fatty liver
NAFLD	non-alcoholic fatty liver disease
NASH	non-alcoholic steatohepatitis
$NF_{\kappa}B$	nuclear factor kappa-light-chain-enhancer of activated B cells
NLR	NOD-like receptor
NLRP3	nucleotide-binding containing pyrin domain 3
NOD	nucleotide-binding oligomerization domain-like
OGTT	oral glucose tolerance test
PA	phosphatidic acid
PAP	phosphatidic acid phosphatase
PC	phosphatidylcholine
PE	phosphatidylethanolamine
PEMT	phosphatidylethanolamine N-methyltransferase
PG	phosphatidylglycerol
PI	phosphatidylinositol
PKB	protein kinase B
PKC	protein kinase C
PLA_2	phospholipase A_2
PNPLA3	patatin-like phospholipase domain-containing protein 3
PP2A	protein phosphatase 2A
PPAR	peroxisome proliferator-activator receptor
PS	phosphatidylserine
PUFA	polyunsaturated fatty acid
Q-TOF	quadrupole time-of-flight
R_a	rate of appearance
RNA	ribonucleic acid
SAT	saturated fat
SCD1	stearoyl-CoA desaturase 1
sCD14	soluble cluster of differentiation 14

SEM	standard error of mean
SFA	saturated fatty acid
shRNA	short hairpin RNA
siRNA	small interfering RNA
SREBP1c	sterol regulatory element-binding protein 1c
TAG	triacylglycerol
TE	echo time
TG	triglyceride
TLR-4	toll-like receptor 4
TM6SF2	transmembrane 6 superfamily member 2
TR	repetition time
UHPLC	ultra high-performance liquid chromatography
UNSAT	unsaturated fat
VLDL	very low-density lipoprotein

1. INTRODUCTION

The spectrum of 'Metabolic NAFLD' and associated risk of disease. Non-alcoholic fatty liver disease (NAFLD) is a spectrum of disease ranging from simple steatosis (non-alcoholic fatty liver, NAFL) to nonalcoholic steatohepatitis (NASH) to cirrhosis (Yki-Järvinen, 2014). It has become the most prevalent cause of liver disease worldwide affecting up to one-quarter of population, increasing in parallel with obesity (Younossi *et al.,* 2016).

NAFLD is strongly associated with hepatic insulin resistance and features of the metabolic syndrome (MetS) ('Metabolic NAFLD') (Yki-Järvinen, 2014). In 'Metabolic NAFLD', insulin fails to suppress the production of glucose and triglycerides in the liver, resulting in hyperinsulinemia, hyperglycemia, hypertriglyceridemia and low high-density lipoprotein concentrations (Yki-Järvinen, 2014). This common form of NAFLD is associated with increased risk of type 2 diabetes, cardiovascular disease and advanced liver disease (**Figure 1**) (Anstee *et al.,* 2013).

Insulin action and sources of FAs in 'Metabolic NAFLD'. Intrahepatic triglycerides (IHTGs), the hallmark of NAFLD, are synthesized from fatty acids originating either from the adipose tissue, dietary fat, or hepatic *de novo* lipogenesis (Donnelly *et al.,* 2005). Adipose tissue lipolysis is the major source, contributing to more than half of the fatty acids in IHTGs. In addition, the liver partially takes up dietary fat, and can also produce fatty acids from non-lipid substrates, such as sugars *via* the *de novo* lipogenesis (DNL) pathway (Donnelly *et al.,* 2005). DNL is the relatively most increased fatty acid source in NAFLD, and produces exclusively saturated fatty acids (Lambert *et al.,* 2014).

Bioactive lipids. IHTGs themselves are inert lipids, while at least two classes of bioactive lipids, diacylglycerols (DAGs) and ceramides have been suggested to mediate insulin resistance (Petersen *et al.,* 2017). DAGs are the immediate precursors of TGs, while ceramides can be synthesized *via* the *de novo* synthetic pathway from saturated fatty acids, *via* sphingomyelin hydrolysis or *via* the salvage pathway from hexosylceramides (Chaurasia *et al.,* 2015). Recent studies in mice have identified C16:0-ceramide, formed *via* the *de novo* ceramide synthetic pathway as the principal mediator of obesity-related insulin resistance (Hla *et al.,* 2014). There are no human data to examine which if any of these pathways contributes to changes in ceramide concentrations in the human liver.

'PNPLA3 NAFLD'. Not all phenotypes of NAFLD are associated with insulin resistance. In 2008, a single-nucleotide polymorphism (rs738409 [G], encoding I148M) in the patatin-like phospholipase domain-containing 3 (*PNPLA3*) was found to increase liver fat content but not insulin resistance (**Figure 1**) (Romeo *et al.,* 2008). Depending on ethnicity, 20-50% of all subjects carry this gene variant (Romeo *et al.,* 2008). *In vitro*, this gene variant inhibits lipolysis of TGs in the liver (Huang *et al.,* 2011) and may also act as a gain-of-function mutation to increase TG synthesis by acting as a lysophosphatidic acyltransferase (LPAAT) converting lysophosphatidic acid into phosphatitidic acid (Kumari *et al.,* 2012).

'MBOAT7 NAFLD'. A common variant in membrane bound O-acyltransferase domain containing 7 (MBOAT7) at rs641738, carried by 58-67% of population, was discovered to increase the risk and severity of NAFLD but not

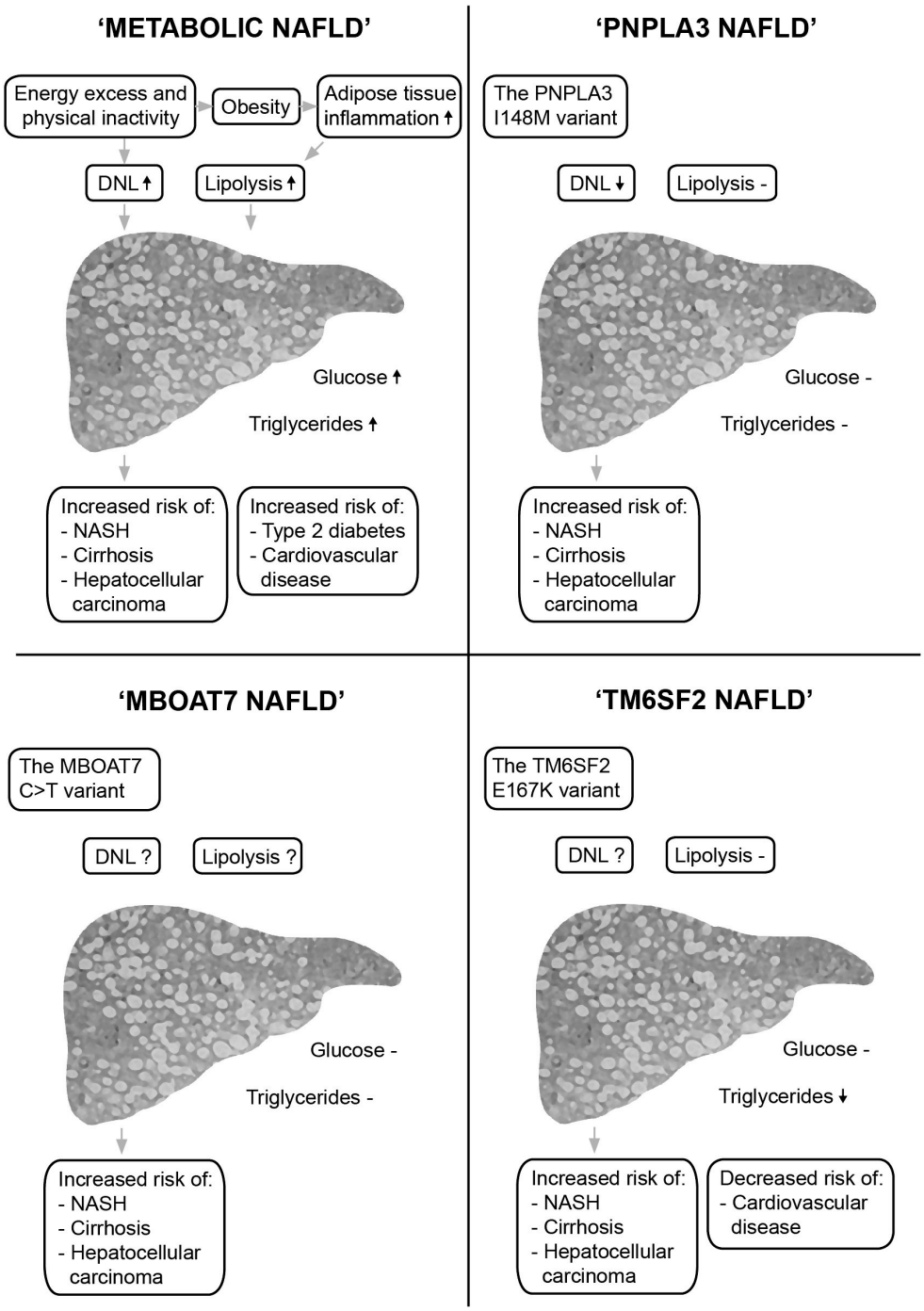

Figure 1. Heterogeneity of the metabolic features and disease risks associated with subtypes of NAFLD.

insulin resistance (**Figure 1**) (Mancina *et al.,* 2016). MBOAT7 functions as a lysophosphatidylinositol acyltransferase, catalyzing the fatty acyl-chain remodeling of phosphatidylinositols (PIs). In keeping with this function, carriers of the variant have lower plasma concentrations of polyunsaturated PIs (Mancina *et al.,* 2016).

'TM6SF2 NAFLD'. A third genetic variant increasing the risk of NAFLD, transmembrane 6 superfamily member 2 (TM6SF2) at rs58542926, was described in 2014 (Kozlitina *et al.,* 2014). In contrast to 'Metabolic NAFLD', carriers of this variant ('TM6SF2 NAFLD') are not more insulin resistant than non-carriers and have normal or decreased plasma TG concentrations and a decreased risk of cardiovascular disease (**Figure 1**) (Kozlitina *et al.,* 2014; Mahdessian *et al.,* 2014). Knockdown of *TM6SF2* increases intracellular TG content and decreases TG secretion, while overexpression has an opposite effect (Mahdessian *et al.,* 2014). In animal models, a similar phenotype, i.e. hepatic steatosis, decreased TG secretion and protected against cardiovascular disease, can result from impaired synthesis or remodeling of phosphatidylcholines (Rong *et al.,* 2015).

Dissociation of IHTG and IR. All of these genetic variants increase liver fat content and histological severity of NAFLD, but in contrast to the 'Metabolic NAFLD', none are associated with metabolic disturbances (**Figure 1**) (Romeo *et al.,* 2008; Mancina *et al.*, 2016; Kozlitina *et al.,* 2014). Whether these dissociations can be attributed to different lipid profiles in the human liver remains unknown.

Dietary modulation of NAFLD. While excessive energy consumption is the primary acquired risk factor of NAFLD, it does not occur in all subjects who are overweight (Browning *et al.,* 2004). Whether macronutrient composition modulates metabolic effects of the diet overconsumed is unclear. Excess intakes of sugar (Sevastianova *et al.,* 2012), and saturated but not polyunsaturated fat (Rosqvist *et al.,* 2014) have been reported to increase IHTGs. Overfeeding of simple sugars increases IHTG *via* DNL (Sevastianova *et al.,* 2012). However, there are no studies investigating the effects of overfeeding saturated or unsaturated fat or simple sugars on IHTG content, sources of hepatic fatty acids (adipose tissue lipolysis and hepatic DNL), insulin resistance, and associated metabolic effects in the gut, adipose tissue and plasma.

The present series of studies aimed to elucidate the heterogeneity of human NAFLD, with a special emphasis on the regulation of hepatic lipid metabolism by genetic and nutritional factors. In study I, we characterized the human liver lipidome in the insulin-resistant 'Metabolic NAFLD' and the insulin-sensitive 'PNPLA3 NAFLD'. In study II, we investigated the effects of the MBOAT7 variant at rs641738 on the human liver histology and lipidome. In study III, we sought to elucidate the pathogenesis of the 'TM6SF2 NAFLD' by characterizing the human liver and serum lipidome and liver transcriptome in carriers of the TM6SF2 E167K variant, and by determining the effects of TM6SF2 knockdown on fatty acid metabolism *in vitro*. Finally, we examined the metabolic effects of three weeks of overfeeding of diets enriched either in saturated or unsaturated fat or simple sugars using a combination of state-of-the-art *in vivo* (imaging, stable isotope tracers and hyperinsulinemic-euglycemic clamp) and *ex vivo* (plasma lipidome, adipose tissue transcriptome and gut microbiome) techniques.

2. REVIEW OF THE LITERATURE

2.1 INTRODUCTION TO NAFLD

2.1.1. Definitions

NAFLD is defined as hepatic steatosis in the absence of other causes such as excess alcohol intake (> 30 g/day in men, > 20 g/day in women), viral or autoimmune hepatitis, or use of hepatotoxic drugs or other compounds (Yki-Järvinen, 2014). It comprises a spectrum of disease ranging from NAFL to NASH, a more aggressive form characterized by hepatocellular injury (ballooning necrosis, mild inflammation and possibly fibrosis), and cirrhosis (Yki-Järvinen, 2014).

Although NAFLD commonly coexists with insulin resistance and the features of the metabolic syndrome ('Metabolic NAFLD'), three common genetic variants increase the risk of NAFLD ('Genetic NAFLD') without affecting insulin sensitivity (**Figure 1**). A single-nucleotide polymorphism in PNPLA3 (rs738409 [G], encoding I148M) increases the risk of NAFL, NASH and fibrosis ('PNPLA3 NAFLD') (Romeo *et al.,* 2008). Genetic variations in MBOAT7 (rs641738 [T]) and TM6SF2 (rs58542926 [T], encoding E167K) also increase the risk of full spectrum of liver disease in NAFLD ('MBOAT7 NAFLD' and 'TM6SF2 NAFLD', respectively) (Mancina *et al.,* 2016; Kozlitina *et al.,* 2014). Given the high prevalence of the metabolic syndrome and these genetic variants, both metabolic and genetic causes of NAFLD may coexist.

2.1.2. Diagnosis

The gold standard method for the diagnosis of NAFLD is histological evaluation of a liver biopsy, which provides quantification of all qualities of the disease: steatosis, ballooning, lobular inflammation and fibrosis (Brunt *et al.,* 1999). NASH can only be diagnosed using a liver biopsy. Despite being highly informative, the utility of a liver biopsy is limited by its invasiveness, cost and sampling variability (European Association for the Study of the Liver (EASL) *et al.,* 2016).

Hepatic steatosis can be assessed using non-invasive imaging modalities such as proton magnetic resonance spectroscopy (^{1}H-MRS), magnetic resonance imaging (MRI), ultrasound, and computer tomography (European Association for the Study of the Liver (EASL) *et al.,* 2016). Using ^{1}H-MRS, NAFLD is commonly defined as intrahepatocellular triglyceride content exceeding 5.56%, based on the 95th percentile of IHTG in the healthy subjects in the population-based Dallas Heart Study (Szczepaniak *et al.,* 2005).

Fibrosis can be assessed indirectly by measuring liver stiffness, using non-invasive techniques such as transient elastography (Fibroscan®) or magnetic resonance elastography. In addition, several risk scores have been developed based on biochemical and anthropometric measurements for assessing the risk of advanced fibrosis in NAFLD, such as the FIB-4 and the NAFLD fibrosis score (European Association for the Study of the Liver (EASL) *et al.,* 2016).

2.1.3. Prevalence and significance

NAFLD has become the most prevalent cause of chronic liver disease worldwide affecting up to one-quarter of population, increasing in parallel with obesity (Younossi *et al.,* 2018). The prevalence of NASH is difficult to estimate, as it requires a liver biopsy. The prevalence of NASH in Finland was estimated by first developing a score based on liver biopsies obtained from 296 patients undergoing bariatric surgery, and then by validating

the score in 380 Italian mainly non-bariatric surgery patients. The score was applied to a Finnish population-based cohort in which the prevalence of NASH was found to be approximately 5% in 45-74-year olds (Hyysalo *et al.,* 2014). This prevalence is consistent with the 3-6% reported in studies of healthy liver donors (Anstee *et al.,* 2013).

Subjects with NAFLD have an increased risk of mortality from cardiovascular disease, liver cirrhosis and hepatocellular carcinoma (Ekstedt *et al.,* 2015). Amongst the histological features of NAFLD, especially fibrosis has been shown to predict overall and liver-related mortality (Dulai *et al.,* 2017, Hagström *et al.,* 2017).

2.1.3.1. Type 2 diabetes and the metabolic syndrome

The liver is the main glucose-producing organ in the body after an overnight fast (Yki-Järvinen, 1993). In the insulin-resistant 'Metabolic NAFLD', insulin fails to inhibit hepatic glucose production, leading to hyperglycemia. In order to maintain euglycemia, the pancreas compensatorily secretes more insulin, resulting in hyperinsulinemia. If this compensatory capacity of the pancreatic beta cells is exceeded, overt hyperglycemia and type 2 diabetes ensues (Yki-Järvinen, 2014).

According to a recent systematic review, NAFLD predicted the development of type 2 diabetes independently of age and BMI in 4 out of 6 studies in which NAFLD was diagnosed by ultrasound, and in 12 out of 14 studies in which the diagnosis was based on liver enzymes (ALT, AST or GGT) (Lallukka *et al.,* 2016).

Liver fat content correlates tightly with the features of the metabolic syndrome (i.e. waist circumference, hypertension, hyperglycemia, hypertriglyceridemia and low HDL cholesterol concentrations) (Kotronen *et al.,* 2007).

2.1.3.2. Cardiovascular disease

The liver is the major organ producing triglyceride-rich lipoproteins into the circulation after an overnight fast. In the insulin-resistant 'Metabolic NAFLD', insulin fails to suppress the hepatic secretion of large very low-density lipoprotein particles (Adiels *et al.,* 2007). This results in high triglyceride and low HDL cholesterol concentrations in plasma. In addition, the 'Metabolic NAFLD' is associated with increased activities of coagulation factors (Kotronen *et al.,* 2011; Lallukka *et al.,* 2016) and impaired fibrinolysis (Verrijken *et al.,* 2014; Tripodi *et al.,* 2011), which may further contribute to an increased risk of cardiovascular disease in subjects with NAFLD.

Indeed, cardiovascular disease is the leading cause of death in subjects with NAFLD (Ekstedt *et al.,* 2006).

2.1.3.3. Advanced liver disease and hepatocellular carcinoma

NAFLD can progress from NAFL to NASH and cirrhosis. NAFLD also increases the risk of hepatocellular carcinoma (HCC) (Anstee *et al.,* 2013). According to a recent meta-analysis the rate of disease progression is slower in patients with NAFL (one fibrosis stage over 14.3 years) as compared to patients with NASH (7.1 years) (Singh *et al.,* 2015). In paired-biopsy studies, steatosis (Pais *et al.,* 2013) and fibrosis stage (Nasr *et al.,* 2017) have been shown to predict the progression from NAFL to NASH and fibrosis. The only curative treatment for end-stage cirrhosis is liver transplantation, for which NAFLD is currently the second most common indication in the US (Wong *et al.,* 2015). NAFLD is the most common cause of HCC in both the United States (Sanyal *et al.,* 2010) and the United Kingdom (Dyson *et al.,* 2014).

2.1.4. Risk factors for NAFLD

Age is associated with the prevalence of ultrasound-diagnosed NAFLD, increasing approximately by 3-fold in subjects over 60 years old compared to those under 30 years of age in the population-based Third National Health and Nutrition Examination Survey comprising of 12,454 subjects (Lazo *et al.,* 2013). Male gender is also associated with increased prevalence of NAFLD (Lazo *et al.,* 2013).

The prevalence and severity of NAFLD is positively correlated with obesity (Lazo *et al.,* 2013; Fabbrini *et al.,* 2010). Histological assessment of liver biopsies obtained from liver donors, car crash victims, autopsies and clinical liver biopsies indicate that the prevalence of steatosis and steatohepatitis are approximately 15% and 3% in non-obese subjects, 65% and 20% in subjects with a BMI 30.0-39.9 kg/m^2, and 85% and 40% in subjects with a BMI over 40 kg/m^2 (Fabbrini *et al.,* 2010).

Subjects with NAFLD are characterized by low level of physical activity (Gerber *et al.,* 2012), while lifestyle interventions have been consistently shown to reduce liver fat content (Thoma *et al.,* 2012; Vilar-Gomez *et al.,* 2015). Nutritional factors also play a major role in the pathophysiology of NAFLD, and are discussed in detail later.

Liver fat content is closely correlated with insulin resistance in the adipose tissue (Marchesini *et al.,* 2001; Bugianesi *et al.,* 2005; Gastaldelli *et al.,* 2007; Kotronen *et al.,* 2008; Seppälä-Lindroos *et al.,* 2002), the skeletal muscle (Marchesini *et al.,* 2001; Bugianesi *et al.,* 2005; Kotronen *et al.,* 2008; Korenblat *et al.,* 2008) and the liver (Seppälä-Lindroos *et al.,* 2002; Kotronen *et al.,* 2008).

NAFLD is found in up to 70 % of subjects with type 2 diabetes, the prevalence being up to 3-fold higher than in the population (Doycheva *et al.,* 2016). This is not explained by obesity since subjects with type 2 diabetes have significantly higher IHTG content than age-, gender-, and BMI-matched subjects without diabetes (Kotronen *et al.,* 2008).

A growing body of evidence indicates that NAFLD is heritable. Family histories of both diabetes (Loomba *et al.,* 2012) and advanced liver disease (Caussy *et al.,* 2017) are associated with increased risk of NASH and fibrosis. Heritability estimates of NAFLD have ranged between 20 and 70 %, depending on the study design, ethnicity and the diagnostic methods used (Sookoian *et al.,* 2017). A portion of this heritability may be mediated by common genetic variants in PNPLA3, MBOAT7 and TM6SF2 (*vide infra*).

2.2. PATHOGENESIS OF NAFLD

2.2.1. 'Metabolic NAFLD'

2.2.1.1. Sources of hepatic fatty acids

Increased intrahepatic triglyceride (IHTG) content is the defining feature of NAFLD. TGs are composed of a glycerol backbone and three variable fatty acyl-groups. Hepatic uptake of fatty acids is mainly determined by their delivery (Frayn *et al.,* 2006). These fatty acids can originate either from the adipose tissue, dietary fat, or from non-lipid substrates *via* hepatic *de novo* lipogenesis (Donnelly *et al.,* 2005) (**Figure 2**).

2.2.1.1.1. Adipose tissue lipolysis

Contribution to IHTG. After an overnight fast, adipose tissue lipolysis is the major source of hepatic fatty acids. Direct measurements using stable isotopes in humans have shown that more than half of the fatty acids in IHTGs in subjects with NAFLD originate from lipolysis (Donnelly *et al.,* 2005).

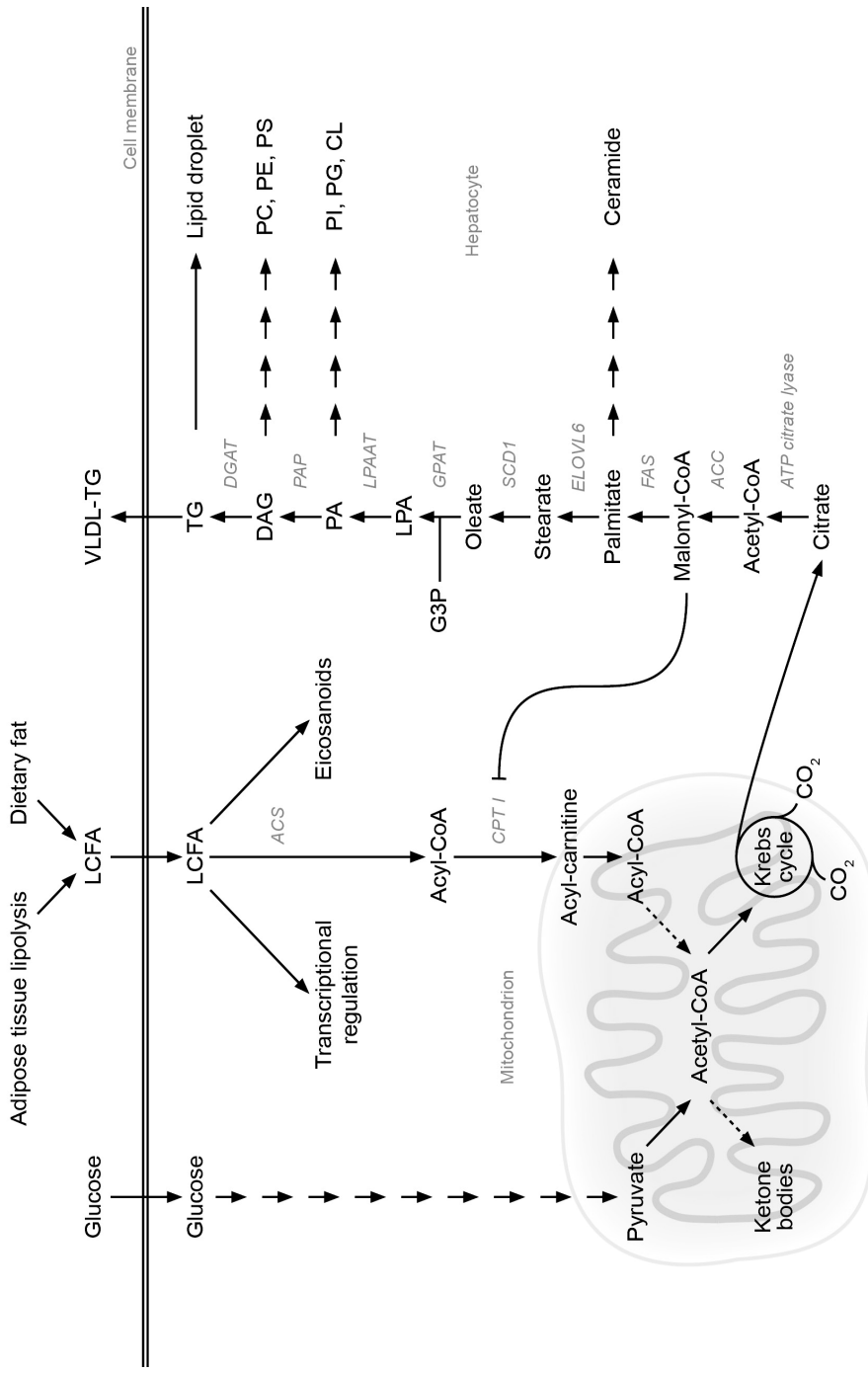

Figure 2. Sources and fates of hepatic fatty acids. LCFA = long-chain fatty acid; ACS = acyl-CoA synthase; CPT I = carnitine palmitoyltransferase I; G3P = glycerol 3-phosphate; ACC = acetyl-CoA carboxylase; FAS = fatty acid synthase; ELOVL6 = fatty acid elongase 6; SCD1 = stearoyl-CoA desaturase 1; GPAT = glycerol phosphate acyltransferase; LPAAT = lysophospholipid acyltransferase; PAP = phosphatidic acid phosphatase; DGAT = diacylglycerol acyltransferase; LPA = lysophosphatidic acid; PA = phosphatidic acid; DAG = diacylglycerol.

In response to a meal, insulin inhibits lipolysis by inhibiting hormone-sensitive lipase (HSL) and adipose tissue switches from net release to net uptake of free fatty acids (FFAs) (Frayn *et al.,* 2006). This decreases the delivery of FFAs to the liver (Frayn *et al.,* 2006).

Regulation of lipolysis. In healthy subjects, adipose tissue lipolysis is stimulated under conditions of energy demand (*e.g*. stress and fasting) and suppressed after a meal under conditions of energy surplus (Frayn *et al.,* 2006). Hormones such as catecholamines, growth hormone and glucocorticoids, and cytokines such as tumor necrosis factor alpha stimulate lipolysis in humans. Inhibitors of lipolysis include insulin and nicotinic acid (Langin, 2006). Polyunsaturated fatty acids may also inhibit adipose tissue lipolysis *via* activation of G-protein coupled receptor 120 (GPR120), which mediates anti-inflammatory and insulin-sensitizing effects and is expressed in adipocytes and macrophages (Oh *et al.,* 2010; Wang *et al.,* 2017; Satapati *et al.,* 2017). HSL, adipose triglyceride lipase (ATGL) and monoacylglycerol lipase (MGL) are the main lipases that mediate the responses to regulators of lipolysis (Frayn *et al.,* 2006; Nielsen *et al.,* 2014).

Insulin resistance in adipose tissue in NAFLD. The increase in lipolysis in NAFLD is characterized by an inability of insulin to normally inhibit lipolysis (Marchesini *et al.,* 2001; Bugianesi *et al.,* 2005; Gastaldelli *et al.,* 2007; Kotronen *et al.,* 2008; Seppälä-Lindroos *et al.,* 2002), thereby increasing the flux of free fatty acids and glycerol into circulation and their availability for uptake in the liver.

The exact mechanism leading to adipose tissue insulin resistance in humans is unclear but it is well established that adipose tissue is inflamed in insulin-resistant conditions such as obesity (Weisberg *et al.,* 2003) and NAFLD (Kolak *et al.,* 2007). Inflamed adipose tissue is characterized by adiponectin deficiency (Arita *et al.,* 1999) and it overproduces adipokines such as monocyte chemotactic protein-1, tumour necrosis factor alpha and interleukins 1 and 6, which in mouse models induce insulin resistance (Shoelson *et al.,* 2006). Adiponectin deficiency seems of particular relevance in human NAFLD. Multiple studies have documented serum adiponectin concentrations to be inversely related with liver fat content (Turer *et al.,* 2012; Polyzos *et al.,* 2016).

Increased adipose tissue lipolysis could stimulate glucose production and induce insulin resistance in the liver by several mechanisms. Free fatty acids taken up by the liver can be metabolized into bioactive, insulin resistance-inducing intermediates, such as ceramides and diacylglycerols (*vide infra*) (Samuel *et al.,* 2016). Hepatic free fatty acids can also be oxidised in the liver into acetyl coenzyme A (acetyl-CoA), which in turn can allosterically activate pyruvate carboxylase and thereby stimulate gluconeogenesis (Perry *et al.,* 2015). Finally, increased glycerol availability can increase gluconeogenesis by a substrate push mechanism (Perry *et al.,* 2015).

According to a systematic review comprising 7,354 healthy subjects, oleic acid (C18:1) makes up 43.5%, palmitic acid (C16:0) 21.5%, linoleic acid (C18:2) 13.9%, palmitoleic acid (C16:1) 7.2%, and stearic acid (C18:0) 3.4% of the fatty acids in TGs of subcutaneous adipose tissue (Hodson *et al.,* 2008). Thereby lipolysis in the adipose tissue could be expected to supply the liver with mostly saturated and monounsaturated fatty acids.

2.2.1.1.2. Dietary fat

In the postprandial state, dietary triglycerides undergo hydrolysis in the intestinal lumen by lipases and are then

taken up by enterocytes and re-esterified into TGs (Frayn *et al.,* 2006). These TGs are secreted into the lymph in chylomicron particles. The majority of chylomicron triglycerides are hydrolysed intravascularly by lipoprotein lipase and taken up by peripheral tissues. The resulting chylomicron remnant particles are taken up by the liver. The fraction of fatty acids that are released in the hydrolysis of chylomicrons intravascularly but are not immediately taken up by adipose tissue and skeletal muscle spill over to the circulation and are available for uptake by the liver (Lambert *et al.,* 2014). This spillover pathway appears to be unchanged in subjects with high as compared to those with low liver fat content (Lambert *et al.,* 2014).

2.2.1.1.3. *De novo* lipogenesis

Hepatic *de novo* lipogenesis synthesizes saturated fatty acid palmitate (C16:0) from cytosolic citrate (Postic *et al.,* 2008) (**Figure 2**). Conversion of citrate to acetyl-CoA is catalyzed by ATP citrate lyase, which is subsequently metabolized to malonyl-CoA by acetyl-CoA carboxylase (ACC) and subsequently elongated by fatty acid synthase (FAS). Cytosolic citrate is produced in the Krebs cycle in mitochondria during oxidation of substrates such as glucose, fructose and amino acids. Unlike glucose, fructose is metabolized only in the liver and stimulates DNL more than glucose in humans (Hellerstein *et al.,* 1996).

Palmitate can be elongated by elongases such as fatty acid elongase 6 (ELOVL6) to form longer saturated fatty acids such as oleate (C18:0) (Postic *et al.,* 2008). Saturated fatty acids are converted to monounsaturated fatty acids via the action of stearoyl-CoA desaturase 1 (SCD-1). Importantly, saturated fatty acids cannot be converted to polyunsaturated fatty acids because their synthesis requires essential fatty acids such as linoleate (C18:2) as a precursor (Hodson *et al.,* 2008).

Hyperglycemia upregulates DNL by stimulating activation of the transcription factor carbohydrate-responsive element-binding protein (ChREBP) which increases the synthesis of FAS and SCD-1, and also simply by increasing the availability of pyruvate in mitochondria (Hellerstein *et al.,* 1996) (**Figure 2**). Insulin stimulates sterol regulatory element-binding protein 1c (SREBP1c) expression in the liver, which increases the transcription of ACC, FAS and ELOVL6 (Yilmaz *et al.,* 2016).

Stimulation of glucose utilization by exercise in skeletal muscle acutely decreases hepatic DNL (Rabøl *et al.,* 2011).

In normal subjects studied after an overnight fast, 4.6-10.1% of fatty acids in VLDL-TGs, which reflect the composition IHTGs, originate from DNL (Diraison *et al.,* 2003; Donnelly *et al.,* 2005). In subjects with high liver fat content, the contribution of DNL to VLDL-TG averaged 14.9-23.2% which was approximately 3-fold higher than in subjects with low liver fat content (Diraison *et al.,* 2003; Lambert *et al.,* 2014). These data imply that that the fatty acid composition of IHTG could be relatively enriched with saturated TGs at least in part because of increased DNL. When measured directly across the splanchnic bed using the hepatic venous catheterization technique, the human fatty liver overproduces triacylglycerols containing saturated fatty acids (Westerbacka *et al.,* 2010). Adipose tissue DNL appears neglible in humans (Diraison *et al.,* 2003).

2.2.1.2. Fates of hepatic fatty acids

In the liver, fatty acids can be channeled into distinct metabolic pathways (**Figure 2**). They can be utilized for synthesis of

TGs, which may either be stored in lipid droplets, or secreted into circulation in VLDL particles (Grevengoed *et al.,* 2014). By definition, the amount of TGs in hepatic lipid droplets is increased in NAFLD. In subjects with NAFLD, TGs are overproduced to the circulation in VLDL particles, and this production is less inhibited by insulin as compared to normal subjects independent of age, gender and obesity (Adiels *et al.,* 2007).

Another fate of fatty acids is metabolism into non-TG lipid species such as diacylglycerols, ceramides, phospholipids or cholesterol esters (*vide infra*).

Fatty acids can undergo oxidation in mitochondria (or in peroxisomes in case of very long chain polyunsaturated fatty acids) to produce acetyl-CoA, which can be utilized to generate adenosine triphosphate (ATP) or ketone bodies (Grevengoed *et al.,* 2014). In studies assessing hepatic lipid oxidation either indirectly by measuring plasma 3-hydroxybutyrate concentrations (Kotronen *et al.,* 2009), or directly by *in vivo* ^{13}C magnetic resonance spectroscopy (Petersen *et al.,* 2016), no changes have been found in subjects with NAFLD as compared to healthy controls. Whether hepatic lipid oxidation is altered in more advanced disease states, such as in NASH, remains unclear (Männistö *et al.,* 2015; Sunny *et al.,* 2017).

Polyunsaturated fatty acids can also be metabolized into bioactive derivatives such as eicosanoids, which are important modulators of inflammation (Grevengoed *et al.,* 2014). Increased circulating concentrations of polyunsaturated fatty acid-derived eicosanoids characterize patients with NASH (Puri *et al.,* 2009; Loomba *et al.,* 2015).

In addition to being substrates for the aforementioned various metabolic pathways, FFAs may modulate metabolism *via* acting as ligands for nuclear transcriptional factors, such as peroxisome proliferator activators alpha, gamma and delta (Grevengoed *et al.,* 2014).

2.2.1.2.1. Triacylglycerols

TGs, i.e. triacylglycerols, are composed of three variable fatty acyl-groups and a glycerol backbone. The energy density of TGs is approximately 37 kJ/g, while that of glycogen is approximately 17 kJ/g, and further decreased as glycogen binds three times its own mass of water. Therefore, TGs are a bioenergetically efficient storage form of chemical energy in the body (Frayn *et al.,* 2006).

Synthesis of TGs starts by formation of the glycerol backbone. Glycerol 3-phosphate acyltransferase (GPAT) acylates glycerol 3-phosphate (G3P) with a fatty acid to form lysophosphatidic acid (LPA). This is acylated by lysophosphatidic acid acyltransferase (LPAAT) to form phosphatidic acid, which can be metabolized into diacylglycerol. Finally, diacylglycerol is acylated by diacylglycerol acyltransferase (DGAT) into a TG (Postic *et al.,* 2008) (**Figure 2**).

As mentioned earlier, the fatty acids in intrahepatic TGs can be derived from the dietary fat, adipose tissue lipolysis, or hepatic *de novo* lipogenesis. The fatty acid composition of VLDL-TGs reflects that of their fatty acid sources (Lambert *et al.,* 2014), and that of hepatic TGs in the fasting state (Donnelly *et al.,* 2005).

A previous study on hepatic lipidome in 27 subjects (9 controls, 9 subjects with NAFL and 9 subjects with NASH) using thin-layer chromatography reported that IHTGs were 9.4-fold increased in NAFL and 7.6-fold in NASH as compared to controls. Saturated, monounsaturated and polyunsaturated fatty acids represented approximately 40, 40 and 20 mol-% of fatty acids in IHTGs,

respectively. Saturated and monounsaturated fatty acids tended to increase and polyunsaturated fatty acids were decreased in IHTGs in NAFL and NASH as compared to controls (Puri *et al.,* 2007).

Even though hepatic TG content correlates closely with insulin resistance (Ryysy *et al.,* 2000; Sanyal *et al.,* 2001; Seppälä-Lindroos *et al.,* 2002; Gastaldelli *et al.,* 2007; Kotronen *et al.,* 2008; Korenblat *et al.,* 2008), several phenotypes characterized by hepatic steatosis without features of insulin resistance also exist, such as in subjects with familial hypobetalipoproteinemia (Amaro *et al.,* 2010), or carrying genetic variants in PNPLA3, MBOAT7 and TM6SF2 (*vide infra*). These findings in humans, and in a plethora of animal models (Sun *et al.,* 2013) suggest that TGs are inert and by themselves not sufficient or necessary to cause insulin resistance (Cohen *et al.,* 2011). Rather than TGs, accumulation of lipotoxic derivatives of fatty acids, such as diacylglycerols and ceramides (*vide infra*) have been suggested to mediate insulin resistance (Samuel *et al.,* 2018; Chaurasia *et al.,* 2015).

2.2.1.2.2. Diacylglycerols

Diacylglycerols (DAGs) are the immediate precursors of TGs (**Figure 2**). These bioactive lipids are composed of two variable fatty acyl chains and a glycerol backbone. DAGs were first associated with insulin resistance in the skeletal muscle, where they impair insulin signaling by activating protein kinase C theta (PKCθ) (Samuel *et al.,* 2016).

DAGs were subsequently hypothesized to mediate IR in the liver. Indeed, in the rat liver, increased concentrations of DAGs activate protein kinase C epsilon (PKCε), which is associated with decreased activation of insulin receptor tyrosine kinase (Samuel *et al.,* 2004; Samuel *et al.,* 2007). This mechanism may mainly affect insulin regulation of net hepatic glycogen synthesis (ter Horst *et al.,* 2017). The specific molecular mechanism underlying inhibition of insulin receptor kinase by PKCε was found to be the phosphorylation site Thr1160 (Petersen *et al.,* 2016b). Both deletion of *prkce,* and inactivation of this phosphorylation site protects mice from high fat diet-induced insulin resistance (Raddatz *et al.,* 2011; Petersen *et al.,* 2016b).

Total hepatic DAG concentrations have been shown to correlate with insulin resistance in two human studies with 37 and 16 subjects (Kumashiro *et al.,* 2011; Magkos *et al.,* 2012). One study with 29 subjects did not find significant correlation between total hepatic DAG content and insulin resistance (ter Horst *et al.,* 2017). However, when subcellular fractions were analysed separately, cytosolic DAG content was found to be increased while membrane DAG content was decreased in insulin resistant as compared to insulin sensitive subjects. Amongst 13 different cytosolic species, four correlated positively with insulin resistance: C18:1-C16:0, C18:0-C18:0, C16:0-C16:0 and C18:1-C18:1, i.e. species with saturated and monounsaturated fatty acyl chains (ter Horst *et al.,* 2017).

Regarding hepatic DAG content in NAFLD, a 4-fold increase was reported in 8 subjects with NAFL as compared to 8 healthy controls matched for age, gender and BMI (Kotronen *et al.,* 2009). Another study described a 2.6-fold increase in hepatic DAG content in 9 subjects with NAFL and a 1.7-fold increase in 9 subjects with NASH as compared to 9 controls (Puri *et al.,* 2007). One study examined the hepatic DAGs with respect to distinct species in 12 subjects with normal liver, 17 subjects with steatosis and 9 subjects with cirrhosis (Gorden *et al.,* 2011). In this study, the increase in hepatic DAGs in steatotic as compared to normal liver was due to increase in species with 32 to

36 carbons and 0 to 3 double bonds. Of note, in this study the groups differed with respect to size, gender distribution, body mass index and age.

There are no studies comparing the hepatic DAG content and composition in insulin-resistant 'Metabolic NAFLD' and in insulin-sensitive 'PNPLA3 NAFLD'.

2.2.1.2.3. Ceramides

Ceramides, a part of the sphingolipid family, are another type of fatty acid intermediates which have been suggested to mediate insulin resistance. Like DAGs, ceramides were first reported to mediate insulin resistance in the skeletal muscle and subsequently hypothesized to mediate it also in the liver (Chavez *et al.,* 2012). They can be synthesized either from saturated fatty acids (*e.g.* palmitate) *via de novo* synthesis, or *via* sphingomyelin hydrolysis, or from hexosylceramides *via* salvage pathway (Chaurasia *et al.,* 2015) (**Figure 3**). In studies using lipid infusions or cell cultures, ceramides have been associated especially with saturated-, but not unsaturated fatty acid-induced insulin resistance (Holland *et al.,* 2007; Hu *et al.,* 2011).

Recently, a distinct species of ceramides, C16:0-ceramide, from the *de novo* synthetic pathway was described as principal mediator of obesity-related insulin resistance in the liver (Hla *et al.,* 2014; Turpin *et al.,* 2014; Raichur *et al.,* 2014). First substrates in the *de novo* ceramide synthetic pathway are palmitoyl-CoA and serine (**Figure 3**). After two intermediate steps, a sphinganine molecule is formed. Then, one of ceramide synthase (CerS) enzymes acylates the sphinganine, producing a dihydroceramide, the immediate precursor of ceramides. There are six different isoforms of CerS (CerS1-6), which have a variable substrate preference. For example, C16:0-dihydroceramides are produced mainly by CerS5 and CerS6 (**Figure 3**). The resulting dihydroceramides are metabolized by dihydroceramide desaturase to form ceramide (Chaurasia *et al.,* 2015).

In high-fat diet-fed mice, both whole-body and liver-specific deletion of CerS6 decreases concentrations of C16:0-ceramides in the liver and increases fatty acid oxidation and glucose tolerance (Turpin *et al.,* 2014). Consistently, CerS2 haploinsufficient mice fed a high-fat diet are characterized by increased C16:0-ceramide concentration in the liver, decreased lipid oxidation, decreased glucose tolerance and hepatic steatosis (Raichur *et al.,* 2014). CerS6 knockdown by anti-sense oligonucleotides in ob/ob mice decreases CerS6 expression selectively in the liver by ~80% and hepatic C16:0-ceramide concentration by ~50% while increasing glucose tolerance by ~50% as compared to control ob/ob mice (Bielohuby *et al.,* 2017).

Inflammation. In addition to availability of the substrate, i.e. palmitoyl-CoA, the *de novo* ceramide synthetic pathway is upregulated by inflammatory mediators *via* nuclear factor kappa-light-chain-enhancer of activated B cells B ($NF_{\kappa}B$) (Chavez *et al.,* 2012). These inflammatory mediators include ligands of the Toll-like receptor 4 (TLR-4), such as endotoxin (also known as lipopolysaccharide, LPS), a component of gram-negative bacteria (Holland *et al.,* 2007) (**Figure 3**).

Degradation. Ceramide concentrations in the liver may also increase *via* diminished degradation. Adiponectin, an insulin-sensitizing and anti-inflammatory cytokine produced by adipocytes (Scherer *et al.,* 1995), exhibits ceramidase activity (Holland *et al.,* 2011b; Holland *et al.,* 2017) (**Figure 3**). In mice, overexpression of acid ceramidase in the liver reduces hepatic C16:0-, C18:0- and C20:0-ceramides, decreases hepatic

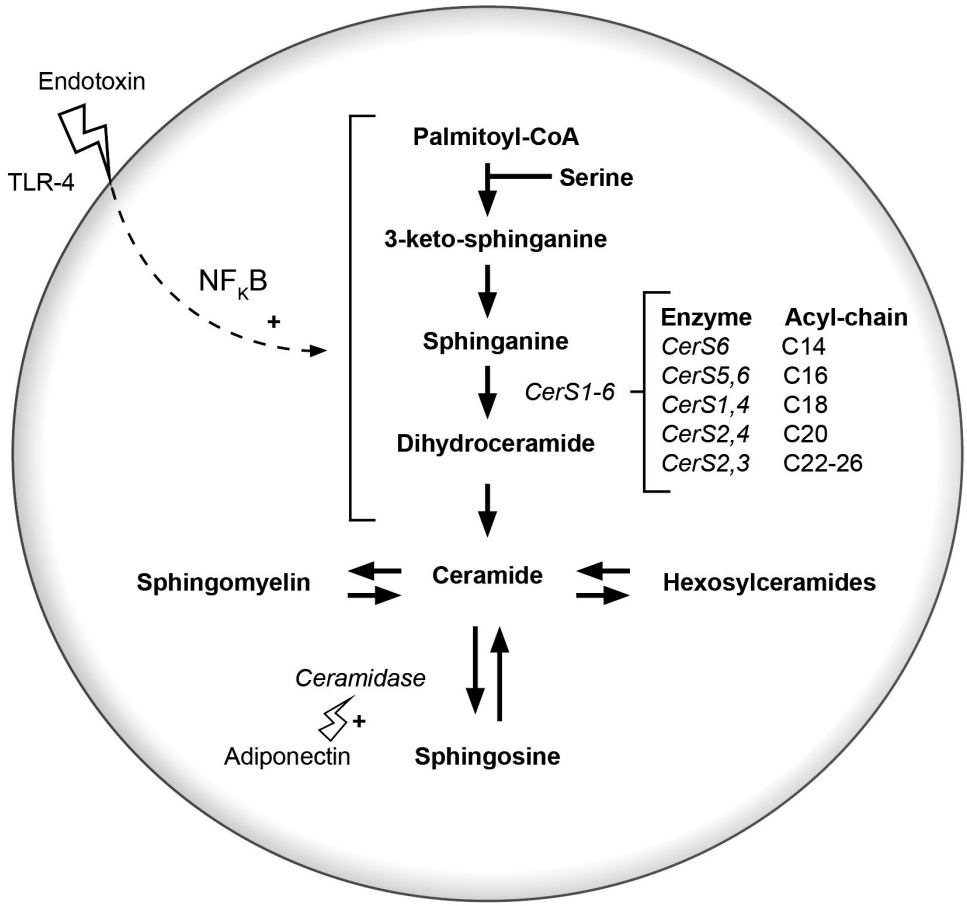

Figure 3. Pathways of ceramide metabolism. TLR-4 = toll-like receptor 4; NF_KB = nuclear factor kappa-light-chain-enhancer of activated B cells; CerS = ceramide synthase.

steatosis and hepatic glucose production, and improves glucose tolerance (Xia *et al.,* 2015).

Mechanisms. Ceramides may promote insulin resistance *via* several mechanisms. In muscle, ceramide accumulation has been shown to inhibit protein kinase B (Akt/PKB) phosphorylation by activating protein phosphatase 2A (PP2A), and blocking the translocation of Akt/PKB to the plasma membrane through activation of PKCζ (Stratford *et al.,* 2004; Hajduch *et al.,* 2008).

In the adipose tissue, ceramides can activate the nucleotide-binding oligomerization domain-like receptor containing pyrin domain 3 (NLRP3) inflammasome and thereby induce inflammation, which is associated with insulin resistance in mice (Vandanmagsar *et al.,* 2011). The adipose tissue in subjects with high liver fat content is infiltrated with macrophages and enriched in ceramides as compared to weight-, age- and gender-matched subjects with normal liver fat content (Kolak *et al.,* 2007). In another study, adipose tissue was enriched in ceramides

in visceral obesity, and their concentration correlated with the gene expression of the components of the inflammasome in the adipose tissue (Kursawe *et al.,* 2016). Thus, ceramides may promote insulin resistance by promoting inflammation in the adipose tissue *via* activation of the inflammasome.

In the mouse liver, ceramides induce translocation of the lipid transport protein CD36 to the cell membrane *via* PKCζ to stimulate fatty acid uptake (Turpin *et al.,* 2014; Xia *et al.,* 2015). Hepatic ceramides also impair lipid oxidation by inhibiting mitochondrial citrate synthase and electron transport chain activities (Xie *et al.,* 2017; Turpin *et al.,* 2014; Raichur *et al.,* 2014). In addition, ceramides increase hepatic mitochondrial acetyl-CoA concentrations and pyruvate carboxylase activities, thereby stimulating gluconeogenesis (Xie *et al.,* 2017).

Human liver studies in IR. Three small studies with 37 (Kumashiro *et al.,* 2011), 16 (Magkos *et al.,* 2012) and 29 (ter Horst KW *et al.,* 2017) subjects have found no correlation between total hepatic ceramide concentration and insulin resistance. However, different ceramides species exhibit markedly different metabolic effects, and only specific ones have been associated with insulin resistance in mice (Hla T *et al.,* 2014; Xia *et al.,* 2015). Only one study has examined the correlation of different species of hepatic ceramides and insulin resistance in humans (ter Horst KW *et al.,* 2017). In this study, neither total hepatic ceramides or total hepatic DAGs differed between insulin sensitive and insulin resistant subjects, and no correlation was found between hepatic ceramide species and insulin resistance. The authors concluded that these conflicting results may be due to experimental techniques or limited sample size (ter Horst *et al.,* 2017).

Human liver studies in NAFLD. Only one study has examined the total concentration of ceramides in the human liver in NAFLD (Kotronen *et al.,* 2009). In this study, 8 subjects with NAFL were compared to 8 age-, sex- and body mass index-matched controls without NAFL, and no significant difference in total liver ceramide content was found. Of note, there were no significant differences in fasting serum insulin concentrations, a surrogate for insulin resistance, between these groups.

Human plasma studies in IR and CVD. In the postabsorptive conditions, plasma ceramides reside in liver-derived very-low and low density lipoprotein particles in humans (Kotronen *et al.,* 2009). Cross-sectionally, plasma ceramide concentrations have been reported to correlate with insulin resistance (Haus *et al.,* 2009; de Mello *et al.,* 2009; Bergman *et al.,* 2015). The plasma ceramide concentrations are also reported to correlate with the improvement in insulin sensitivity during thiazoledinedione treatment, and after bariatric surgery (Huang *et al.,* 2011; Warshauer *et al.,* 2015). In addition to insulin resistance, plasma ceramide concentrations are reported to predict cardiovascular events and death in five prospective studies, even independently of LDL cholesterol (Tarasov *et al.,* 2014; Cheng *et al.,* 2015; Laaksonen *et al.,* 2016; Havulinna *et al.,* 2016; Wang *et al.,* 2017). Thus, ceramides may have, in addition to insulin resistance and NAFLD, implications in cardiovascular disease (Summers, 2018).

There are no studies reporting the concentrations of distinct ceramide species in the human liver, or which, if any, pathway of ceramide metabolism is altered.

2.2.1.2.4. Phospholipids

Phospholipids are a major lipid class which form the matrix of cellular

membranes. In addition, they serve as first and second messengers during cellular signal transduction (van Meer *et al.,* 2008). They also serve as precursor pools of various lipid mediators, such as eicosanoids derived from polyunsaturated fatty acids, *e.g*. arachidonic acid (Shindou *et al.,* 2008). Phospholipids include six major subspecies, i.e. phosphatidylcholines (PCs), phosphatidyl-inositols (PIs), phosphatidylserines (PSs), phosphatidylglycerols (PGs), phosphatidyl-ethanolamines (PEs) and cardiolipins (CLs) (Shindou *et al.,* 2009).

In the *de novo* synthetic pathway (also known as the Kennedy pathway) of phospholipids, lysophosphatidic acid (LPA) is formed from glycerol 3-phosphate by glycerol-3-phosphate acyl transferase (GPAT) (**Figure 2**). Subsequently, LPA is metabolized to phosphatidic acid (PA) by lysophosphatidic acid acyltransferase (LPAAT). PA is metabolized into one of two glycerol derivatives: DAG or cytidine diphospho-DAG. The former is can be converted to TG, PC or PE. PS is derived from either PC or PE. Cytidine diphospho-DAG can be metabolized into PI, PG and CL (Shindou *et al.,* 2009).

The fatty acyl composition of phospholipids have an important role in the membrane structure and cellular signaling. The composition can be altered in the remodeling pathway (also known as the Lands' cycle) through removal of the existing fatty acyl group by phospholipase A_2 (PLA_2), and replacement by lysophospholipid acyltransferase (LPLAT) (Shindou *et al.,* 2009) (**Figure 4**). Several isoforms of each enzymes exist, and more are being found (Shindou *et al.,* 2009).

Phosphatidylcholines have an important role in triglyceride-rich lipoprotein metabolism and cardiovascular disease. Animal models with impaired PC synthesis, such as those with deletion in CTP:phosphocholine cytidylyltransferase alpha, phosphatidylethanolamine N-methyltransferase and lysophosphatidylcholine acyltransferase 3 are characterized by hepatic steatosis, reduced hepatic TG secretion and reduced risk of atherosclerotic disease, but no features of insulin resistance (Sun *et al.,* 2013; Cole *et al.,* 2012; Rong *et al.,* 2014). A similar phenotype also characterizes animals consuming a PC deficiency-inducing methionine-choline-deficient diet, a widely used experimental model for NAFLD and NASH (Cole *et al.,* 2012; Rinella *et al.,* 2004).

Regarding PIs, alterations in their metabolism have been associated with various disorders, such as neural and cardiac development, neurological disorders, cancer, immune dysfunction, metabolic disease and inflammation (D'Souza *et al.,* 2014).

In the human liver, concentrations of PCs are reported to be 25% decreased in 9 subjects with NAFL as compared to 9 control subjects (Puri *et al.,* 2007). In a study comparing the lipidome in 12 normal, 17 steatotic and 9 cirrhotic human livers, hepatic concentrations of PI(38:3) and PI(38:4) decreased from normal to steatotic to cirrhotic livers (Gorden *et al.,* 2011). In contrast, concentrations of PI(38:5), PI(36:3), PI(36:4), PI(34:1), PI(34:2) and PI(32:1) were increased with the severity of NAFLD.

No studies have reported the contents or compositions of PCs or PIs in the human liver in NAFLD due to different aetiologies.

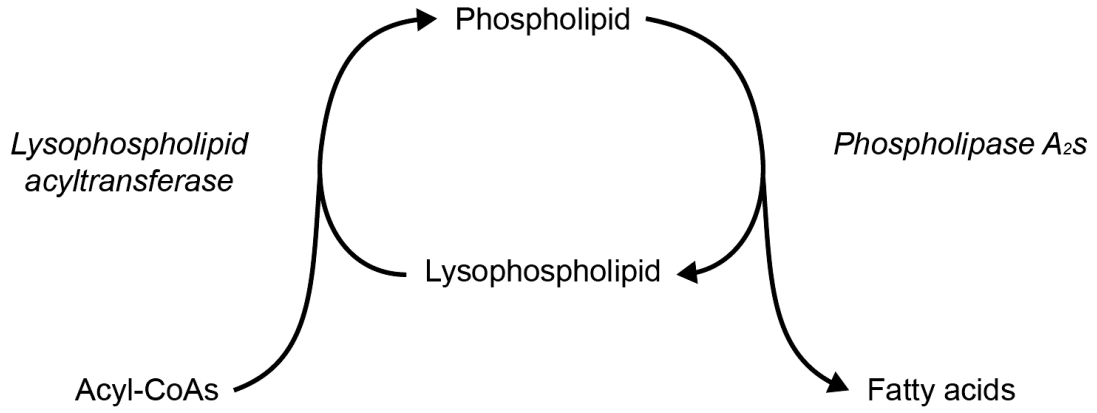

Figure 4. Phospholipid remodeling pathway, also known as the Lands' cycle.

2.2.1.3. Hepatocellular injury and fibrosis

Histological scoring. In the histological assessment of a liver biopsy, macrovesicular steatosis, lobular inflammation, hepatocellular ballooning and fibrosis are evaluated (Brunt *et al.,* 1999; Bedossa *et al.,* 2012).

In the histological score developed by Brunt *et al.*, macrovesicular steatosis is assessed as the percent of hepatocytes involved. Necroinflammation is evaluated using a grading from 1 to 3. Grade 1 (mild) is characterized by steatosis up to 66%, possible occasional ballooned perivenous hepatocytes; possible small amount of intra-acinar inflammatory infiltrates. This grade meets the minimum criteria for the diagnosis of non-alcoholic steatohepatitis. In grade 2 (moderate), the steatosis may be of any degree; hepatocyte ballooning is always present and predominantly seen in the perivenous region; ballooning is seen adjacent to hepatocytes most distended by the steatosis; perivenous fibrosis may be present; mild to moderate portal and intra-acinar chronic inflammation is present. In grade 3 (severe), steatosis is panacinar; ballooning is always present and seen predominantly in the perivenous region; lobular inflammation is more pronounced as compared to grade 2 (Brunt *et al.,* 1999).

Fibrosis is assessed by a staging from 1 to 4. Stage 1 is characterized by focal or extensive perivenous fibrosis. In addition to these features, stage 2 includes various degrees of portal fibrosis. Stage 3 adds focal or extensive bridging fibrosis between perivenous and periportal regions. Stage 4 represents cirrhosis (Brunt *et al.,* 1999).

Mortality. Amongst these histological features, especially fibrosis has been shown to predict mortality from both overall and liver-related causes (Dulai *et al.,* 2017). According to a recent meta-analysis with 1,495 NAFLD patients with 17,452 patient years of follow-up, all-cause mortality rate ratio was 1.58 (95% CI 1.19-2.11) in stage 1; 2.52 (95% CI 1.85-3.42) in stage 2; 3.48 (95% CI 2.51-4.83) in stage 3; and 6.40 (95% CI 4.11-9.95) in stage 4 as compared to subjects with no fibrosis (stage 0). The risk was more pronounced with respect to liver-related mortality ratio: 1.41 (95% CI 0.17-11.95) in stage 1; 9.57 (95% CI 1.67-54.93) in stage 2; 16.69 (95% CI 2.92-95.36) in stage 3; and 42.30 (95% CI 3.51-510.34)

in stage 4 as compared to subjects with stage 0 (Dulai et al 2017).

Predictors. In paired biopsy studies, features that have predicted the progression of disease severity include changes in hepatic steatosis (Pais *et al.,* 2013; Ekstedt *et al.,* 2006) and waist circumference (Wong *et al.,* 2010). In addition, greater weight gain, more severe insulin resistance (Ekstedt *et al.,* 2006), and higher prevalence of type 2 diabetes (McPherson *et al.,* 2015; Nasr *et al.,* 2017) characterize subjects with disease progression as compared to non-progressors. In a recent meta-analysis with 411 subjects with biopsy-proven NAFLD and 2,145 patient-years of follow-up, the rate of disease progression was slower in patients with NAFL (one fibrosis stage over 14.3 years; 95% CI 9.1-50.0 years) compared to patients with NASH (7.1 years; 95% CI 4.8-14.3 years) (Singh *et al.,* 2015). In addition to these acquired factors, genetic variants in PNPLA3, TM6SF2 and MBOAT7 predispose to advanced liver disease (*vide infra*).

Fibrogenesis. Hepatic stellate cells are the dominant source of extracellular matrix and fibrosis in the liver (Mederacke *et al.,* 2013). In a quiescent, non-proliferative state, stellate cells store retinyl esters, but they can also be activated into proliferative myofibroblasts characterized by enhanced extracellular matrix production (Tsuchida *et al.,* 2017). A repetitive or chronic activation may promote progressive fibrogenesis, and can thereby lead to cirrhosis (Diehl *et al.,* 2017). Factors regulating the progression of NAFLD from NAFL to NASH to advanced fibrosis and cirrhosis are not fully known. Fatty acids and their lipotoxic intermediates, such as DAGs, ceramides and arachidonic acid-derived proinflammatory eicosanoids have been suggested to play a role (Neuschwander-Tetri 2010; Chen *et al.,* 1997; Nieto *et al.,* 2000; Ishihara *et al.,* 2012; Loomba *et al.,* 2015; Puri *et al.,* 2009). In addition, deficiency of hepatic PCs (George *et al.,* 2003) and local hypoxia (Jungermann *et al.,* 2000; Cannito *et al.,* 2014) have been proposed to stimulate disease progression.

There are no reports whether the hepatic lipid composition is associated with liver injury in NAFLD due to different causes in humans.

2.2.1.4. Role of the gut in the pathogenesis of NAFLD

Low-grade inflammation. It is well established that conditions related to insulin resistance, such as diabetes and obesity are characterized by a low-grade inflammation, which origin is unknown (Hotamisligil, 2006; Weisberg *et al.,* 2003). The human gut is estimated to harbour up to 100 trillion microbial cells, outnumbering the human cells by 10-fold (Ley *et al.,* 2006). These microbes are a rich source of inflammatory mediators, such as endotoxin (a component of Gram-negative bacteria, also known as lipopolysaccharide, LPS), and could thereby contribute to the low-grade inflammation in metabolic disease.

Toll-like receptor 4 (TLR-4). One of the pathways *via* which endotoxin may mediate its proinflammatory action is through the TLR-4. In this pathway, endotoxin interacts with lipopolysaccharide-binding protein (LBP) and cluster of differentiation 14 (CD14, a glycoprotein) (Chow *et al.,* 1999). CD14 can exist in the circulation in a soluble form (soluble CD14; sCD14), or as a membrane protein. The former acts in neutralization of endotoxin, while the latter is a necessary co-receptor with TLR-4 in mediating the proinflammatory signal within the cell (Fernandez-Real *et al.,* 2003). TLR-4 is expressed in various metabolic organs in the human body, such as in the adipose tissue (Bés-

Houtmann *et al.,* 2007), and in the liver (Sharifnia *et al.,* 2015).

Endotoxemia. Cross-sectional studies in humans have reported endotoxemia to associate with histological severity in 237 patients with NAFLD (Pang *et al.,* 2017). It is also associated with insulin resistance (Lassenius *et al.,* 2011), the features of the metabolic syndrome, and type 2 diabetes (Pussinen *et al.,* 2011). Infusion of endotoxin induces adipose tissue inflammation and insulin resistance in mice (Cani *et al.,* 2007) and in humans (Mehta *et al.,* 2010), and stimulates lipolysis *in vitro* (Zu *et al.,* 2009).

Dietary regulation. Gut-derived endotoxin can enter the circulation by permeating the intestinal barrier. This occurs in humans in response to a single high-fat meal enriched in butter (Erridge *et al.,* 2007) or cream (Deopurkar *et al.,* 2010), but not after consuming equicaloric amount of orange juice, or water (Deopurkar *et al.,* 2010). Endotoxemia can also be elicited by a 4-week saturated fat-enriched diet in humans (Pendyala *et al.,* 2012). In mice, high-fat feeding increases the proportion of endotoxin-containing bacteria in the gut and plasma concentrations of endotoxin, and induces insulin resistance (Cani *et al.,* 2007). Another study in mice reported that especially saturated but not polyunsaturated fat feeding increases the abundance of gram-negative Bilophila and Bacteroides, and induces endotoxemia and Toll-like receptor activation and inflammation in the adipose tissue (Caesar *et al.,* 2015).

In addition to TLR-4, several other receptors in the innate immune system can recognize bacterial structures, such as nucleotide-binding oligomerization domain-like (NOD)-like receptors (NLRs) (Stienstra *et al.,* 2011).

Gut flora and NAFLD. In a cross-sectional study, Wong *et al.* reported lower abundance of Gram-positive *Ruminococci* in 16 subjects with biopsy-proven NAFLD as compared to 22 control subjects (Wong *et al.,* 2013). Mouzaki *et al.* described decreased abundance of Gram-negative *Bacteroidetes* in 22 subjects with NASH and 11 subjects with NAFL compared to 17 controls (Mouzaki *et al.,* 2013). Zhu *et al.* found that Gram-negative *Bacteroides* and *Proteobacteria* were increased and Gram-positive *Firmicutes* were decreased in 22 children with biopsy-proven NASH compared to 16 controls (Zhu *et al.,* 2013). Munukka *et al.* studied 31 subjects with ^{1}H-MRS, and reported low abundance of Gram-positive, butyrate-producing *Faecalibacterium prausnitzii*, and high abundance of Gram-negative *Enterobacteria* in 21 subjects with high as compared to 10 subjects with low liver fat content (Munukka *et al.,* 2014).

There are no studies examining the effect of overfeeding of diets with different macronutrient composition on the gut microbiota in human NAFLD.

2.2.2. 'Genetic NAFLD'

2.2.2.1. The PNPLA3 I148M variant

In 2008, a single-nucleotide polymorphism (rs738409 [G], encoding I148M) in the patatin-like phospholipase domain-containing 3 (*PNPLA3, adiponutrin*) was discovered in a genome-wide association study to increase liver fat content by more than two-fold (Romeo *et al.,* 2008). The finding has been replicated in a large number of studies (Kotronen *et al.,* 2009; Sookoian S *et al.,* 2009; Sookoian *et al.,* 2011). In addition to steatosis, the variant allele predisposes to NASH (Sookoian *et al.,* 2009; Sookoian *et al.,* 2011), fibrosis (Valenti *et al.,* 2010; Sookoian *et al.,* 2011) and cirrhosis (Shen *et al.,* 2015). The variant allele also increases the risk

of hepatocellular carcinoma (Trépo *et al.,* 2014; Singal *et al.,* 2014). Obesity potentiates these hepatic effects conferred by this gene variant (Stender *et al.,* 2017). In addition to NAFLD, the PNPLA3 I148M variant predisposes to alcoholic liver disease and alcoholic cirrhosis (Tian *et al.,* 2010; Trépo *et al.,* 2011).

Depending on ethnicity, 20-50% of all subjects carry this gene variant (Romeo *et al.,* 2008). In a Finnish population-based study, 39 % carried the variant allele (Hyysalo *et al.,* 2013).

In contrast to the 'Metabolic NAFLD', insulin resistance or dyslipidemia does not characterize NAFLD due to the I148M variant in PNPLA3 ('PNPLA3 NAFLD') (Romeo *et al.,* 2008) (**Figure 1**). According to a recent systematic review with 14 studies, insulin sensitivity as determined by HOMA-IR, the hyperinsulinemic euglycemic clamp method, or fasting or post-glucose insulin or glucose, does not differ between carriers and non-carriers of this variant (Petäjä *et al.,* 2016).

In the majority of studies, serum triglycerides have been reported to be similar in carriers and non-carriers (Petäjä *et al.,* 2016). However, some studies have reported that carriers have lower serum triglycerides as compared to non-carriers (Pirazzi *et al.,* 2012; Del Ben *et al.,* 2014; Di Constanzo *et al.,* 2018; Liu *et al.,* 2017). This decrease in circulating lipids may contribute to the paradoxical reduction in the risk of cardiovascular disease in subjects with 'PNPLA3 NAFLD' (Simons *et al.,* 2017; Liu *et al.,* 2017).

With respect to sources of hepatic fatty acids available for IHTG synthesis, adipose tissue is not insulin-resistant in carriers as compared to non-carriers of the variant (Kotronen *et al.,* 2009). Expression of inflammation-related genes in adipose tissue in carriers and non-carriers of the variant is also unchanged (Lallukka *et al.,* 2013). One study reported decreased hepatic *de novo* lipogenesis, as assessed by a stable isotope technique and indirectly by hepatic SREBP1c gene expression, in carriers of the variant as compared to non-carriers (Mancina *et al.,* 2015). Taken together, neither adipose tissue lipolysis nor hepatic DNL seem to explain the increase in IHTG in 'PNPLA3 NAFLD'.

In humans, *PNPLA3* is mainly expressed in the liver, skin, adipose tissue and retina (Huang *et al.,* 2010; Pirazzi *et al.,* 2014). In the mouse liver, PNPLA3 is expressed predominantly in hepatocytes, and to a much lesser degree in hepatic stellate cells (Huang *et al.,* 2010).

In HuH7 cells, PNPLA3 is localized to the endoplasmic reticulum and lipid droplets (He *et al.,* 2010). Wild-type human PNPLA3 protein was described to hydrolyze triolein time- and dose-dependently, while PNPLA3-I148M virtually abolished this activity (He *et al.,* 2010). Adenovirus-mediated overexpression of human PNPLA3-I148M decreases TG hydrolase activity, and increases accumulation of TGs and CEs in the liver as compared to wild-type PNPLA3 overexpressing C57BL/6J mice. The authors concluded that PNPLA3-I148M promotes TG accumulation by limiting TG hydrolysis (He *et al.,* 2010).

PNPLA3 has also been suggested to function as a lysophosphatidic acid acyltransferase (LPAAT) converting lysophosphatidic acid into phosphatitidic acid with palmitoyl-, oleyl-, linoleyl- and arachidonyl-CoAs as the preferred substrates (Kumari *et al.,* 2012). Purified mouse and human PNPLA3 I148M protein derived by site-directed mutagenesis and overexpressed in E. coli was reported to increase this LPAAT activity by two-fold (Kumari *et al.,* 2012). This finding was not replicated in primary hepatocytes from mice overexpressing

either human wild-type PNPLA3 or PNPLA3-I148M (Li *et al.,* 2012), or in mouse PNPLA3 I148M knock-in mice (BasuRay *et al.,* 2017).

The PNPLA3 gene expression is regulated by liver X receptor and SREBP-1c, and increased by carbohydrate feeding and decreased by fasting in C57BL/6J mice (Huang *et al.,* 2010). PNPLA3 is one of the most insulin-responsive genes in human adipose tissue (Soronen *et al.,* 2012). Post-translationally, saturated fatty acid palmitate (C16:0), monounsaturated fatty acid oleate (C18:1) and polyunsaturated fatty acid linoleate (C18:2) increased PNPLA3 protein expression, while very long chain polyunsaturated fatty acids, such as C20:4, C20:5 had no effect (Huang *et al.,* 2010).

Purified human wild-type PNPLA3 but not PNPLA3-I148M hydrolyzes TGs, DAGs, monoacylglycerols and oleyl-CoA (Huang *et al.,* 2011). Human PNPLA3 hydrolyzes TGs containing C14:0, C16:0, C18:1, C18:2 and C20:4, of which TGs containing C18:1 were the preferred substrates (Huang *et al.,* 2011).

Chow-fed C57BL/6J mice constitutively overexpressing human PNPLA3-I148M in the liver develop hepatic steatosis due to accumulation of TGs and CEs in the liver as compared to mice expressing human wild-type PNPLA3 (Li *et al.,* 2012). The hepatic fatty acid composition was enriched in monounsaturated fatty acids, while the abundance of polyunsaturated fatty acids was decreased in PNPLA3-I148M transgenic as compared to wild-type PNPLA3 transgenic mice. Steatosis was not accompanied by changes in body composition or features of insulin resistance, but was amplified by a high-sucrose diet. There were no changes in TG synthesis in mice overexpressing human wild-type and PNPLA3-I148M as determined by incorporation of labeled glycerol, acetate and oleate into TG, or in the rate of VLDL-TG secretion. However, incorporation of tritium from tritiated water into fatty acids and TGs was increased in PNPLA3-I148M transgenic mice as compared to control mice, while there was no difference between wild-type and PNPLA3-I148M transgenic mice. No differences were found in VLDL-TG secretion rates, or in fatty acid oxidation *in vivo* or in primary hepatocytes of these mouse lines. In contrast, PNPLA3-I148M transgenic mice had significantly increased expression of SREBP-1c target genes associated with lipid synthesis, such as *Acc2, Fas, Scd1, Acly* and *Elovl6* (Li *et al.,* 2012).

Two studies reported that global deletion of *PNPLA3* in mice by gene targeting does not affect body composition, insulin sensitivity, serum lipids or hepatic TG content (Chen *et al.,* 2010; Basantani *et al.,* 2011). Since neither deletion of wild-type murine PNPLA3 nor overexpression of wild-type human PNPLA3 results in hepatic fat accumulation, the effects of the PNPLA3 I148M variant may not be attributable simply to a loss or gain of the activity of the wild type PNPLA3.

C57BL/6J mice with an endogenous I148M mutation in mouse PNPLA3 accumulated hepatic TGs on a high-sucrose but not on a chow diet (Smagris *et al.,* 2015). This was not accompanied by insulin resistance or changes in hepatic mRNA profile or in the fatty acid composition of major lipids (Smagris *et al.,* 2015). There were no differences in fatty acid or TG synthesis as determined from incorporation of tritium from tritiated water into fatty acids and TGs, or from labeled palmitate into TGs in I148M knock-in mice as compared to control mice (BasuRay *et al.,* 2017). There were also no differences in VLDL-TG secretion or fatty acid oxidation rates between the groups (BasuRay *et al.,* 2017). However, the I148M knock-in mice accumulated PNPLA3 protein on hepatic lipid droplets as compared to controls (Smagris *et al.,*

2015). This accumulation of PNPLA3 protein was subsequently proposed to be due to disrupted ubiquitylation and proteosomal degradation (BasuRay *et al.,* 2017). The authors concluded that the I148M variant in PNPLA3 does not cause hepatic steatosis by increasing TG synthesis, or by reducing TG removal through VLDL-TG secretion or fatty acid oxidation, but does so by impairing mobilization of TGs from lipid droplets (LDs) due to accumulation of PNPLA3-I148M protein (BasuRay S *et al.,* 2017).

In addition to hepatocytes, PNPLA3 has been reported to function as a retinyl palmitate hydrolase in hepatic stellate cells and the I148M was shown to impair this activity (Pirazzi *et al.,* 2014), and to promote a fibrogenic phenotype (Bruschi *et al.,* 2017).

One study reported the fatty acid composition of hepatic TGs to be relatively deficient in C18:0, C20:0, C24:0, C20:3, C20:4, C22:4 and C22:5, and relatively enriched in C18:3n3 in 19 carriers (2 homozygous and 17 heterozygous) as compared to 33 non-carriers of the I148M variant allele (Peter *et al.,* 2014).

There are no studies on changes in distinct hepatic TG species with respect to carbons and double bonds, or DAGs or ceramides in 'PNPLA3 NAFLD' and no data comparing NAFLD attributable to the PNPLA3 I148M gene variant to that characterizing NAFLD associated with insulin resistance.

2.2.2.2. The MBOAT7 rs641738 C>T variant

In 2015, a rs641738 C>T mutation in the *membrane bound O-acyltransferase domain containing 7* (*MBOAT7)* gene was discovered to predispose to alcohol-related cirrhosis (Buch *et al.,* 2015). The variant was subsequently reported to increase the risk of NAFLD (Mancina *et al.,* 2016). Depending on the ethnicity, 58-67% of all subjects carry the variant (Mancina *et al.,* 2016).

Among 2,736 subjects studied with ^{1}H-MRS in the Dallas Heart Study, carriers of the MBOAT7 variant had increased IHTG content compared to non-carriers (Mancina *et al.,* 2016). The variant allele carriers also had more severe histological steatosis, necroinflammation and fibrosis in a cohort of 1,149 subjects in the Liver Biopsy Cross-Sectional Cohort (Mancina *et al.,* 2016). In a study including 218 subjects with NAFLD and 227 controls, the MBOAT7 T allele was significantly associated with the presence of NAFLD (Di Costanzo *et al.,* 2018). The association of MBOAT7 rs641738 variant with fibrosis was replicated in a study comprising 320 subjects (Krawczyk *et al.,* 2017). The variant allele was also associated with increased risk of hepatocellular carcinoma (OR 2.0, 1.33-3.31) in a cohort of 913 subjects (Donati *et al.,* 2017). In addition to NAFLD, the variant allele in MBOAT7 confers an increased risk of inflammation and fibrosis in subjects with hepatitis B and C (Thabet *et al.,* 2017; Thabet *et al.,* 2016).

There were no differences in BMI, prevalence of impaired fasting glucose or type 2 diabetes, or of concentrations of total, LDL and HDL cholesterol or TGs in the circulation between the MBOAT7 genotype groups in 4,591 subjects in the Dallas Heart Study, or in the 1,149 subjects in the Liver Biopsy Cross-Sectional Cohort (Mancina *et al.,* 2016). In keeping with these data, in a study including 218 subjects with NAFLD and 227 controls, subjects with NAFLD carrying the variant allele were not characterized by any differences in clinical, anthropometric and biochemical measures as compared to non-carriers (Di Costanzo *et al.,* 2018). The MBOAT7 genotype at rs641738 has not been associated with changes in the risk of

cardiovascular disease (Simons *et al.,* 2017).

In humans, *MBOAT7* is expressed in the liver, ovaries, uterus, brain, lymphocytes, bone marrow and retina (Mancina *et al.,* 2016). In the liver, *MBOAT7* is expressed in hepatocytes, hepatic stellate and sinusoidal epithelial cells (Mancina *et al.,* 2016). Endogenous MBOAT7 locates in the endoplasmic reticulum, mitochondria-associated membrane and lipid droplets in the human liver. Carriers of the variant have lower expression of both the gene and the MBOAT7 protein in the liver as compared to non-carriers (Mancina *et al.,* 2016).

In mice, MBOAT7 functions as a lysophosphatidylinositol acyltransferase, catalyzing the fatty acyl-chain remodeling of polyunsaturated phosphatidylinositols (PIs) (Anderson *et al.,* 2013). In *Caenorhabditis elegans*, MBOAT7 was identified to be required for incorporation of especially PUFAs, such as arachidonic acid (C20:4) and eicosapentaenoic acid (C20:5n3) into lysophosphatidylinositols to form PIs (Lee *et al.,* 2008). MBOAT7 was also found to function as a lysophosphatidylinositol acyltransferase with substrate specificity towards arachidonyl-CoA in human neutrophils, where it regulates the availability of free arachidonic acid for the synthesis of eicosanoids and thereby the inflammatory response (Gijón *et al.,* 2008). Consistent with the proposed function in the fatty acyl-chain remodeling of PIs, the plasma concentration of PI species 32:1, 34:1, 34:2, 36:1, 36:2 and 36:3 were increased, while those of 36:4, 38:3, 38:5, 38:6, 40:4 and 40:5 were decreased in carriers as compared to non-carriers of the MBOAT7 variant (Mancina *et al.,* 2016).

There are no studies comparing the lipid composition of the human liver between carriers and non-carriers of the MBOAT7 variant.

2.2.2.3. The TM6SF2 E167K variant

In 2014, a variant in transmembrane 6 superfamily member 2 (TM6SF2) at rs58542926 ([T], encoding E167K) was reported to increase liver fat content (Kozlitina *et al.,* 2014). Approximately 10-17% of all subjects carry the variant allele (Kozlitina *et al.,* 2014).

In addition to steatosis, the variant increased the risk of steatohepatitis and fibrosis in 349 NAFLD patients (Liu *et al.,* 2014) and 983 bariatric surgery patients (O'Hare *et al.,* 2017). Adiposity potentiates the effects of this gene variant on hepatic outcomes (Stender *et al.,* 2017). The variant allele was shown to independently predict the development of fatty liver in a 21-year follow-up study of 2,042 children (Suomela *et al.,* 2016). In addition to NAFLD, the TM6SF2 variant allele increases the risk of alcohol-related cirrhosis (Buch S *et al.,* 2015), the risk of hepatocellular carcinoma in alcoholic cirrhosis (Falleti *et al.,* 2016), and the risk of steatosis, fibrosis and cirrhosis in hepatitis C (Liu *et al.,* 2017).

In several studies, carriers of the variant have neither been more obese nor insulin-resistant compared to non-carriers (Kozlitina *et al.,* 2014; Zhou *et al.,* 2015; Sookoian *et al.,* 2015; Goffredo *et al.,* 2016; Grandone *et al.,* 2016; Eslam *et al.,* 2016; Mancina *et al.,* 2016b; Musso *et al.,* 2016; Dongiovanni *et al.,* 2015; Kim *et al.,* 2017; Petäjä *et al.,* 2016).

Hepatic and adipose tissue insulin sensitivities, as assessed by the euglycemic hyperinsulinemic clamp technique combined with a glucose tracer, are unchanged in carriers as compared to non-carriers of the variant in 111 subjects (Zhou *et al.,* 2015).

In studies with less than 400 subjects, fasting serum TG concentrations have been reported to be unchanged between carriers and non-carriers of the variant

(Zhou *et al.,* 2015; Sookoian *et al.,* 2015; Musso *et al.,* 2016; Goffredo *et al.,* 2016). In contrast, in studies with more than 400 and up to 300,000 subjects, carriers of the variant have consistently had lower circulating TG concentrations in the fasting state than non-carriers (Kozlitina *et al.,* 2014; Grandone *et al.,* 2016; Eslam *et al.,* 2016; Mancina *et al.,* 2016; Dongiovanni *et al.,* 2015; Kim *et al.,* 2017; O'Hare *et al.,* 2017; Liu *et al.,* 2017; Di Costanzo *et al.,* 2018).

Lower concentrations of circulating TGs in carriers as compared to non-carriers have also been reported under postprandial conditions (Musso *et al.,* 2016; O'Hare *et al.,* 2017). Humans carrying the TM6SF2 E167K variant have reduced concentrations of large, triglyceride-rich $VLDL_1$ particles in the postprandial state (Musso *et al.,* 2016). In 6,929 Finnish men, the T allele was associated with lower circulating apolipoprotein B-100, VLDL and LDL particles, lower total, VLDL and LDL triglyceride concentrations, and lower total, VLDL and LDL cholesterol concentrations (Kim *et al.,* 2017). The T allele was not associated with body mass index or insulin sensitivity as determined by Matsuda index (Kim *et al.,* 2017).

Consistent with the reduced circulating TG concentrations, carriers of the E167K variant have a reduced risk of cardiovascular disease (Dongiovanni *et al.,* 2015; Holmen *et al.,* 2014; Simons *et al.,* 2017; Liu *et al.,* 2017).

In humans, *TM6SF2* mRNA is expressed in the liver and the intestine (Mahdessian *et al.,* 2014; O'Hare *et al.,* 2017). In HuH7 and HepG2 human hepatoma cells, TM6SF2 is located in the endoplasmic reticulum (Mahdessian *et al.,* 2014). In primary hepatocytes of C57BL/6N mice, TM6SF2 is located in the endoplasmic reticulum, *cis*/medial Golgi, and Golgi matrix (Smagris *et al.,* 2016).

Carriers of the E167K variant have lower *TM6SF2* mRNA concentrations in the liver than non-carriers (Mahdessian *et al.,* 2014). In hepatocytes, the TM6SF2 E167K variant allele decreases TM6SF2 protein expression (Kozlitina *et al.,* 2014). It was suggested that in Huh7 cells stably expressing E167K, reduced protein stability might contribute to decreased protein expression (Ehrhardt *et al.,* 2017).

Silencing of TM6SF2 by small interfering RNA in HuH7 and HepG2 cells increases cellular TG content and decreases TG secretion, while overexpression of TM6SF2 has the opposite effect (Mahdessian *et al.,* 2014). In C57BL/6J mice, knockdown of *TM6SF2* in the liver by adeno-associated virus-mediated small hairpin RNA induced hepatic steatosis due to accumulation of hepatic TGs and cholesterol esters (CEs), the main components of the hydrophobic core of very low-density lipoprotein particles (Kozlitina *et al.,* 2014).

Mice with chronic inactivation of Tm6sf2 develop hepatic steatosis due to a 3-fold decrease in VLDL-TG secretion, resulting in increased TG and cholesteryl ester concentrations in the liver (Smagris *et al.,* 2016). This decrease in VLDL-TG secretion was not due to reduced apolipoprotein B-100 secretion, but rather due to reduced TG content per particle. The VLDL particles in knockout mice were significantly smaller than in wild-type mice. The livers in these mice were deficient in lipid species with polyunsaturated fatty acyl chains, such as 20:4 and 22:6 (Smagris *et al.,* 2016). These mice were also characterized by modestly decreased TG and cholesterol absorption, and TG accumulation in the intestine after a high-fat diet (Smagris *et al.,* 2016).

There are no data on the lipid composition of the human liver between carriers and non-varriers of the TM6SF2 E167K variant allele.

2.3. NUTRITIONAL MODULATION OF NAFLD

2.3.1. Energy intake

Excess energy intake is the most important nutritional determinant of hepatic fat accumulation (Yki-Järvinen, 2015). Overfeeding human subjects increases IHTG content (Kechagias *et al.,* 2008; van der Meer *et al.,* 2008; Bortolotti *et al.,* 2009; Sobrecases *et al.,* 2010; Sevastianova *et al.,* 2012; Rosqvist *et al.,* 2014; Fabbrini *et al.,* 2016).

Overfeeding 1000 extra kilocalories per day of a diet with similar macronutrient composition as their habitual diet in 27 obese subjects lead to an increase in body weight by ~6%, and an increase in IHTG from 4.8 to 7.1% (^{1}H-MRS) (Fabbrini *et al.,* 2016). The mechanisms underlying the increase in IHTG was attributed to an increase in DNL and a decrease in hepatic fatty acid oxidation as determined by beta-hydroxybutyrate turnover (Fabbrini *et al.,* 2016).

Hypocaloric diets have been consistently shown to reduce liver fat content (Petersen *et al.,* 2005; Tamura *et al.,* 2005; Larson-Meyer *et al.,* 2006; Shah *et al.,* 2009; Sevastianova *et al.,* 2011; Browning *et al.,* 2011; Haufe *et al.,* 2011). This is why weight loss is recommended to all overweight and obese subjects with NAFLD (European Association for the Study of the Liver (EASL) *et al.,* 2016).

2.3.2. Macronutrient composition of the diet

Hypocaloric studies. Hypocaloric diets decrease liver fat content very rapidly as compared to the decrease in body weight. For example, two to six days of daily energy deficiency of 1000 kilocalories results in 30-45% loss in liver fat content in the face of small weight loss (Kirk *et al.,* 2009; Sevastianova *et al.,* 2011). Ketogenic low-carbohydrate diets decreased liver fat content more than standard hypocaloric diets in the face of similar caloric deficiency in two (Kirk *et al.,* 2009; Browning *et al.,* 2011) but not in one study (Haufe *et al.,* 2011).

A hypocaloric diet lowers plasma glucose and insulin concentrations and increases the basal rate of adipose tissue lipolysis (Sevastianova *et al.,* 2011). Despite increased lipolysis, liver fat content decreases on a hypocaloric diet, since free fatty acids are channeled towards oxidation and ketogenesis rather than triglyceride synthesis (Sevastianova *et al.,* 2011). Since glucose and insulin also upregulate *de novo* lipogenesis, the lower plasma insulin concentrations during the hypocaloric diet would also be expected to result in reduced rates of DNL (Topping *et al.,* 1982; Hellerstein *et al.,* 1996). This indeed happens during a 5-day hypocaloric low-carbohydrate diet (Schwartz *et al.,* 1995).

Isocaloric studies. Cross-sectionally, intake of saturated fat correlates with liver fat content (Tiikkainen *et al.,* 2003). Similarly, higher intakes of saturated fatty acids and cholesterol and lower intakes of fiber, protein and polyunsaturated fatty acids characterize subjects with NASH as compared to age-, gender-, and body mass index-matched controls (Musso *et al.,* 2003). In another cross-sectional study, increased intakes of simple sugars from soft drinks and protein from meat, and decreased intakes of fish rich in omega-3 polyunsaturated fatty acids were associated with increased risk of NAFLD (Zelber-Sagi *et al.,* 2007).

Isocaloric studies comparing high-fat, low-carbohydrate as compared to low-fat, high-carbohydrate diets lasting for two (Westerbacka *et al.,* 2005), three (van Herpen *et al.,* 2011) and four (Utzschneider *et al.,* 2013) weeks in humans have consistently shown the former to increase IHTG content compared to the latter.

Regarding the quality of fat, in an isocaloric study comparing high-saturated fat/low polyunsaturated fat diet to low-saturated fat/high-polyunsaturated fat, the former increased liver fat content as compared to the latter (Bjermo *et al.,* 2012).

Hypercaloric studies. In a 7-week overfeeding study comparing a diet enriched with saturated fat to a diet enriched with polyunsaturated fat, only a diet enriched in saturated fat but not that enriched with polyunsaturated fat increased liver fat content in the face of similar energy excess (Rosqvist *et al.,* 2014). In another overfeeding study, 7 days of overfeeding of fat (30% energy excess) increased liver fat content by 86%, overfeeding of fructose (35% energy excess) by 16%, and overfeeding of both fat and fructose (65% energy excess) increased liver fat content by 116% but these differences were not statistically significant (Sobrecases *et al.,* 2010).

Regarding the causes underlying increased deposition of FAs into IHTG during overfeeding, pathways leading to IHTG need to be considered. DNL has been shown to increase and lead to liver fat accumulation in response to excess sugar intake (Sevastianova *et al.,* 2012). However, there are no studies comparing effects of overfeeding saturated or unsaturated fat or sugars on lipolysis in humans. In addition, no studies have compared effects of such diets on DNL.

3. AIMS OF THE STUDY

The aims of this series of studies were:

i. to determine whether the human liver lipidome (triglycerides, free fatty acids and insulin resistance-inducing lipids such as ceramides and diacylglycerols) differs between 'Metabolic NAFLD' and 'PNPLA3 NAFLD' (*study I*);

ii. to determine which, if any, pathway of ceramide metabolism is altered in 'Metabolic NAFLD' (*study I*);

iii. to determine whether the human liver lipidome (phosphatidylinositols) is altered in 'MBOAT7 NAFLD' (*study II*);

iv. to determine whether the human liver and serum lipidome (phosphatidylcholines, triglycerides and cholesteryl esters) and hepatic gene expression are altered in 'TM6SF2 NAFLD' (*study III*);

v. to determine whether the incorporation of different fatty acids into complex lipids is altered in *TM6SF2* knockdown cells (*study III*); and

vi. to determine in healthy overweight humans whether three weeks of overfeeding diets enriched either in saturated or unsaturated fat or simple sugars differentially influences IHTG content, rates of adipose tissue lipolysis and hepatic *de novo* lipogenesis, adipose tissue transcriptome, insulin resistance, plasma lipidome, gut microbiota and markers of endotoxemia (*study IV*).

4. SUBJECTS AND METHODS

4.1. SUBJECTS AND STUDY DESIGNS

The ethics committee of the Hospital District of Helsinki and Uusimaa approved the study protocols of all studies. All studies were conducted in accordance with the Declaration of Helsinki. Each participant provided written informed consent after being explained the nature and potential risks of the study.

4.1.1. Studies I-III

In studies I-III (the 'Liver Biopsy Cohort'), the subjects were recruited amongst those undergoing laparoscopic bariatric surgery. The inclusion criteria were: a) age 18 to 75 years; b) no known acute or chronic disease except for obesity or type 2 diabetes or hypertension on the basis of medical history, physical examination and standard laboratory tests (*vide infra*); c) alcohol consumption less than 20 g/day for women and less than 30 g/day for men; d) no evidence of pre-existing liver conditions other than NAFLD such as autoimmune, drug-induced or viral liver disease. Subjects with diabetes were excluded from the study III.

One week before surgery, all subjects arrived for a clinical visit after an overnight fast for metabolic characterization. Body weight, height and waist circumference were measured. An intravenous cannula was inserted in an antecubital vein for withdrawal of blood for measurement of HbA_{1c}, serum insulin and adiponectin, plasma glucose, LDL- and HDL-cholesterol, triglyceride, albumin, AST, ALT, ALP and GGT concentrations and for genotyping of PNPLA3 rs738409, MBOAT7 rs641738 and TM6SF2 rs58542926. After basal blood sampling and anthropometric measurements, an oral glucose (75 grams) tolerance test (OGTT) was performed (DeFronzo *et al.,* 2010). During the day of surgery, wedge biopsies were obtained at the beginning of surgery. One part was flash-frozen in liquid nitrogen and another part was sent to pathologist for histological assessment.

In study I, the subjects (N=125) were divided into two groups based on HOMA-IR, a surrogate of insulin resistance. Because of a lack of universally accepted consensus regarding the cut-off threshold of HOMA-IR between the insulin-resistant and sensitive subjects, median HOMA-IR was used to divide the subjects into 'High HOMA-IR' (HOMA-IR > 3.19) and 'Low HOMA-IR' (HOMA-IR ≤ 3.19) groups. The same subjects were divided into two groups based on their PNPLA3 rs738409 genotype (I148M variant carriers, '$PNPLA3^{148MM/MI}$'; and non-carriers, '$PNPLA3^{148II}$'. In study II, the subjects (N=115) were divided into three groups based on their *MBOAT7* genotype at rs641738 (CC, CT and TT). In study III, the subjects (N=90) were divided into groups based on their TM6SF2 rs58542926 genotype (E167K variant allele carriers, $TM6SF2^{EK/KK}$; and non-carriers, $TM6SF2^{EE}$).

4.1.4. Study IV

In study IV, the subjects (N=38) were recruited by newspaper advertisements or by contacting subjects who had previously participated in metabolic studies. The exclusion criteria were: a) type 1 or 2 diabetes; b) pre-existing autoimmune, viral or drug-induced liver disease; c) alcohol consumption over 20 g/day for women and over 30 g/day for men; d) evidence of any other acute or chronic disease; e) extreme obesity (BMI ≥ 40 kg/m^2); f) use of drugs influencing glucose or lipid metabolism; g) pregnancy or lactation.

One day before the metabolic study visit, a blood sample was taken for measurement of background enrichment of ^2H in plasma water and palmitate in VLDL-TG for measurement of *de novo* lipogenesis. Subjects consumed deuterated water (^2H_2O) (3 g/kg body water) in the evening prior to the metabolic study visit, to achieve a plasma water enrichment of 0.3% for the measurement of DNL. IHTG was measured by proton magnetic resonance spectroscopy (^1H-MRS). Subjects collected fecal samples which were stored immediately at −20°C, and within 24 h at -80°C until analysis.

The subjects arrived at the clinical research unit after an overnight fast on the following morning. Body composition (InBody 720, Biospace, Seoul, Korea), weight, height and waist circumference were measured. After indirect calorimetry measurements, an intravenous cannula was inserted in an antecubital vein for withdrawal of blood for measurement of DNL and for liver function tests, fasting glucose, FFA, insulin, total, HDL and LDL cholesterol and TG concentrations. A needle aspiration biopsy from abdominal subcutaneous adipose tissue was obtained. After the basal sampling, a euglycemic-hyperinsulinemic clamp combined with infusion of [$^2H_5$]glycerol for measurement of lipolysis was performed.

The subjects were randomized to one of three dietary intervention groups to consume a 3-week hypercaloric (1000 excess kcal/day) diet enriched either in saturated fat (SAT, 76% from saturated fatty acids, 21% from monounsaturated fatty acids and 3% from polyunsaturated fatty acids), unsaturated fat (UNSAT, 57% from monounsaturated fatty acids, 22% from polyunsaturated fatty acids, 21% from saturated fatty acids), or simple sugars (CARB, 100% simple sugars). The extra energy was provided to participants as foodstuffs, which consisted in the SAT group of 30 g coconut oil, 40 g butter and 100 g of 40% fat-containing blue cheese; in the UNSAT group of 36 g olive oil, 26 g pesto, 54 g pecan nuts and 20 g of butter; and in the CARB group of 2.8 dl orange juice, 4.3 dl of a sugar-sweetened beverage, and 200 g of candy. Of the extra energy, 2%, 91% and 7% came from carbohydrate, fat and protein in the UNSAT group, and 1%, 86% and 13% from these sources in the SAT group, respectively and 100% from simple sugars in the CARB group. Baseline measurements were repeated after 3 weeks of consuming the hypercaloric diets.

Adherence was reinforced by the study dietician, who contacted the subjects on a weekly basis. The subjects filled 3-day dietary records before and after 3 weeks on the diet. The food records were analyzed using the AivoDiet software (version 2.0.2.3, Aivo Finland, Turku, Finland). As an objective biomarker of recent dietary intake, the FA composition of fasting VLDL-TG was measured (Hodson *et al.,* 2008).

4.2. METHODS

4.2.1. Liver fat content (I-IV)

Biopsies. During the day of surgery, wedge biopsies from the liver were obtained at the beginning of surgery. One part was flash-frozen in liquid nitrogen for subsequent analysis of hepatic lipidome, and another part was sent to pathologist for histological assessment. The time from obtaining the biopsy to flash-freezing of the sample in liquid nitrogen was approximately one minute. An experienced liver pathologist (J.A.) performed the histological assessment of the liver biopsy in a blinded fashion according to the criteria by Brunt *et al.* (Brunt *et al.,* 1999). Liver fat content in liver biopsies was quantified as the percentage of hepatocytes with macrovesicular steatosis.

MRS. Liver fat content was determined by ^{1}H-MRS using 1.5T Siemens Avanto^{fit} (Siemens Healthcare Diagnostics, Erlangen, Germany). MR spectra were acquired using a point resolved spectroscopy sequence with TE (echo time) of 30 ms and 16 acquisitions. Prior to MRS measurements, transaxial and coronal T2-weighted localization images were collected. A 25x25x25 mm^3 voxel was carefully positioned in the right lobe of the liver avoiding large vessels, bile ducts, and gall bladder. Respiratory motion was triggered using a navigator belt keeping TR (repetition time) > 3000 ms. All spectra were analyzed with the jMRUI v5.2 software using AMARES algorithm (Stefan *et al.,* 2009; Vanhamme *et al.,* 1997). Resonances of methylene groups in the fatty acid chains and water were determined using line-shape fitting with prior knowledge. Signal intensities were corrected for T2 relaxation using the equation $I_m = I_0 \exp(-TE/T2)$. T2 values of 46 ms and 58 ms were used for water and fat, respectively. Liver fat content was expressed as a ratio of signal from methylene group to total signal of methylene and water. Liver fat content was converted from signal ratio to a weight fraction, applying method validated by Longo *et al.* (Longo *et al.,* 1995) and Szczepaniak *et al.* (Szczepaniak *et al.,* 2005). The following experimentally determined factors were used: (1) the ratio of the number of lipid protons in the fitted $(CH2)_{n-2}$ signal to the total number of lipid protons is 0.6332 (Szczepaniak *et al.,* 1999); (2) proton densities of fat and water are 110 and 111 mol/l, respectively; (3) 1 g liver tissue contains 711 mg water; (4) densities of the liver tissue, fat in the liver, and water are 1.051 g/ml, 0.900 g/ml, and 1.000 g/ml; respectively. This measurement has been validated against histologically determined lipid content and against estimates of fatty infiltration by computed tomography (Ryysy *et al.,* 2000). The coefficient of variation of repeated measurements of liver fat in non-diabetic subjects as determined on two separate occasions in our laboratory was 11%.

4.2.2. Lipidomics (I-IV)

Hepatic lipidomics analyses using UHPLC-MS (I-III). Liver tissue (approx. 5 mg) was homogenized when frozen (Covaris, CryoPrep CP02, MA), and weighted. An aliquot (20 µL) of an internal standard mixture containing PC(17:0/0:0), PC(17:0/17:0), PE(17:0/17:0), phosphatidylglycerol(17:0/17:0)[rac], Ceramide(d18:1/17:0), PS(17:0/17:0), phosphatidic acid(17:0/17:0) (Avanti Polar Lipids, Alabaster, AL), monoacylglycerol(17:0/0:0/0:0)[rac], DAG(17:0/17:0/0:0)[rac] and TAG(17:0/17:0/17:0) were added. The lipids were extracted using a mixture of HPLC-grade chloroform and methanol (2:1; 400 µL). 50 µl of 0.9% sodium chloride was added and the lower phase (200 µL) was collected and 20 µL of an internal standard mixture containing labeled PC(16:1/0:0-D_3), PC(16:1/16:1-D_6) and TAG(16:0/16:0/16:0-$^{13}C3$) was added. The extracts were run on a Waters Q-TOF Premier mass spectrometer combined with an Acquity Ultra Performance LC™.

The column (at 50 °C) was an Acquity UPLC™ BEH C18 2.1 × 100 mm with 1.7 µm particles. The solvent system included A. ultrapure water (1% 1 M NH_4Ac, 0.1% HCOOH) and B. LC/MS grade acetonitrile/isopropanol (1:1, 1% 1M NH_4Ac, 0.1% HCOOH). The gradient started from 65% A / 35% B, reached 80% B in 2 min, 100% B in 7 min and remained there for 7 min. The flow rate was 0.400 ml/min and the injected amount was 2.0 µl (Acquity Sample Organizer, at 10 °C). Reserpine was used as the lock spray reference compound. The lipid profiling was carried out using electrospray ionization mode and the data

were collected at a mass range of m/z 300-1200 with a scan duration of 0.2 sec.

The data processing included alignment of peaks, peak integration, normalization and identification. The lipid identification was based on an internal library which had been constructed based on accurate mass measurements in combination with tandem mass measurements. For specific lipids, the composition of fatty acid chains had been determined with separate measurements, and for those the fatty acid composition was specified, e.g. TAG(14:0/16:0/18:0). The data were normalized using one or more internal standards representative of each class of lipid present in the samples: the intensity of each identified lipid was normalized by dividing it with the intensity of its corresponding standard and multiplying it by the concentration of the standard.

All monoacyl lipids except cholesterol esters, such as monoacylglycerols and monoacylglycerophospholipids, were normalized with PC(17:0/0:0), all diacyl lipids except ethanolamine phospholipids were normalized with PC(17:0/17:0), all ceramides with Cer(d18:1/17:0), all diacyl ethanolamine phospholipids with PE(17:0/17:0), and TAG and cholesterol esters with TAG(17:0/17:0/17:0). Other (unidentified) molecular species were normalized with PC(17:0/0:0) for retention times < 300 s, PC(17:0/17:0) for a retention time between 300 s and 410 s, and TAG(17:0/17:0/17:0) for longer retention times.

Quality control of the method showed that the day-to-day repeatability of control serum samples, and the relative standard deviation for identified lipids was on average 14.1% in electrospray ionization positive mode and 9.5% in electrospray ionization negative mode. The internal standards added to all samples in the study had an average relative standard deviation of 10.8% in electrospray ionization positive mode and 8.0% in electrospray ionization negative mode.

Hepatic lipidomics analyses using GC-MS (I-III). Liver tissue was homogenized when frozen (Covaris, CryoPrep CP02, MA) and weighted (ca. 10 mg). The homogenate was spiked with 10 µl of internal standard mixture (DL-Valine at 37 mg/l, heptadecanoic acid at 186.5 mg/l, succinic acid-d4 at 62.9 mg/l and DL-Glutanic acid-d5 at 103.5 mg/l) and the samples were extracted with 400 µl MeOH/H2O 1:1 (v/v). The supernatant was collected and evaporated to dryness under gentle flow of nitrogen. The fatty acids were then converted into their methoxime and trimethylsilyl derivatives by a two-step derivatization. First, 25 µL of methoxamine reagent was added to the residue, and the mixture was incubated for 60 min at 45 °C. Next, 25 µL of N-methyl-N-trimethylsilyltrifluoroacetamide was added, and the mixture was incubated for 60 min at 45 °C. Finally, a retention index standard mixture (n-alkanes) and an injection standard (4,4'-dibromooctafluorobiphenyl), both in hexane, were added to the mixture.

Two-dimensional gas chromatography-time-of-flight mass spectrometry (GC×GC–TOFMS) experiments were performed on an Agilent 6890 gas chromatograph equipped with a split/splitless injector (Agilent Technologies, Santa Clara, CA), cryogenic dual-stage modulator and time-of-flight mass spectrometer (Leco Corp., St. Joseph, MI, USA). A multipurpose sampler with Maestro software (Gerstel, Mülheim an der Ruhr, Germany) was used for derivatization and sample introduction. A 10 m × 0.18 mm I.D. Rxi-5ms (Restek Corp., Bellefonte, PA, USA) column with film thickness 0.18 µm was used as the first column and a 1.5 m × 0.1 mm I.D. BPX-50 (SGE Analytical Science, Austin, TX, USA) column with film thickness of 0.1 µm as the second column.

A phenyl methyl deactivated retention gap column (1.5 m × 0.53 mm I.D.) was installed in front of the first column. The injector was used in the splitless mode at 240 °C for injecting 1 µl of a sample. The splitless period was 90 s. High-purity helium (Aga, Espoo, Finland) was used as the carrier gas in a constant-pressure mode with initial pressure of 276 kPa. The first column oven temperature program was as follows: 50 °C (isothermal for 2 min) then 7 °C/min to 240 °C, and, finally, 25 °/min to 300 °C (3 min). The second dimension column oven temperature was maintained 20 °C higher and the programming rate and hold times were similar than in the first dimension. The temperature of the transfer line was maintained at 260 °C and ion source at 200 °C. Modulation time was 4 s. Electron impact ionization was applied at 70 eV, and the mass range from 45 to 700 amu with 100 spectra/s were measured.

Automatic peak detection and mass spectrum deconvolution were carried out using a peak width set to 0.2 s. Peaks with signal-to-noise values lower than 100 were rejected. The signal-to-noise values were based on the masses chosen by the software for quantification. ChromaTOF version 4.32 was used for the raw data processing. The peak areas from total ion chromatography were used for most of the compounds; for compounds that were quantified with the ChromaTOF software, peak areas of selected characteristic m/z were used. Next, the data files obtained by the ChromaTOF software were exported to text files and in-house developed software Guineu16 was used for aligning and normalization of compounds in different data sets for further analyses. The original GC×GC–TOFMS data includes retention times, retention indices (I), spectral information for possible identification, spectral similarity value (S=0-999), and peak response data. The linear retention indices were calculated based on the total (=sum of the first and the second dimension) retention times of the compounds and the retention times of the retention index standards (n-alkanes). The second dimension retention time is so short (1-3.5 s) that its contribution to the retention index is not significant. The alignment of the data was performed based on retention indices, second dimension retention times and spectra. After alignment of the GC×GC–TOFMS data, two filtration criteria was utilised for positive identification: spectral similarity > 850 and maximum allowed difference in retention index between experimental and literature values < 25. The literature values were obtained from NIST 2008 Mass Spectral Library or they were determined experimentally with GC×GC-TOFMS instrument in our laboratory with authentic standards (in-house determined library). Golm metabolome database was used for further identification of the metabolites.

Quantitation was based on external calibration of each specific fatty acid, normalised by the internal standard. Quality control of the method showed that the day-to-day repeatability of control serum samples, and the relative standard deviation for fatty acids was on average 10.3%. The internal standards added to all samples in the study had an average relative standard deviation of 12.3%.

Serum/plasma lipidomics using UHPLC-MS (III and IV). The plasma samples were analysed for global profiling of lipids using an ultra-high-performance liquid chromatography quadrupole time-of-flight mass spectrometry method (UHPLC-Q-TOF-MS) developed for lipidomics purposes. The samples were prepared following the Folch procedure (Folch *et al.,* 1957) with minor modifications. PE(17:0/17:0), SM(d18:1/17:0), Cer(d18:1/17:0), PC(17:0/17:0), LP(17:0), PC(16:0/d31/18:1), PC(14:0/d13),

TG(16:0/16:0/16:0)-$^{13}C_3$ and TG(8:0/8:0/8:0)-$^{13}C_3$ were used as internal standards. The calibration curve (using PC(16:0e/18:1(9Z)), PC(18:0p/18:1(9Z)), LPC(18:0), PC(18:0p/22:6), PI(18:0/20:4), DG(18:0/20:4), LPC(16:0), TG(17:017:0/17:0) and CE(18:2)) was prepared to the following concentration levels: 100, 500, 1000, 1500, 2000, 2500, 3000, 3500, 4000, 4500 and 5000 ng/ml including 250 ng/ml of each quality control standard. All samples were randomized before sample preparation and again before the analysis.

10 µL of 0.9% NaCl, 40 µl of $CHCl_3$: MeOH (2:1, v/v) and 80 µL of the 3.5 µg/ml working standards solution were added to 10 µl of each plasma sample. The samples were vortex mixed and allowed to stand on ice for 30 min after which they were centrifuged (9400 × g, 3 min, 4 °C). 60 µL from the lower layer of each sample was then transferred to a glass vial with an insert and 60 µL of $CHCl_3$:MeOH (2:1, v/v) was added. The samples were then stored at -80 °C until analysis.

The UHPLC system used in this study was 1290 Infinity system from Agilent Technologies. The system was equipped with a multisampler using 10% DCM in MeOH and ACN:MeOH:IPA:H_2O (1:1:1:1, v/v/v/v) + 0.1% HCOOH as needle wash solutions after each injection for 7.5 s each, a quaternary solvent manager and a column thermostat (maintained at 50 °C). Separations were performed in a ACQUITY UPLC® BEH C18 column (2.1 mm × 100 mm, particle size 1.7 µm) by Waters (Milford, USA). The flow rate was 0.4 mL/min and the injection volume was 1 µL. H_2O + 1% NH_4Ac (1M) + 0.1% HCOOH (A) and ACN:IPA (1:1, v/v) + 1% NH_4Ac + 0.1% HCOOH (B) were used as the mobile phases for the gradient elution. The gradient was as follows: from 0 to 2 min 35-80% B, from 2 to 7 min 80-100% B and from 7 to 14 min 100% B. Each run was followed by a 7 min re-equilibration period under initial conditions (35% B).

A 6550 iFunnel quadrupole time of flight (Q-TOF) mass spectrometer from Agilent Technologies (Agilent) interfaced with a dual jet stream electrospray ion source. Nitrogen generated by a nitrogen generator (PEAK Scientific, Scotland, UK) was used as the nebulizing gas at a pressure of 21 psi, as the drying gas at a flow rate of 14 L/min (at 193 °C) and as the sheath gas at a flow rate of 11 L/min (at 379 °C). Pure nitrogen from Praxair (Fredericia, Denmark) was used as the collision gas. The capillary voltage and the nozzle voltage were kept at 3643 V and 1500 V, respectively. The reference mass solution including ions at m/z 121.0509 and 922.0098 was prepared according to instructions by Agilent and was introduced to the mass spectrometer through the other nebulizer in the dual electrospray ionization ion source using a separate Agilent series 1290 isocratic pump at a constant flow rate of 4 mL/min (split to 1:100 before the nebulizer). The acquisition mass range was m/z 100-1700 and the instrument was run using the extended dynamic range with an approximate resolution of 30,000 FWHM (full width at half maximum) measured on the ion at m/z 1521.9715 (which is included in the tune mixture) during calibration of the instrument. MassHunters B.06.01 (Agilent) was used for all data acquisition. MS data processing was performed using MZmine 2.17.

VLDL-TG fatty acid composition (IV). To determine the fatty acid composition of VLDL-TG, VLDL was isolated by ultracentrifugation (Havel *et al.,* 1955). VLDL total lipids were extracted according to the method of Folch et al (Folch *et al.,* 1957) and fatty acid methyl esters (FAMEs) prepared from triglyceride as previously described (Heath *et al.,* 2003). Separation and

quantification (expressed as mol%) of FAMEs was performed on a HP6890 GC (Agilent Technologies, Stockport, UK) with flame ionisation detection.

4.2.3. Hepatic gene expression (III)

Hepatic gene expression analyses were carried out using RNA sequencing. Of the original cohort of Study III, liver samples were available from 69 subjects and an additional 25 subjects were recruited using the same criteria as the original cohort.

For RNA sequencing, samples were prepared using Illumina's TruSeq RNA Sample preparation kit and sequencing was performed using a paired-end 101 bp protocol on HiSeq2000 platform (Illumina, San Diego, CA). STAR (v2.4.1a) (Dobin *et al.,* 2013) was used to align output reads to human reference genome (GRCh38). FeatureCounts program (Liao *et al.,* 2014) was used to count uniquely mapped fragment against genomic features defined by the genecode annotation file (gencode.v22.annotation.gtf). The read counts were adjusted for aligned library, size counts per million and $\log_2$ adjusted. In the analysis, we used autosomal genes present in >= 80% samples with an average expression >= 1 counts per million.

To evaluate whether genes significantly correlated with *TM6SF2* are enriched in specific biological pathways, over-representation tests were performed of this set of genes against 737 Reactome (Fabregat *et al.,* 2014; Milacic *et al.,* 2012) database pathways downloaded from https://data.broadinstitute.org/mpg/depict/documentation.html (October 4, 2016). Those 1485 genes (out of 13,644 tested autosomal genes) for which the P-value for Pearson correlation passed the 1% false discovery rate threshold (i.e. q-value < 0.01, q-values were calculated using the qvalue R package) were focused on. P-values for over-representation of this gene set in the tested Reactome pathways were calculated using hypergeometric test in R. To account for possible biases in the over-representation analysis, we performed permutations to further test the significance of the enrichment of our gene set in the Reactome pathways. Specifically, we sampled 1000 random sets of genes of the size of the original significantly correlated gene set from the full set of 13,644 genes and tested the enrichment of these gene sets in the pathways as above. Finally, we computed a permuted P-value for each pathway by taking the proportion permutations, which gave a more extreme P-value than the original gene set in the over-representation test. We conservatively considered only pathways where permuted P-value was below 0.001, i.e. none of 1000 permutations gave a P-value as significant as the original gene set, significantly enriched.

4.2.4. Adipose tissue gene expression (IV)

In study IV, needle aspiration biopsies from abdominal subcutaneous adipose tissue were obtained under 1% lidocaine anesthesia and immediately frozen in liquid nitrogen and stored at −80°C until analysis. Total RNA was isolated using the RNeasy Lipid Tissue Mini Kit (Qiagen, Valencia, CA).

Bioinformatics. The Illumina HumanHT12v4 microarray chips (Illumina, San Diego, CA) were annotated using the IlluminaHumanv4.db from Bioconductor. A standard non-specific filtering approach was used to extract genes most likely to be expressed in the tissue and to ultimately limit the number of tests to genes of interest. Specifically, probes without annotation to a gene were removed, and if multiple probes matched to a gene, only the probe with the highest interquartile range across samples was

included. Only genes with inter-quartile range greater than the median of all genes were included. Kyoto Encyclopedia of Genes and Genomes (KEGG) pathways were downloaded from the Molecular Signatures Database (http://software.broadinstitute.org/gsea/msigdb/collections.jsp#C2). To limit the number of tests to pathways of interest, unrelated pathways were removed *e.g.* Huntington's disease.

Statistical analysis. The pre/post comparisons within each diet were computated using LIMMA (Bioconductor). Specifically, the two factors (time and diet) were converted into a single factor with 6 levels, and after running the full model, contrast tests between levels of interest were performed (*e.g.* Diet 1-Pre vs. Diet 1-Post). The model was analyzed as a multi-level model to account for repeated measures. Array-quality weights were estimated and included in the model. For the reporter features analysis, $\log_2$ fold-change and unadjusted p-values from the LIMMA analysis were used as input. Statistical significance was determined from the null distribution and gene sets were limited to those with more than 3 and no more than 200 genes. Otherwise, default parameters were used. Distinctly up- and down-regulated pathways were used to determine pathway enrichment in the specific direction. P-values were adjusted to the Benjamini-Hochberg false discovery rate.

4.2.5. Adipose tissue lipolysis (IV)

Insulin action on serum FFA and glycerol rate of appearance (R_a) were determined using the euglycemic hyperinsulinemic clamp technique (Yki-Järvinen *et al.,* 1991). The duration of the insulin infusion was 120 min (120-240 min) and rate of the continuous insulin infusion was 0.4 mU/kg·min (DeFronzo *et al.,* 1979). The low insulin infusion rate was chosen to optimize the conditions detecting changes in lipolysis, which is half-maximally suppressed already at insulin concentrations of 13 mU/L in normal subjects (Nurjhan *et al.,* 1986). The concentrations needed to inhibit hepatic glucose production or stimulate glucose disposal in normal subjects are ~50 mU/L and ~100 mU/L (Yki-Järvinen *et al.,* 1987). Before start of the infusions, two 18 gauge catheters (Venflon, Viggo-Spectramed, Helsingborg, Sweden) were inserted, one in an antecubital vein and another retrogradely in a heated (+65 °C) dorsal hand vein for sampling of arterialized venous blood for insulin (0, 120, 180 and 240 min), FFA (0, 100, 120, 130, 135, 140, 150, 180, 240 min), and concentrations of glycerol and its isotopic enrichment (0, 100, 120, 130, 140, 150, 180, 240 min).

The rate of whole-body lipolysis and effect of insulin on lipolysis were determined by infusing [$^2H_5$]glycerol for 120 min before (0-120 min) and for 120 min during the insulin infusion (120-240 min).

[$^2H_5$]glycerol enrichment was measured by GC/MS (Gastaldelli *et al.,* 1999). After deproteinization, plasma samples were derivatized with pyridine and acetic anhydride (1:1), and then reconstituted with ethyl acetate (80 µl). Thereafter, samples were injected (2 µl) in the GC/MS (Agilent, Palo Alto, CA), and enrichment was assessed as the peak area ratio between fragments of mass 148 and 145, after correction for baseline values. During the last 20 min of the tracer equilibration period, both plasma glycerol concentrations and [$^2H_5$]glycerol enrichments were stable in all subjects. Therefore, the R_a of endogenous glycerol was calculated as the ratio of the tracer infusion rate to the plasma tracer enrichment (mean of 3 determinations). During the clamp, glycerol R_a was calculated from [$^2H_5$]glycerol enrichment using the Steele's equation (Gastaldelli *et al.,* 1999).

4.2.6. *De novo* lipogenesis (IV)

Fasting *de novo* lipogenesis was assessed based on the incorporation of deuterium from ^2H_2O in plasma water (Finnigan GasBench-II, ThermoFisher Scientific, UK) into VLDL-TG palmitate using gas chromatography/mass spectrometry (GC/MS) with monitoring ions with mass-to-charge ratios (m/z) of 270 (M+0) and 271 (M+1) (Semple *et al.,* 2009). Absolute DNL was calculated by multiplying %DNL and the concentration of TG in VLDL (Santoro *et al.,* 2015).

4.2.7. Body composition (I-IV)

Body weight was measured to the nearest 0.1 kg using a calibrated digital scale (Soehnle, Monilaite-Dayton, Finland) wearing light indoor clothing without shoes. Height was measured to the nearest 0.5 cm using a non-stretching tape. Body mass index (BMI) was calculated as weight in kilograms divided by the square of height in meters. Waist circumference was measured from the midway between the lower rib margin and the superior iliac spine, and hip circumference at the greater trochanter level. Visceral and subcutaneous fat was determined by magnetic resonance imaging using 1.5T Siemens Avanto^{fit} (Siemens Healthcare Diagnostics, Erlangen, Germany). A series of T1-weighted trans-axial images with frequency selective fat excitation were obtained for the determination of visceral and subcutaneous fat by magnetic resonance imaging from a region extending from 8 cm above to 8 cm below the fourth and fifth lumbar intervertebral disk (16 slices; field of view, 437.5 x 500 mm^2; matrix size, 448 x 512; slice thickness, 10 mm; repetition time, 91 ms; echo time, 5.24 ms) in two breath holds. Visceral and subcutaneous fat areas were measured using an image analysis program (SliceOMatic v5.0, Tomovision, Montreal, Quebec, Canada, http://www.perceptive.com/ALICE.HTM). The areas of subcutaneous and visceral fat measured for each slice using a region-growing routine. The results were expressed as total volumes of visceral and subcutaneous fat. Body fat percentage, body water mass and fat free mass were determined using the bioelectric impedance method (InBody 720, Biospace, Seoul, Korea).

4.2.8. Energy expenditure and substrate oxidation (IV)

Indirect calorimetry using a computerized flow-through canopy system (Deltatrac, Datex, Helsinki, Finland) was used to measure respiratory gas exchange and rates of resting energy expenditure for 40 min before, and for 40 min during euglycemic hyperinsulinemia (Yki-Järvinen *et al.,* 1991). Protein oxidation was calculated from urinary urea nitrogen excretion (Ferrannini *et al.,* 1988). Rates of carbohydrate and lipid oxidation were calculated from the gas exchange data as described (Yki-Järvinen *et al.,* 1991).

4.2.9. Intestinal microbiota (IV)

Bacterial DNA was extracted from fecal samples using mechanical cell lysis. Illumina MiSeq paired-end sequencing of the hypervariable V3-V4 regions of the 16S rRNA gene was performed according to the manual, except that the libraries were prepared with single-step polymerase chain reaction, i.e. by amplifying the 16S rRNA gene fragment together with barcoded primers, adapted from Kozich et al (Kozich *et al.,* 2013). The multiplex polymerase chain reaction was comprised of 1 ng/ul template, 1X Phusion® Master Mix (ThermoFisher, F-531L), 0.25 uM V3-V4 locus specific primers and 0.375 uM dual-index barcodes. The polymerase chain reaction was run under the following settings: 98 °C for 30 s, 27 cycles of 98 °C for 10 s, 62 °C for 30 s, 72 °C for 15 s and finally 10 min at 72 °C, where after the samples were stored at 4 °C. The size of the

polymerase chain reaction product was expected to be ~640 base pairs (bp) and verified on a Bioanalyzer DNA 1000 chip (Agilent Technology, Santa Clara, CA, USA). The polymerase chain reaction clean-up was performed with AMPure XP beads (Beckman Coulter, Copenhagen, Denmark) and confirmation of the right size of the target was performed on a Bioanalyzer DNA 1000 chip (Agilent Technology, CA, USA). The pooled libraries were sequenced at the sequencing unit of the Institute for Molecular Medicine Finland, Helsinki, Finland with an Illumina MiSeq instrument using paired end 2 × 300 bp reads and a MiSeq v3 reagent kit with 5% PhiX as spike-in.

Sequencing data preprocessing, analysis and statistics. The forward reads were truncated to length of 150 bases with mare's "ProcessReads" command. We used default settings for minimum quality score and maximum expected errors. Reads with prevalence below 0.01% were removed. Chimera removal and dereplication of the reads was done using USEARCH8 (Edgar *et al.,* 2010). Truncated, filtered and dereplicated reads were annotated using the Silva database (Quast *et al.,* 2012). The median read count per sample after preprocessing was 68797 (range 296 –148 604). The data analysis was done without rarefaction or transformations utilizing statistical and visualization tools included in the mare-package (Korpela 2016). The number of reads was used as an offset in all statistical models. Community dissimilarity was estimated with principal coordinates analysis using Bray-Curtis dissimilarity as the distance measure. This was calculated with capscale function of R package vegan and Bray-Curtis dissimilarities with function vegdist of the same package (Oksanen *et al.,* 2011). Permutational multivariate analysis of variance using distance matrices was performed with adonis function in package vegan to calculate the relative contribution of different factors in the microbiota variation. Taxonomic richness was estimated as the number of observed operational taxonomic units after clustering the reads to operational taxonomic units using USEARCH8. Comparison of the abundance of bacterial genera between two time points in each intervention group was performed using generalized linear mixed models within "GroupTest" function of the mare package using subject as the random factor. This function uses the glmmADMB package (generalized linear mixed models built on AD Model Builder) of R software on background and assumes negative binomial distribution of abundance.

4.2.10. Genotyping (I-IV)

The TaqMan polymerase chain reaction method (Applied Biosystems, Foster City, CA, USA) was used according to the manufacturer's instructions for genotyping of PNPLA3 at rs739409, MBOAT7 at rs641738 and TM6SF2 at rs58542926 from approximately 10 ng of genomic DNA extracted from whole blood. Post-polymerase chain reaction allelic discrimination was performed by allele-specific fluorescence measurements by an ABI Prism Sequence Detection System ABI 7900HT (Applied Biosystems). The success rate for genotyping was >95%.

4.2.11. Other analytical procedures (I-IV)

Fasting plasma glucose was measured using a hexokinase method on an autoanalyser (Roche Diagnostics Hitachi 917; Hitachi, Tokyo, Japan) and fasting serum insulin concentration by time-resolved fluoroimmunoassay using the Insulin Kit (AUTOdelfia; Wallac, Turku, Finland). Homeostasis model assessment of insulin resistance (HOMA-IR) and Matsuda insulin sensitivity index were used as surrogates for IR. HOMA-IR was calculated by using the formula: HOMA-

IR = fS-insulin (mU/l) x fP-glucose (mmol/l) / 22.5 (Matthews *et al.,* 1985). Matsuda insulin sensitivity index was calculated from insulin and glucose concentrations measured at 0, 30 and 120 minutes during the OGTT (DeFronzo *et al.,* 2010). HbA_{1c} (%) was measured by HPLC using a fully automated Glycosylated Hemoglobin Analyzer System (BioRad, Richmond, CA, USA), and HbA_{1c} (mmol/mol) was calculated from the formula: (HbA_{1c} [%] – 2.15) × 10.929. LDL- and HDL-cholesterol and triacylglycerol concentrations were measured with the respective enzymatic kits (Roche Diagnostics Hitachi 917). Serum creatinine, alanine aminotransferae (ALT), aspartate aminotransferase (AST), alkaline phosphatase (ALP) and gamma glutamyltransferase (GGT) were measured as recommended by the European Committee for Clinical Laboratory Standards. Free fatty acids were measured by an enzymatic colorimetric assay (NEFA-HR, Wako Chemicals, Neuss, Germany) using a Konelab 60i Analyzer (Thermo Electron Corporation, Vantaa, Finland). Plasma albumin was measured using a photometric method on an autoanalyzer (Modular Analytics EVO; Hitachi High-Technologies Corporation, Tokyo, Japan). Serum adiponectin was measured using the Human Adiponectin ELISA kit from B-Bridge International (Cupertino, CA, USA). Serum lipopolysaccharide-binding protein (LBP) and soluble cluster of differentiation 14 (sCD14) were measured by quantitative enzyme-linked immunosorbent assay (ELISA) using human LBP DuoSet® ELISA and human CD14 DuoSet® ELISA kits (R&D Systems, Minneapolis, MN, USA).

4.2.12. *In vitro* experiments (III)

HuH-7 human hepatoma derived cell line was cultured in Minimal essential medium Eagle AQ™ media (Sigma-Aldrich, St. Louis, MO) containing 10% fetal bovine serum, 100 U/ml penicillin, 100 µg/ml streptomycin. At 70% confluency the cells were transduced with lentiviral particles expressing shRNA against TM6SF2 (TRCN0000254085, Sigma-Aldrich) according to the manufacturer's protocol. Sigma-Aldrich SHC002V was used as control non-targeting shRNA. Control and TM6SF2 shRNA transduced cell pools were selected using 5 µg/ml of puromycin.

Quantitative PCR. To analyse *TM6SF2* knockdown efficiency in transduced HuH-7 cells and transiently silenced HuH-7 cells, RNA from the puromycin selected cells was isolated using PureLink® RNA Mini Kit (Ambion/Thermo Fisher, Waltham, MA) according to the manufacturer's protocol. Reverse transcription was carried out with Moloney murine leukemia virus reverse transcriptase (Invitrogen, Carlsbad, CA) and Oligo dT priming. Real time quantitative polymerase chain reaction was performed in Light Cycler 480 II (Roche Applied Science, Penzberg, Germany) using Roche SYBR-Green® master mix. The primers used for TM6SF2 were forward: ACAGCTATGTGGTGGGCTTC; reverse: CCCAGCCAGTAGAGTCCAAA. Data were normalised to the geometric mean of two house keeping genes, Succinate dehydrogenase complex, subunit A (forward: CATGCTGCCGTGTTCCGTGTGGG; reverse: GGACAGGGTGTGCTTCCTCCAGTGCTC C and β-actin, forward: GACAGGATGCAGAAGGAGATT, reverse: TGATCCACATCTGCTGGAAGG.

Lipid droplet quantification. Control and *TM6SF2* knockdown HuH-7 cells were fixed using 4% paraformaldehyde in phosphate buffered saline. Cells were then permeabilised using 0.1% Triton X-100 for 5 mins and washed twice with phosphate buffered saline, followed by staining with BODIPY® 493/503

(Molecular Probes, Eugene, OR). Cells were washed three-times in phosphate buffered saline and mounted in Mowiol (Calbiochem, La Jolla, CA) containing 50 mg/ml 1,4-Diazabicyclo-[2.2.2] octane, 5 (Sigma–Aldrich) and 5 µg /ml DAPI (Molecular Probes). The cells were imaged using Zeiss Axio Observer Z1 microscope (Carl Zeiss Imaging Solutions GmbH, Oberkochen, Germany) with a 60X objective with numerical aperture 1.4 and Colibri laser. The lipid droplet area in each cell was quantified (total lipid area in a field/number of cells in the field) by using FIJI (ImageJ) software; 150 cells from both control and *TM6SF2*-silenced specimens were analysed.

Incorporation of labeled fatty acids to lipids. HuH-7 control and *TM6SF2* knockdown cells were cultured in 6 well plates as described above. Cells were incubated with radioactive lipids in full media for 24 hours after 48 hours of reaching confluency. [9,10-^{3}H(N)]-oleic acid (1.5 µCi/mL), [9,10-^{3}H(N)]-palmitic acid (1.5 µCi/mL) and [5,6,8,9,11,12,14,15-^{3}H(N)]-arachidonic acid (100nCi/mL) (PerkinElmer, Waltham, MA) were used. Total lipids were isolated using the Bligh and Dyer method and the extracts were separated using thin layer chromatography. Hexane/diethyl ether/acetic acid/water (65:15:1:0.25,V/V) and chloroform/methanol/acetic acid/water (50:30:8:3.5 V/V) were used as solvents for separating neutral and phospholipids, respectively. After the run thin layer chromatography plates were stained with iodine. Triolein, DOPC and CE(18:1) were used as standards to identify TGs, PCs and CEs. These lipid spots were scraped and the radioactivity was measured using a liquid scintillation counter. The radioactivity values were normalised to total cell protein content. Fatty acid incorporation experiments were also carried out in transiently silenced HuH-7 and control cells using tritiated [9,10-^{3}H(N)]-palmitic acid and [5,6,8,9,11,12,14,15-^{3}H(N)]-arachidonic acid as described above. Silencing was done in HuH-7 cells using siRNA (65 nM) against TM6SF2 (SI04187946, Qiagen) for 48 hours and labeled for another 24 hours with radioactive fatty acids. Lipofectamine® RNAiMAX transfection reagent was used for transfecting siRNA according to manufacturers protocol. AllStars Negative Control siRNA (SI03650318, Qiagen) was used as negative control.

4.2.13. Statistical analyses (I-IV)

Studies I-III. Continuous variables were tested for normality using the Kolmogorov-Smirnov test. The independent two-sample Student t test and Mann-Whitney U test were used to compare normally and non-normally distributed data, respectively. Normally distributed data were reported in means ± standard error of means while non-normally distributed were reported in medians and interquartile ranges. Pearson $\chi 2$ test was used to evaluate if the distribution of categorical variables differ between the groups. Pearson's correlation coefficients were calculated as a measure of statistical dependence between two variables after log-transformation if necessary. Linear regression analyses were performed to evaluate whether the differences in lipids between the groups is dependent on their number of carbons and number of double bonds.

Study IV. Continuous variables were tested for normality using the Kolmogorov-Smirnov test. Changes between groups were compared using one-way analysis of variance followed by Fisher least significant differences test. Nonparametric variables were log-transformed for analysis and back-transformed for presentation or analyzed nonparametrically with the Kruskal-Wallis test. The paired Students t test was used to explore within-group effects of

overfeeding. Categorical variables were analyzed with the Fisher exact test.

Cluster analysis of lipids. In study I, Bayesian model-based clustering analysis was performed to identify the groups of lipids with similar profiles across all the samples. A total of 1,458 lipids were measured and 324 identified. The data were decomposed into 11 lipid clusters. After $\log_2$ transformation, lipidomics data of each lipid species were scaled to zero mean and unit variance. The average profile of each cluster was represented by the mean value of all lipids contained. The comparisons of clusters between subgroups were visualized by bar plots.

Assessment of abundances of lipid species. After $\log_2$ transformation, the mean values of concentrations of all lipids were compared between subgroups based on HOMA-IR, and PNPLA3 and TM6SF2 genotypes. In study II, median values of concentrations of lipids were compared using Kolmogorov-Smirnov and Mann-Whitney *U* tests. The multiple hypotheses testing was done by the Benjamini-Hochberg's method (Hochberg *et al.,* 1990). The comparisons of concentrations of lipids were illustrated by heatmaps, which plot chain length against the number of double bonds. The comparisons of concentrations of ceramides and their precursors were illustrated by heatmaps, which plot fatty acyl chain against sphingoid base. The color intensity of each cell in the heatmap represents the $\log_2$ transformed ratio of mean values of individual lipid molecules of the cases divided by the controls. The concentrations of dihydroceramides as markers of the *de novo* ceramide synthetic pathway, sphingomyelins as markers of sphingomyelin hydrolysis pathway, and hexosylceramides as markers of the salvage pathway.

All statistical analyses were performed by using R 3.1.1 (http://www.r-project.org/), IBM SPSS Statistics 22.0.0.0 version (IBM, Armonk, NY) and GraphPad Prism 6.0f for Mac OS X (GraphPad Software, La Jolla, CA). A p value of less than 0.05 indicated statistical significance.

5. RESULTS

5.1. SUBJECT CHARACTERISTICS (I–IV)

Clinical characteristics of the subgroups based on median HOMA-IR and the PNPLA3 genotype in study I, and those based on the TM6SF2 genotype in study III are shown in **Table 1**. All groups were similar with respect to gender distribution and body mass index (**Table 1, Figure 5**).

Study I – Subgroups based on median HOMA-IR. Macrovesicular steatosis as determined by histological assessment was significantly and 3-fold higher in the 'High HOMA-IR' (15 [5–33]) than in the 'Low HOMA-IR' group (5 [0–20], p<0.002) (**Table 1, Figure 5**). The 'High HOMA-IR' group had significantly higher concentrations of fasting serum insulin (18 mU/l [14–22] vs. 7 mU/l [6–10], p<0.0001) and plasma glucose (6.1 mmol/l [5.6–6.8] vs. 5.5 mmol/l [4.7–6.0], p<0.0001) as compared to the 'Low HOMA-IR' group (**Table 1, Figure 5**). In the 75-gram oral glucose tolerance test, the concentrations of insulin (82 mU/l [56–124] vs. 39 mU/l [21–49], p<0.05) and glucose (9.2 mmol/l [6.9–12.0] vs. 7.5 mmol/l [5.4–10.4], p<0.001) at two hours were higher in the 'High HOMA-IR' than the 'Low HOMA-IR' group (**Figure 1**). Concentrations of plasma triglycerides were higher, and concentrations of HDL cholesterol and adiponectin were lower subjects in the 'High HOMA-IR' as compared to the 'Low HOMA-IR' group (**Table 1 and Figure 5**). The PNPLA3 genotypes were similarly distributed between 'High HOMA-IR' and 'Low HOMA-IR' groups (**Table 1**).

Study I – Subgroups based on the PNPLA3 genotype. Macrovesicular steatosis was significantly and 3-fold higher in the 'PNPLA3$^{148MM/MI}$' (15 [5–30]) as compared to the 'PNPLA3^{148II}' group (5 [0–28], p<0.04) (**Table 1, Figure 5**). Glucose and insulin concentrations during OGTT, HOMA-IR, Matsuda insulin sensitivity index, and serum lipid and adiponectin concentrations were similar between the PNPLA3 subgroups (**Table 1 and Figure 5**). By definition, the distributions of PNPLA3 genotypes were different between the 'PNPLA3$^{148MM/MI}$' and 'PNPLA3^{148II}' groups (p<0.001, **Table 1**).

*Study II***.** The groups defined based on the MBOAT7 genotype at rs641738 (n=35 for CC, n=60 for CT and n=20 for TT) were similar with respect to age, gender, BMI, waist circumference, PNPLA3 I148M and TM6SF2 E167K genotypes. Histologically determined scoring of macrovesicular steatosis (the percentage of grades 0/1/2/3 were 23/60/3/14, 25/62/12/2 and 20/55/25/0, p=0.03 in CC, CT and TT groups, respectively), necroinflammation (the percentage of grades 0/1/2/3 were 74/26/0/0, 87/13/0/0 and 60/35/0/5, p=0.04, respectively) were significantly different between the MBOAT7 groups. The prevalence of subjects with fibrosis stage 2 or greater increased with number of *MBOAT7* variant alleles (0 vs. 5 vs. 25 %, p=0.001, **Figure 6**). Concentrations of fasting serum insulin (13.7 [8.4–17.1], 11.2 [6.5–18.3] and 12.3 [7.0–18.8] mU/l in CC, CT and TT groups), plasma glucose (5.9 [5.0–6.6], 5.8 [5.4–6.6] and 5.7 [5.1–6.1] mmol/l), plasma triglycerides (1.24 [1.06–1.55], 1.29 [0.91–1.69] and 1.08 [1.00–1.59] mmol/l), HDL (1.15 [0.98–1.33], 1.09 [0.93–1.38] and 0.98 [0.86–1.13] mmol/l) and LDL (2.5 [1.9–3.4], 2.3 [1.7–2.9] and 2.4 [1.5–3.5] mmol/l) cholesterol were similar between the MBOAT7 groups.

Table 1. Clinical characteristics of the subjects in studies I and III.

	Low HOMA-IR (n=63)	High HOMA-IR (n=62)	PNPLA3^{148II} (n=64)	PNPLA3$^{148MM/MI}$ (n=61)	TM6SF2^{EE} (n=80)	TM6SF2$^{EK/KK}$ (n=10)
Age (years)	49.2 ± 1.1	46.2 ± 1.1	46.2 ± 1.1	49.3 ± 1.0*	45.2 ± 0.9	49.1 ± 2.8
Gender (% women)	71.4	61.3	70.3	62.3	71.3	70.0
BMI (kg/m^2)	45.2 ± 0.8	46.2 ± 0.6	45.6 ± 0.7	45.8 ± 0.8	45.4 ± 0.7	45.6 ± 1.7
Waist circumference (cm)	127.6 ± 1.8	135.5 ± 1.6**	130.2 ± 1.8	132.9 ± 1.8	128.3 (120.0 – 140.0)	127.3 (117.4 – 135.4)
fP-Glucose (mmol/l)	5.5 (4.7 - 6.0)	6.1 (5.6 – 6.8)***	5.8 (5.2 - 6.4)	5.7 (5.3 - 6.5)	5.6 ± 0.1	5.7 ± 0.3
HbA_{1C} (%)	5.7 (5.5 - 6.1)	6.0 (5.6 - 6.5)	5.7 (5.5 - 6.3)	5.9 (5.5 - 6.3)	5.7 (5.5 - 6.0)	5.7 (5.5 - 6.1)
HbA_{1C} (mmol/mol)	39 (37 – 43)	42 (38 – 47)	39 (37 – 45)	41 (37 – 45)	39 (37 – 42)	39 (37 – 43)
HOMA-IR	1.8 (1.3 – 2.7)	4.8 (3.9 – 5.8)***	3.2 (1.9 - 4.5)	3.2 (1.7 - 5.1)	3.4 ± 0.2	3.6 ± 0.7
Matsuda ISI	89.8 (65.7 – 141.9)	35.5 (27.3 – 45.1)***	53.7 (35.0 – 87.8)	51.2 (34.3 – 96.8)	55.4 (36.0 – 104.9)	56.9 (42.2 – 74.3)
fP-TGs (mmol/l)	1.12 (0.91 - 1.66)	1.34 (1.15 - 1.85)*	1.29 (0.97 - 1.80)	1.26 (1.00 - 1.66)	1.24 (0.91 - 1.69)	1.34 (0.97 - 1.60)
fP-HDL cholesterol (mmol/l)	1.17 (1.00 - 1.44)	1.02 (0.89 - 1.21)**	1.10 (0.95 - 1.36)	1.11 (0.95 - 1.30)	1.13 (0.96 - 1.37)	1.09 (0.96 - 1.55)
fP-LDL cholesterol (mmol/l)	2.4 ± 0.1	2.5 ± 0.1	2.5 ± 0.1	2.4 ± 0.1	2.6 ± 0.1	2.5 ± 0.2
Liver fat (%)	5 (0 - 20)	15 (5 - 33)**	5 (0 - 28)	15 (5 - 30)*	13.8 ± 2.0	27.5 ± 9.5*
P-AST (IU/l)	30 (25 - 37)	31 (26 - 38)	28 (24 - 33)	32 (26 - 41)**	30 (25 - 37)	34 (30 - 41)
P-ALT (IU/l)	28 (22 - 40)	38 (30 - 51)***	31 (24 - 45)	36 (27 - 46)	32 (24 - 45)	42 (28 - 58)
P-ALP (IU/l)	65 ± 2	65 ± 2	66 ± 2	64 ± 2	64 ± 2	70 ± 5
P-GGT (U/l)	26 (19 - 38)	36 (23 - 52)*	28 (20 - 44)	32 (22 - 52)	28 (21 - 45)	50 (26 - 66)
P-Albumin (g/l)	37.6 (36.6 - 39.3)	38.0 (36.1 – 39.7)	37.8 (36.3 - 39.4)	37.9 (36.0 - 39.3)	38.2 ± 0.3	37.9 ± 1.0
B-Platelets (x10^9/l)	246 ± 9	252 ± 8	258 ± 9	240 ± 7	252 ± 6	276 ± 35
PNPLA3 (n, CC/CG/GG)	32/27/4	32/27/3	64/0/0	0/54/7***	41/35/4	6/3/1
TM6SF2 (n, CC/CT/TT)	55/5/0	53/5/1	53/5/1	54/5/1	80/0/0	0/9/1***
MBOAT7 (n, CC/CT/TT)	16/31/11	19/29/9	9/31/16	19/29/11	23/37/12	4/3/2

Data are in n, means ± SEM or median (25th-75th percentile), and statistical tests are Student's t-test, Mann-Whitney U-test and Pearson's χ2-test, as appropriate. *p ≤ 0.05, **p ≤ 0.01, ***p ≤ 0.001 against the respective reference group. Adapted from Luukkonen *et al., Journal of Hepatology.* 2016; 64:1167-75 and from Luukkonen *et al., Journal of Hepatology*. 2017; 67:128-136 and reproduced with the permission of Elsevier.

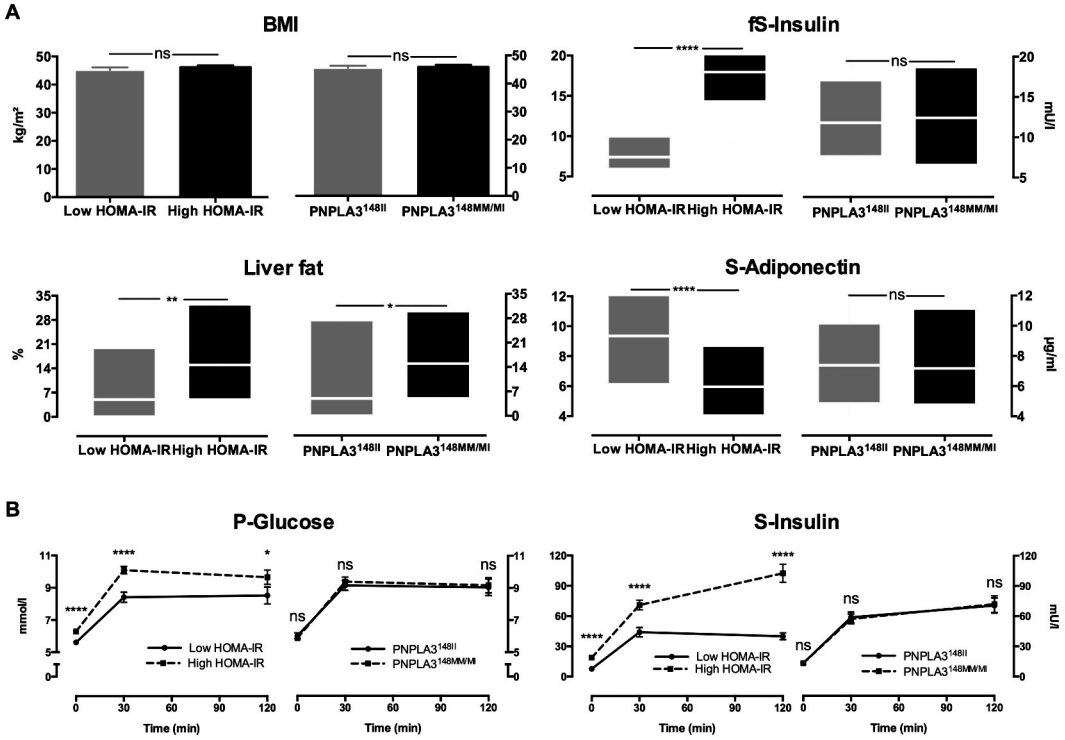

Figure 5. (*A*) Body mass index (top panels on the left), fasting serum insulin concentrations (top panels on the right), liver fat content (bottom panels on the left), and serum adiponectin concentrations (bottom panels on the right) in the 'Low HOMA-IR' vs. 'High HOMA-IR' (leftmost panels in each comparison) and in the 'PNPLA3148II' vs. 'PNPLA3148MM/MI' (rightmost panels in each comparison) groups. Data are in mean ± SEM (bars and whiskers) or in medians and interquartile ranges (box plots), as appropriate. (*B*) Plasma glucose and serum insulin concentrations in the groups during oral glucose tolerance test. Data are in means ± SEM. n.s. p>0.05, *p<0.05, **p<0.01, ***p<0.001. Adapted from Luukkonen *et al., Journal of Hepatology*. 2016; 64:1167-75 and reproduced with the permission of Elsevier.

*Study III***.** Clinical characteristics of the *TM6SF2* genotype groups are shown in **Table 1**. Histologically determined macrovesicular steatosis was 2-fold higher in the TM6SF2$^{EK/KK}$ than the TM6SF2^{EE} group (27.5 ± 9.5 % vs. 13.8 ± 2.0 %, p<0.05, **Table 1**). By definition, the distribution of TM6SF2 genotypes differed between the TM6SF2 groups (**Table 1**). Indices of insulin sensitivity, circulating lipid concentrations and the distribution of *PNPLA3* rs738409 genotype were comparable between the TM6SF2 groups (**Table 1**). The TM6SF2$^{EK/KK}$ group tended to have higher prevalence of hepatic fibrosis (stage 1 or greater) compared to the TM6SF2^{EE} group (60 vs. 31 %, p=0.09).

*Study IV***.** The clinical characteristics of the subjects in study IV at baseline are shown in **Table 2**. The groups consuming hypercaloric diets enriched either in saturated fat (SAT), mono- and polyunsaturated fat (UNSAT) and simple sugars (CARB) were similar with respect to age, gender distribution, body mass index, body composition, IHTG content, blood pressure, the PNPLA3 genotype distribution, and circulating insulin, lipids and liver enzymes (**Table 2**).

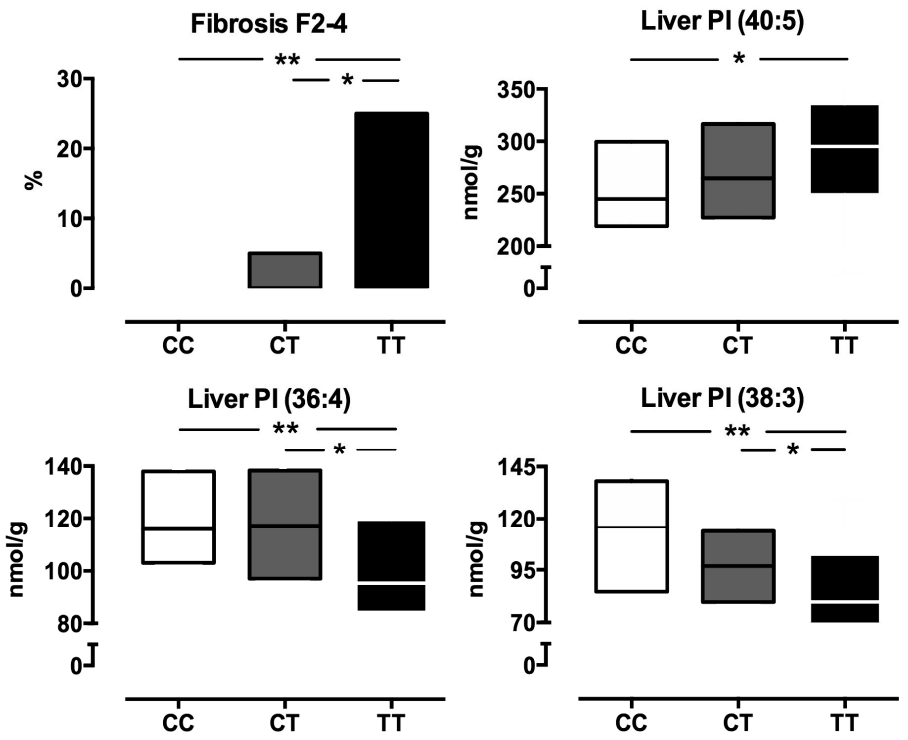

Figure 6. Prevalence of fibrosis (top panel on the left) and concentrations of hepatic phosphatidylinositols PI(40:5) (top panel on the right), PI(36:4) (bottom panel on the left), and PI(38:3) (bottom panel on the right) in groups according to the MBOAT7 genotype at rs641738. Data are in % and median (25^{th}-75^{th} percentile), and were tested using Pearson $\chi 2$ test, Kolmogorov-Smirnov test and Mann-Whitney *U* test, as appropriate. * $p<0.05$, ** $p<0.01$. Adapted from Luukkonen *et al., Journal of Hepatology*. 2016; 65:1263-1265 and reproduced with the permission of Elsevier.

5.2. HUMAN LIVER LIPIDOME (I-III)

In total, 1,458 lipids were measured, of which 324 were identified. The data were decomposed into 11 lipid clusters (LCs). The abundance of LCs containing ceramides and dihydroceramides (LC1), DAGs, saturated and monosaturated TGs (LC5), and polyunsaturated TGs (LC8, LC10 and LC11) were increased in the 'High HOMA-IR' vs. 'Low HOMA-IR' group. The abundance of LCs containing mostly polyunsaturated TGs (LC8, LC9, LC10 and LC11) differed significantly between the $PNPLA3^{148MM/MI}$ and the $PNPLA3^{148II}$ groups. We therefore focused on analyses of these lipid species (TGs, DAGs, ceramides and dihydroceramides) in study I.

5.2.1. 'Metabolic NAFLD' (I)

The increase in liver fat content in 'High HOMA-IR' as compared to the 'Low HOMA-IR' group was predominantly due to increase in TG species with 0 to 3 double bonds and 48 to 54 carbons, i.e. species with mostly saturated and monounsaturated long chain acyl-groups (**Figure 7**).

Table 2. Baseline clinical characteristics of the subjects in study IV according to diet group.

	SAT (n=14)	**UNSAT (n=12)**	**CARB (n=12)**
Age (years)	48 ± 2	52 ± 3	45 ± 3
Gender (n, women/men)	8/6	7/5	6/6
BMI (kg/m^2)	30 ± 2	31 ± 2	33 ± 2
Fat free mass (kg)	58.6 ± 2.6	60.2 ± 3.8	61.9 ± 3.6
Liver fat (^{1}H-MRS, %)	4.9 ± 1.8	4.8 ± 1.4	4.3 ± 1.3
Visceral adipose tissue (MRI, cm^3)	1940 ± 429	2019 ± 383	2014 ± 351
Subcutaneous adipose tissue (MRI, cm^3)	4770 ± 575	4732 ± 708	5133 ± 622
Waist circumference (cm)	97 ± 5	98 ± 4	102 ± 3
Waist-to-hip ratio	0.90 ± 0.03	0.90 ± 0.02	0.92 ± 0.02
LBP-to-sCD14 ratio	4.3 ± 0.3	4.6 ± 0.3	4.9 ± 0.5
fP-Glucose (mmol/l)	5.6 ± 0.2	5.7 ± 0.2	5.9 ± 0.2
fS-Insulin (mU/l)	8.1 (5.8 – 11.9)	9.1 (6.5 – 14.6)	10.3 (6.2 – 19.2)
HOMA-IR	1.9 (1.3 – 3.2)	2.3 (1.6 – 4.0)	2.8 (1.7 – 5.0)
Systolic blood pressure (mmHg)	133 ± 4	134 ± 5	139 ± 6
Diastolic blood pressure (mmHg)	80 ± 3	83 ± 2	85 ± 4
fP-Triglycerides (mmol/l)	1.1 ± 0.3	1.1 ± 0.1	1.4 ± 0.2
fP-HDL cholesterol (mmol/l)	1.62 ± 0.10	1.61 ± 0.14	1.53 ± 0.11
fP-LDL cholesterol (mmol/l)	3.2 ± 0.3	3.4 ± 0.2	3.5 ± 0.2
fS-FFA (µmol/l)	556 ± 58	610 ± 52	639 ± 65
fP-ALT (IU/l)	28 ± 4	26 ± 3	24 ± 3
fP-AST (IU/l)	26 ± 1	27 ± 2	26 ± 2
PNPLA3 (CC/CG/GG) (n)	9/5/0	7/4/1	5/4/2

Data are in n (%), means ± SEM or median (25th-75th percentile), as appropriate. There were no significant differences in any variable between the groups using ANOVA, Kruskal-Wallis and Chi-squared test, as appropriate.

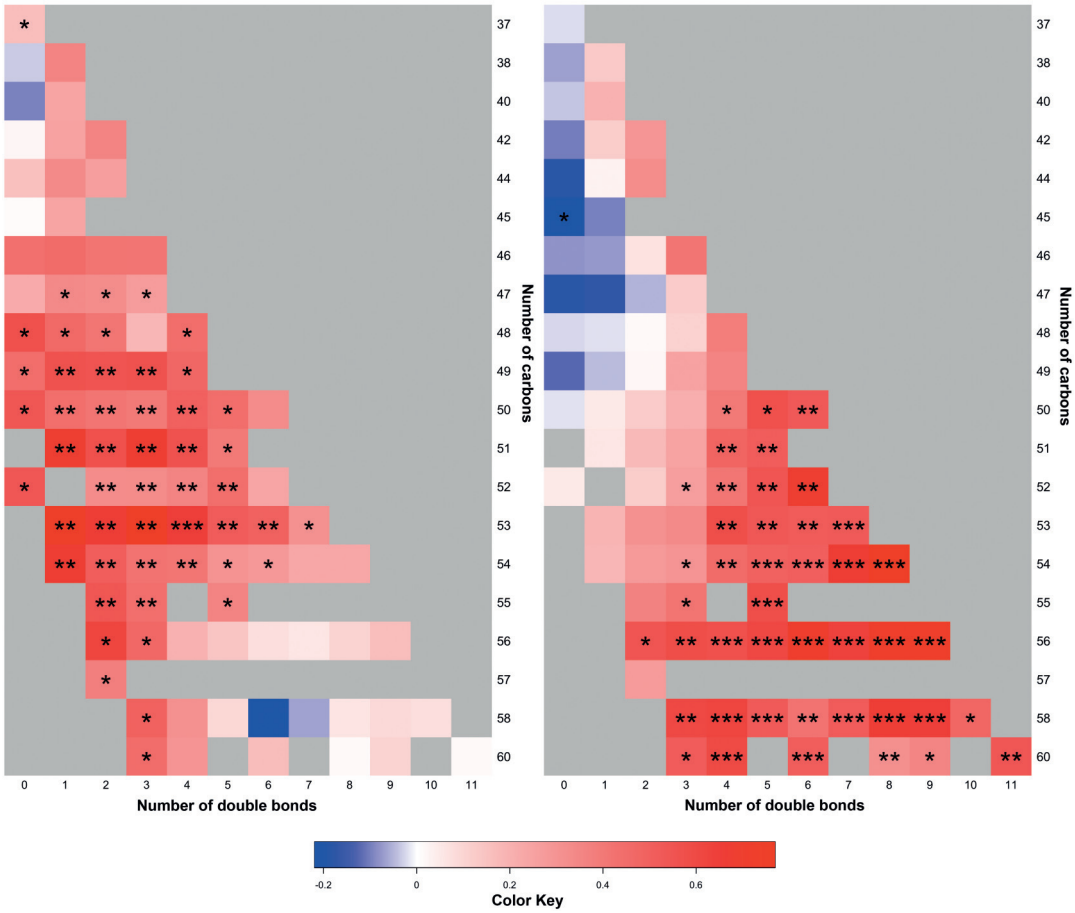

Figure 7. Fold-change of distinct hepatic TGs between groups ('High HOMA-IR' vs. 'Low HOMA-IR', panel on the left; 'PNPLA3$^{148MM/MI}$' vs. 'PNPLA3^{148II}', panel on the right). The color code represents the log of the ratio between means of the groups for an individual TAG. The y-axes denote the number of carbons and the x-axes the number of double bonds. The brighter the red color, the greater increase of absolute concentration of the individual TG in the 'High HOMA-IR' compared to the 'Low HOMA-IR' group or the PNPLA3$^{148MM/MI}$' compared to the 'PNPLA3^{148II}' group. *p<0.05, **p<0.01, ***p<0.001. Adapted from Luukkonen *et al., Journal of Hepatology*. 2016; 64:1167-75 and reproduced with the permission of Elsevier.

The concentrations of free palmitate (C16:0) (372 [296–502] vs. 333 [279–402] nmol/g, p<0.05), stearate (C18:0) (202 [149–250] vs. 164 [135–200], p<0.05) and oleate (C18:1) (188 [140–254] vs. 164 [126– 207], p<0.05) in the liver were greater in the 'High HOMA-IR' group vs. the 'Low HOMA-IR' group. There were no differences in hepatic concentrations of free polyunsaturated fatty acids linoleate (C18:2) and arachidonate (C20:4) in the 'High HOMA-IR' group vs. the 'Low HOMA-IR' group.

The concentrations of 13 out of 17 hepatic ceramide species were significantly increased in the 'High HOMA-IR' vs. the 'Low HOMA-IR' group (**Figure 8**).

Regarding the pathways of ceramide synthesis, hepatic concentrations of dihydroceramides were used as markers

of *de novo* ceramide synthetic pathway, sphingomyelins as markers of sphingomyelin hydrolysis pathway, and hexosylceramides as markers of the salvage pathway (**Figure 9**). Concentrations of 4 out of 5 dihydroceramide species in the liver were significantly increased in 'High HOMA-IR' group vs. the 'Low HOMA-IR' group (**Figure 9**). There were no differences in the hepatic concentrations of sphingomyelins and hexocylceramides between the groups (**Figure 9**).

The concentrations of 4 out of 5 DAG species in the liver (DAG(32:1), DAG(34:1), DAG(36:2) and DAG(36:3)) were significantly ($p<0.05$) increased in the 'High HOMA-IR' vs. the 'Low HOMA-IR' group.

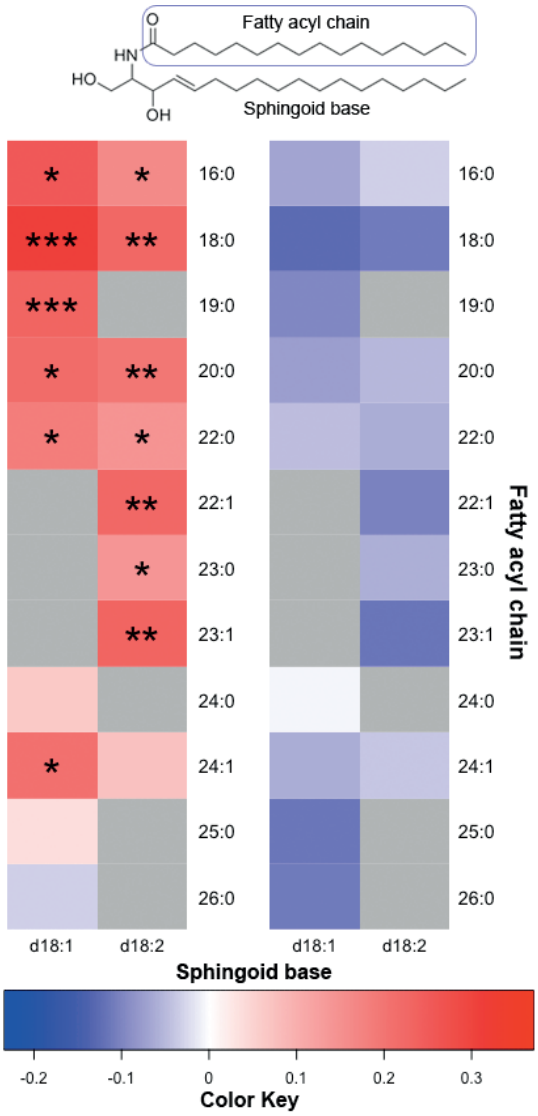

Figure 8. Fold-changes of distinct hepatic ceramides between the groups ('High HOMA-IR' vs. 'Low HOMA-IR', panel on the left; 'PNPLA3$^{148MM/MI}$' vs. 'PNPLA3^{148II}' groups panel on the right). The top panel represents the structure of a ceramide. In the heatmaps, the color code indicates the log of the ratio between means of the groups for an individual ceramide. The y-axes denote the fatty acyl chain and the x-axes the sphingoid base species. The brighter the red color, the greater increase of absolute concentration of the individual ceramide in the 'High HOMA-IR' compared to the 'Low HOMA-IR' group or the PNPLA3$^{148MM/MI}$' compared to the 'PNPLA3^{148II}' group. *$p<0.05$, **$p<0.01$, ***$p<0.001$. Adapted from Luukkonen *et al. Journal of Hepatology*. 2016; 64:1167-75 and reproduced with the permission of Elsevier.

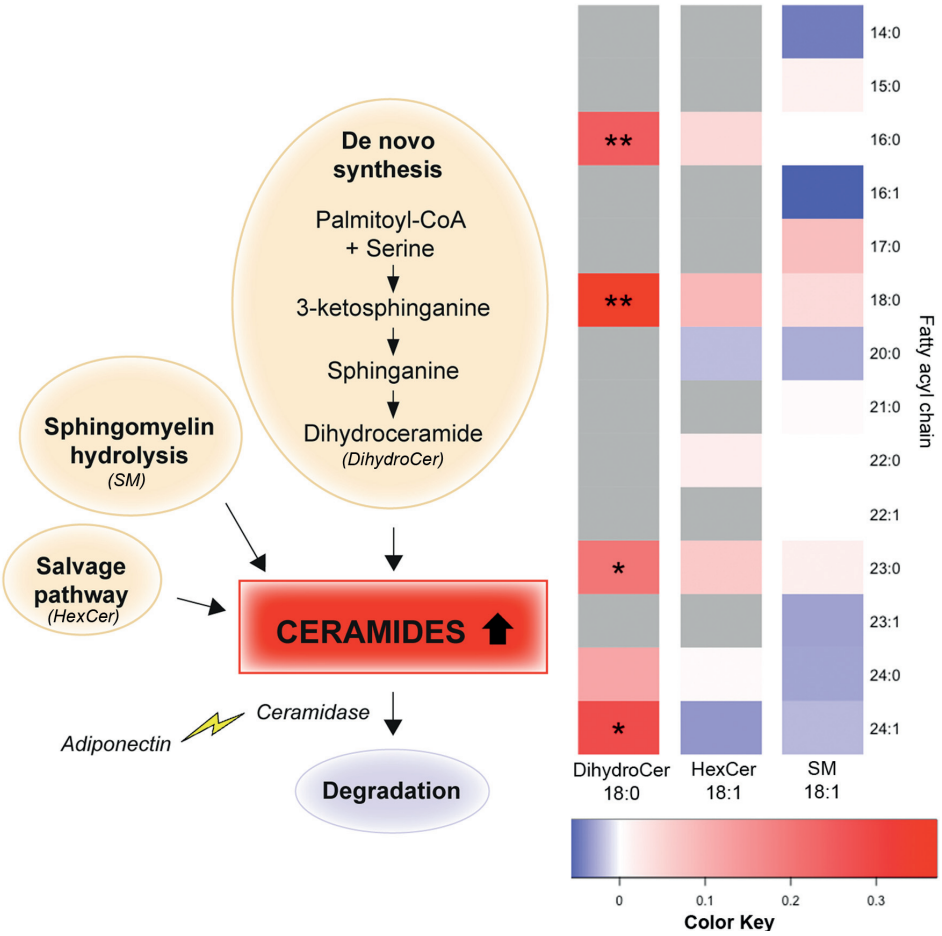

Figure 9. Pathways of ceramide metabolism. The diagram (panel on the left) depicts the pathways of ceramide metabolism. Ceramides can be synthesized *via* the *de novo* synthetic pathway in which palmitate is metabolized to dihydroceramides (*DihydroCer*) prior to formation of ceramides (heatmap on the left). They can also be formed *via* the salvage pathway from hexosylceramides (*HexCer*, middle heatmap) and *via* sphingomyelin hydrolysis (*SM*, heatmap on the right). Ceramides are degraded by ceramidase, which is upregulated by adiponectin. In the heatmaps, the color code indicates the log of the ratio between means of the 'High' vs. 'Low HOMA-IR' groups for an individual lipid. The y-axes denote the fatty acyl chain and the x-axes the sphingoid base. The brighter the red color, the greater increase of absolute concentration of the individual lipid. *p<0.05, **p<0.01. Adapted from Luukkonen *et al., Journal of Hepatology*. 2016; 64:1167-75 and reproduced with the permission of Elsevier.

5.2.2. 'PNPLA3 NAFLD' (I)

In contrast to the differences between the subgroups based on median HOMA-IR, increase in liver fat content in the PNPLA3$^{148MM/MI}$ vs. the PNPLA3^{148II} group was predominantly due to increase in TG species with 4 to 11 double bonds and 50 to 60 carbons, i.e. species with mostly polyunsaturated very long chain acyl-groups (**Figure 7**).

There were no differences in hepatic free fatty acids or ceramides

between the PNPLA3 groups (**Figure 8**). Amongst hepatic DAGs, concentration of one polyunsaturated species, DAG(36:3), was significantly ($p<0.05$) increased in the $PNPLA3^{148MM/MI}$ as compared to the $PNPLA3^{148II}$ group.

5.2.3. 'MBOAT7 NAFLD' (II)

Amongst 7 distinct phosphatidylinositols which were identified in the human liver, concentrations of two species, i.e. PI(36:4) and PI(38:3), decreased significantly as a function of the number of *MBOAT7* variant alleles (**Figure 6**). The concentration of one species, *i.e.* PI(40:5), increased with increasing number of *MBOAT7* variant alleles (**Figure 6**). No significant differences in the concentrations of any other lipid classes, such as triglycerides, cholesterol esters, ceramides, sphingomyelins, hexosylceramides, other phospholipids, or free fatty acids in the liver were observed in the groups based on the *MBOAT7* genotype.

5.2.4. 'TM6SF2 NAFLD' (III)

The increase in the liver fat content in the $TM6SF2^{EK/KK}$ as compared to the $TM6SF2^{EE}$ group (**Table 1**) was predominantly due to an increase in hepatic TG species with saturated and monounsaturated long-chain fatty acyl-groups (**Figure 10**, top panel in the middle).

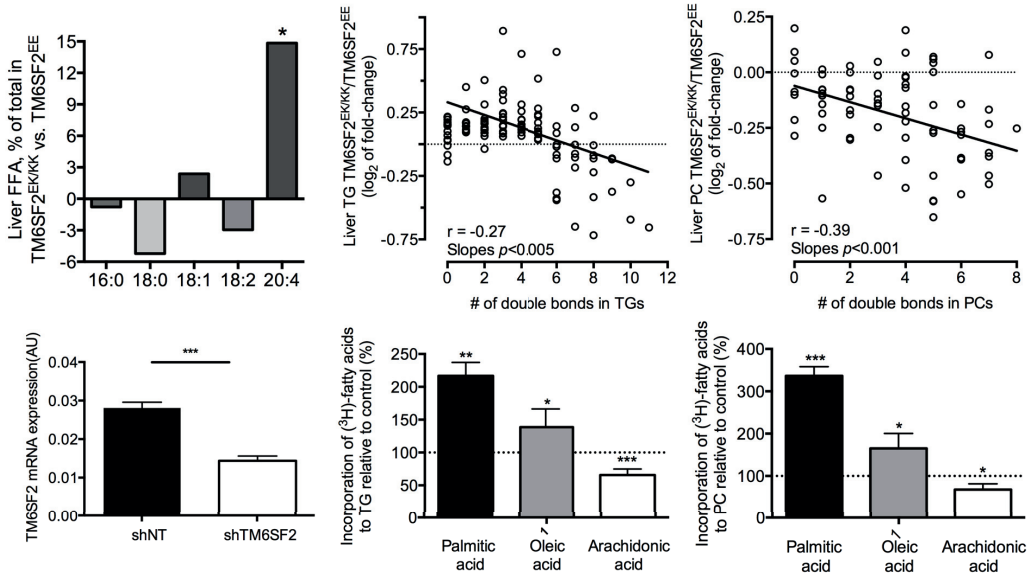

Figure 10. The difference in liver free fatty acids (FFA) as % total in $TM6SF2^{EK/KK}$ as compared to $TM6SF2^{EE}$ (top panel on the left); linear regressions between the number of double bonds in liver TGs and fold-change of liver TG species (top panel in the middle); between the number of double bonds in PCs and fold-change of liver PCs (top panel on the right) in $TM6SF2^{EK/KK}$ and $TM6SF2^{EE}$. *TM6SF2* mRNA expression in control shRNA (shNT) and TM6SF2 shRNA (shTM6SF2) expressing HuH-7 cells (bottom panel on the left). The relative incorporation of (^{3}H)-palmitic acid, (^{3}H)-oleic acid and (^{3}H)-arachidonic acid into triglycerides (bottom panel in the middle), and phosphatidylcholines (bottom panel on the right) expressed in percentage relative to control. Each circle denotes a different lipid. Data are shown as mean ± SD; Student t-test; * $p < 0.05$, ** $p < 0.01$, *** $p < 0.001$. Adapted from Luukkonen *et al., Journal of Hepatology*. 2017; 67:128-136 and reproduced with the permission of Elsevier.

In contrast, concentrations of TGs with 8 or more double bonds, i.e. TGs containing predominantly polyunsaturated fatty acyl-groups were decreased in the TM6SF2$^{EK/KK}$ as compared to the TM6SF2^{EE} group (**Figure 10**, top panel in the middle). As a consequence, the fold-change of concentrations of hepatic TGs between the TM6SF2 groups was inversely correlated (r=-0.27, p<0.005) with the number of double bonds in the TGs (**Figure 10**, top panel in the middle). In addition to TGs, the total concentration of hepatic CEs was significantly higher in the TM6SF2$^{EK/KK}$ as compared to the TM6SF2^{EE} group (+20%, p<0.05).

Total concentration of hepatic phosphatidylcholines (PCs) was significantly lower in the TM6SF2$^{EK/KK}$ as compared to the TM6SF2^{EE} group (-11%, p<0.05). Amongst distinct PC species, concentrations of those with high number of double bonds, i.e. PCs containing predominantly polyunsaturated fatty acyl-groups were decreased in the TM6SF2$^{EK/KK}$ as compared to the TM6SF2^{EE} group (**Figure 10**, top panel on the right). Consequently, the fold-change of concentrations of hepatic PCs between the TM6SF2 groups was inversely correlated with the number of double bonds (r=-0.39, p<0.001) (**Figure 10**, top panel on the right). In addition to the liver, similar inverse correlations between the fold-changes of concentrations of TGs and PCs with the number of double bonds in these lipids were observed in the serum (p<0.0001 for both TGs and PCs).

In contrast to hepatic TGs and PCs, which were characterized by deficiency of species with highly polyunsaturated acyl-chains, the relative abundance of a such fatty acids, i.e. arachidonic acid (C20:4), was significantly higher in the amongst the hepatic free fatty acids in the TM6SF2$^{EK/KK}$ as compared to the TM6SF2^{EE} group (**Figure 10**, top panel on the left).

The absolute concentration of total hepatic free fatty acids was significantly lower in the TM6SF2$^{EK/KK}$ (700 [595 – 822] nmol/g) as compared to the TM6SF2^{EE} group (904 [755 – 1098] nmol/g, p<0.01). Amongst the distinct FFAs, the concentrations of palmitate (16:0, 286 [254 – 346] vs. 383 [307 – 456] nmol/g, p<0.01), stearate (18:0, 131 [125 – 188] vs. 195 [160 – 231] nmol/g, p<0.01), oleate (18:1, 140 [131 – 168] vs. 191 [141 – 247] nmol/g, p<0.05) and linoleate (18:2, 67 [50 – 81] vs. 84 [67 – 102] nmol/g, p<0.05) were significantly lower in the TM6SF2$^{EK/KK}$ as compared to the TM6SF2^{EE} group.

5.3. *IN VITRO* EXPERIMENTS (III)

The relative deficiency of TGs and PCs with polyunsaturated fatty-acyl groups in the liver and serum in the face of relative excess of polyunsaturated fatty acids in the nonesterified pool lead us to consider whether TM6SF2 plays a role in the incorporation of fatty acids into complex lipids, such as TGs and PCs. In the human liver, the expression of *TM6SF2* is decreased in carriers of the E167K variant (Mahdessian *et al.*, 2014). Therefore, we performed *in vitro* experiments in TM6SF2 silenced cells to determine the incorporation of fatty acids with different degree of saturation into complex lipids.

HuH-7 cells were transduced with lentiviral particles expressing short hairpin RNA against *TM6SF2*, which resulted in 52% lower *TM6SF2* mRNA expression than in control HuH-7 cells (p<0.001) (**Figure 10**, bottom panel on the left). The incorporation of palmitic acid (+117 %, p<0.01) and oleic acid (+39%, p<0.05) into TGs in the *TM6SF2* silenced HuH-7 cells were significantly increased, while that of arachidonic acid was significantly decreased (-34%,

p<0.001) (**Figure 10**, bottom panel in the middle). Similarly, the incorporation of palmitic acid (+236%, p<0.001) and oleic acid (+65%, p<0.05) into PCs were increased, while the incorporation of arachidonic acid was significantly decreased in *TM6SF2* knockdown HuH-7 cells as compared to control cells (-32 %, p<0.05) (**Figure 10**, bottom panel on the right). Transient silencing (-78% *TM6SF2* mRNA expression as compared to control cells) of *TM6SF2* with small interfering RNA in HuH-7 cells induced similar changes in fatty acid incorporation into TGs and PCs.

5.4. HEPATIC GENE EXPRESSION (III)

To further elucidate the function of TM6SF2, RNA sequencing was performed in the human liver samples. As reported previously by Mahdessian *et al.,* (Mahdessian *et al.,* 2014), the expression of *TM6SF2* was significantly lower in variant allele carriers as compared to non-carriers as determined from the relationship between *TM6SF2* gene expression and the number of variant alleles at rs58542926, β=-0.41±0.11, p<0.001).

In the pathway analyses of the RNA sequencing data, 3 pathways related to lipids were enriched with genes co-expressing with *TM6SF2*, i.e. 'metabolism of lipids and lipoproteins', 'peroxisomal lipid metabolism' and 'triglyceride synthesis'. Distinct genes whose expression correlated positively with *TM6SF2* (and were therefore decreased in carriers of the TM6SF2 E167K variant) included those associated with synthesis of fatty acids (*fatty acid synthase, acetyl-CoA carboxylase beta*) and triglycerides (*diacylglycerol acyltransferases 1 and 2*), and metabolism of very low-density lipoproteins (*apolipoprotein C-III*). In contrast, genes that correlated negatively with *TM6SF2* (and were therefore increased in carriers of the TM6SF2 E167K variant) included genes related to fatty acid oxidation (*carnitine palmitoyltransferase 1*), *peroxisome proliferator-activator receptors alpha and gamma* and synthesis of polyunsaturated fatty acid-derived eicosanoids (*arachidonate 5-lipoxygenase*).

5.5. METABOLIC EFFECTS OF DIFFERENT OVERFEEDING DIETS (IV)

5.5.1. Macronutrient composition of the diet

At the end of the overfeeding period, fat constituted 60 [54–64] and 59 [53–61] % of total energy intake in the SAT and UNSAT groups. These percentages of fat were 2-fold higher as compared to the CARB group (24 [20–26] %). Saturated fat intake was 2-fold higher in the SAT (33 [28–36] %) compared to the UNSAT (14 [14–18] % (p<0.001) group. Intakes of monounsaturated (28 [23–30] vs. 13 [12–15] %, UNSAT vs. SAT, p<0.001) and polyunsaturated (11 [10–14] vs. 5 [4–5] %, respectively, p<0.001) fat were 2-fold higher in the UNSAT compared to the SAT group. The percentage of total energy intake from carbohydrates was 2.8-fold higher in the CARB (64 [58–68] %) as compared to the UNSAT (23 [19–29] %, p<0.001) or the SAT (26 [23–32] %, p<0.001) groups.

5.5.2. Fatty acid composition of VLDL-TG

In addition to dietary records, analysis of fatty acid composition of fasting plasma VLDL-TG was used to as an objective marker of recent dietary intake to monitor compliance (**Figure 11**). During the SAT diet, the relative abundance of saturated fatty acids C16:0 (26.2±1.0 vs. 30.7±1.0 mol% (p<0.001)), C18:0 (3.1±0.3 vs. 4.1±0.3 mol% (p<0.01)) and C14:0 (1.8±0.2 vs. 4.8±0.5 mol% (p<0.001)) in VLDL-TG increased

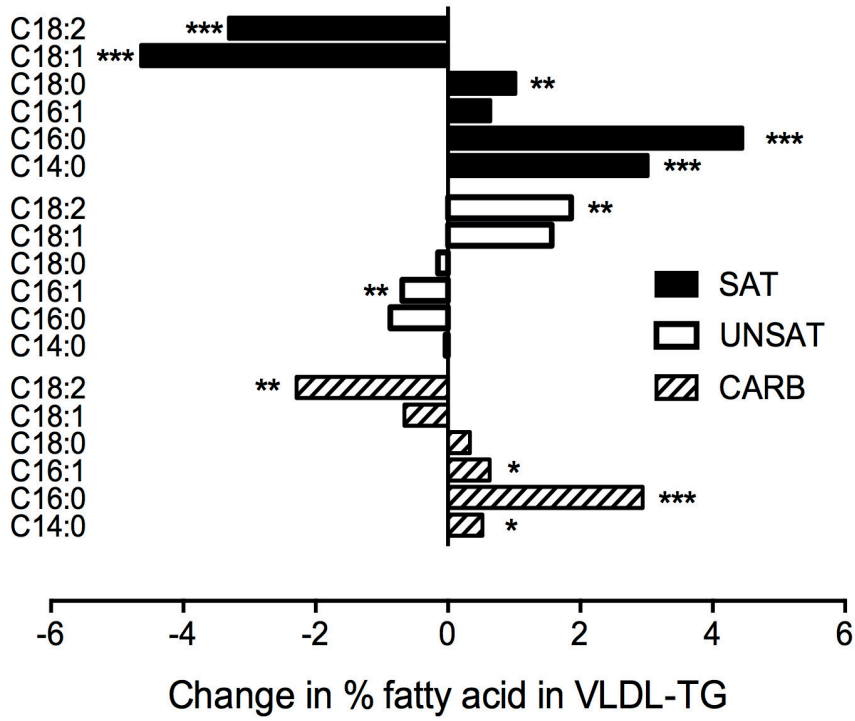

Figure 11. Overfeeding-induced changes in fatty acid composition of VLDL-TG in the groups. Black bars denote the saturated fat (SAT); white bars the unsaturated fat (UNSAT); and hatched bars the simple sugar (CARB) group. The x-axis shows the change in % FA in VLDL-TG after versus before overfeeding and the y-axis the specific fatty acids in VLDL-TG. * p<0.05, ** p<0.01, *** p<0.001. © 2018 by the American Diabetes Association ®. Adapted from Luukkonen *et al., Diabetes Care* 2018 May; dc180071 and reproduced with the permission from the American Diabetes Association ®.

significantly. The abundance of unsaturated fatty acids C18:1 and C18:2 decreased significantly during the SAT diet. During the UNSAT diet, the relative abundance of unsaturated fatty acid C18:2 increased significantly (p<0.01). During the CARB diet, the abundance of C16:0, C14:0 and C16:1 increased, while that of C18:2 decreased significantly (p<0.05) (**Figure 11**).

5.5.3. Body composition and energy expenditure

In all subjects, body weight increased by 1.4±0.2 % from 92.1±2.8 to 93.3±2.8 kg (p<0.001). The increases in body weight were 1.4±0.3 kg in the SAT, 0.9±0.3 kg in the UNSAT and 1.4±0.5 kg in the CARB groups (NS). Visceral and subcutaneous fat contents did not change significantly during overfeeding.

In all subjects, overfeeding increased resting energy expenditure significantly from 7.49±0.22 to 7.62±0.24 MJ/day (p<0.05). Rates of substrate oxidation expressed per kg body weight or fat free mass did not change with overfeeding. The non-protein respiratory quotient remained unchanged.

5.5.4. Liver fat content

Intrahepatic triglyceride content increased by 55% (4.9±1.8 vs. 7.6±2.4% ($p<0.001$)) in the SAT group, by 15% (4.8±1.4 vs. 5.5±1.4% ($p<0.02$)) in the UNSAT group, and by 33% (4.3±1.3 vs. 5.7±1.6% ($p<0.02$)) in the CARB group. The increase in intrahepatic triglyceride content was significantly greater in the SAT as compared to the UNSAT group ($p<0.01$). This difference was independent of changes in body weight as determined from the significantly different intercepts between the regression lines relating change in IHTGs and change in body weight in the SAT as compared to the UNSAT group ($p<0.05$).

5.5.5. *De novo* lipogenesis and adipose tissue lipolysis

Hepatic *de novo* lipogenesis increased significantly during the CARB diet (96 [47–116] vs. 190 [61–303] µmol/L, $p<0.05$) but not during the other diets (**Figure 12**).

In the basal state, whole-body glycerol rate of appearance (R_a) remained unchanged in all groups. After overfeeding compared to baseline, whole-body glycerol R_a during euglycemic hyperinsulinemia increased in the SAT (2.08±0.12 vs. 2.31±0.16 µmol/kg·min, $p<0.05$), decreased in the UNSAT (2.59±0.25 vs. 2.14±0.22 µmol/kg·min, $p<0.05$), and did not change in the CARB (2.15±0.21 vs. 2.27±0.19 µmol/kg·min, p=NS) group (**Figure 12**). Whole-body glycerol R_a during hyperinsulinemia increased significantly more in the SAT compared to the UNSAT ($p<0.001$) and the CARB compared to the UNSAT ($p<0.01$) group (**Figure 12**).

5.5.6. Insulin resistance

HOMA-IR, a marker of insulin resistance, increased significantly during the overfeeding in the SAT group by 23% (1.9 [1.3–3.2] vs. 2.2 [1.4–3.3], $p<0.05$), but remained unchanged in the other groups (**Figure 12**).

5.5.7. Ceramides and endotoxemia

Total plasma ceramide concentration increased significantly by 49% in the SAT group with overfeeding ($p<0.001$, **Figure 12**). There were no changes in total plasma ceramides in the other groups. The increase in total plasma ceramides was significantly higher in the SAT compared to the UNSAT ($p<0.05$) or CARB ($p<0.001$) groups. This difference was independent of changes in body weight as determined from significantly different intercept of the regression lines between changes in total plasma ceramides and those in body weight in the SAT as compared to the UNSAT ($p<0.05$) or the CARB ($p<0.001$) groups. The increase in total plasma ceramides in the SAT groups was due to increases in several long-chain ceramides and dihydroceramides (markers of *de novo* ceramide synthesis).

Regarding circulating lipids, plasma HDL cholesterol increased significantly by 17% in the SAT group (+0.3±0.1 mmol/l, $p<0.01$ for after vs. before) but not in the other groups. Plasma LDL cholesterol increased by 10% in the SAT group (+0.3±0.1 mmol/l, $p<0.01$) but not in the other groups. Plasma triglyceride concentrations remained unchanged in all groups.

The ratio of serum lipopolysaccharide-binding protein and soluble cluster of differentiation 14 (LBP-to-sCD14 ratio), a marker of endotoxemia, increased significantly in the SAT group (4.3±0.3 vs. 4.7±0.3, $p<0.01$) and remained unchanged in the UNSAT and CARB groups. The increase in LBP-to-sCD14 ratio was significantly higher in the SAT as compared to the UNSAT ($p<0.05$) or the CARB ($p<0.001$) groups.

Regarding gut microbiota, the abundance of gram-negative *Proteobacteria* increased by 3.6-fold in the SAT group with overfeeding ($p<0.05$). There were no changes in gut microbiota in the other groups.

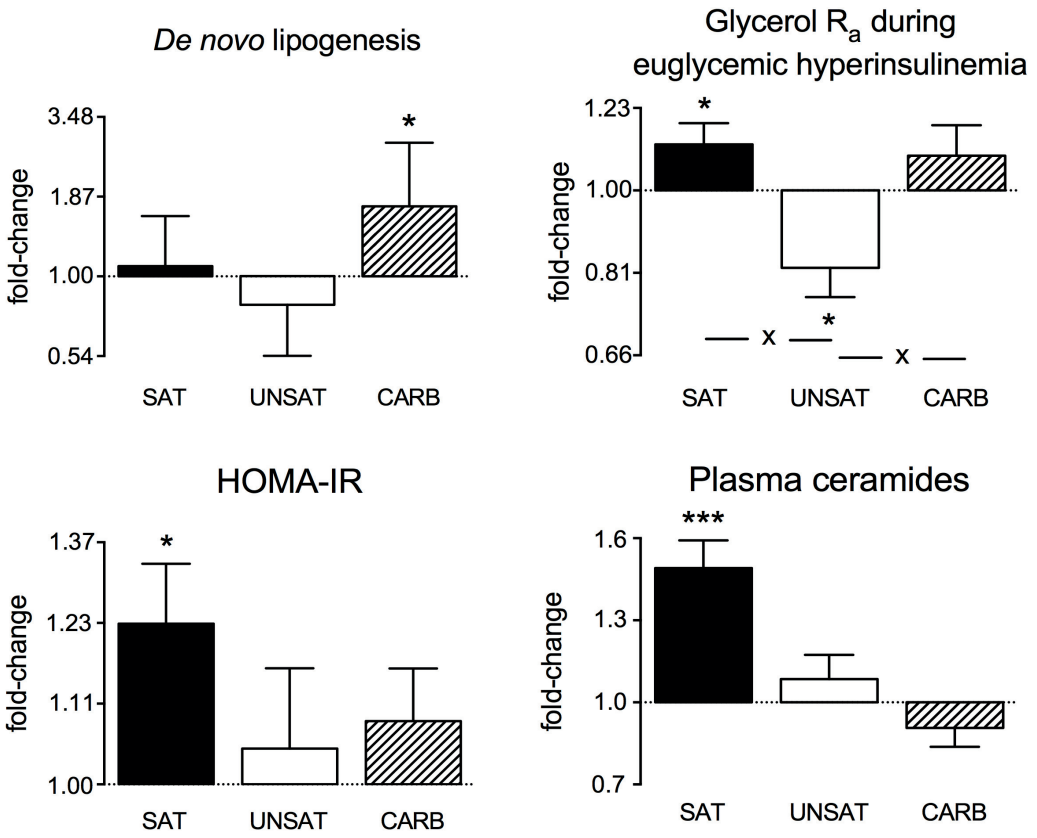

Figure 12. Overfeeding-induced changes in hepatic *de novo* lipogenesis (top panel on the left), glycerol R_a during euglycemic hyperinsulinemia (top panel on the right), HOMA-IR (bottom panel on the left), total plasma ceramides (bottom panel on the right). Black bars denote the saturated fat (SAT), white bars the unsaturated fat (UNSAT), and hatched bars the simple sugar (CARB) group. The y-axes indicate fold-change of mean values after versus before overfeeding within groups. Data are reported as mean ± SEM. *$p<0.05$, ** $p<0.01$, *** $p<0.001$. X = $p<0.05$ between groups. Adapted from Luukkonen *et al., Diabetes Care* 2018 May; dc180071 and reproduced with the permission from the American Diabetes Association ®.

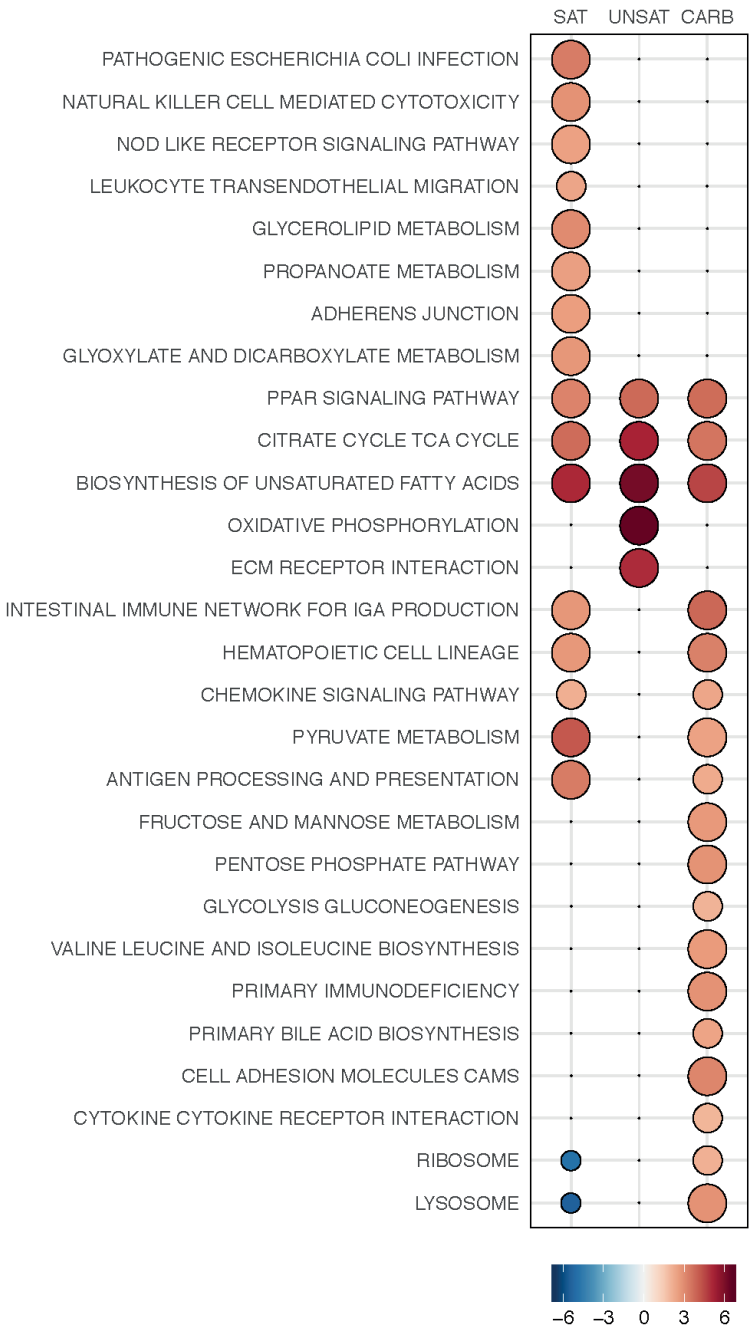

Figure 13. Overfeeding-induced changes in adipose tissue transcriptome in the groups. The bubble grid depicts the reporter test statistics (proportional to size and color intensity) comparing post- relative to pre-overfeeding gene expression. Only the pathways which were significant at <5% false discovery rate in at least one diet are shown. SAT = saturated fat, UNSAT = unsaturated fat, CARB = simple sugar group. Adapted from Luukkonen *et al., Diabetes Care* 2018 May; dc180071 and reproduced with the permission from the American Diabetes Association ®.

5.5.8. Adipose tissue gene expression

A total of 28 reporter pathways out of 134 KEGG pathways were identified in the gene set analysis at a 5% false discovery rate. Both the SAT and CARB diets changed 18 pathways, and the UNSAT diet changed 5 pathways. These changes were highly specific for each of the diets, and only 3 pathways overlapped between all diets (**Figure 13**). The SAT diet upregulated pathways related to inflammation, such as 'pathogenic E. coli infection', 'natural killer cell mediated cytotoxicity', 'NOD like receptor signaling pathway' and 'leukocyte transendothelial migration', and also to 'glycerolipid metabolism'. Changes in some pathways related to inflammation, such as 'antigen processing and presentation', 'chemokine signaling pathway', and 'hematopoietic cell lineage' were similar in the SAT and CARB groups. In addition, the CARB diet upregulated pathways related to carbohydrate metabolism, such as 'fructose and mannose metabolism', 'pentose phosphate pathway' and 'glycolysis gluconeogenesis'. The UNSAT diet upregulated pathways such as 'oxidative phosphorylation' and 'ECM receptor interaction' **(Figure 13)**.

6. DISCUSSION

Insulin-resistant NAFLD is associated with features of the metabolic syndrome and an increased risk of type 2 diabetes and cardiovascular disease ('Metabolic NAFLD') (Yki-Järvinen 2014). In contrast, NAFLD due to the common genetic variants in PNPLA3, MBOAT7 and TM6SF2 ('PNPLA3 NAFLD', 'MBOAT7 NAFLD' and 'TM6SF2 NAFLD', respectively) is not associated with any of these features (Sookoian *et al.,* 2011; Mancina *et al.,* 2016; Kozlitina *et al.,* 2014). All subtypes of NAFLD increase the risk of NASH, liver cirrhosis and hepatocellular carcinoma. The present series of studies aimed to determine whether these marked differences in the phenotypes in 'Metabolic NAFLD', 'PNPLA3 NAFLD', 'MBOAT7 NAFLD' and 'TM6SF2 NAFLD' is associated with distinct hepatic lipidomes that could offer insights to the underlying mechanisms. In addition, while excess energy intake is the major risk factor for NAFLD, not all obese subjects develop NAFLD (Yki-Järvinen, 2014). Study IV was undertaken to investigate the effect of dietary macronutrient composition on the metabolic effects of a hypercaloric diet.

6.1. 'METABOLIC NAFLD'

In study I, the human liver lipidome was analyzed in two subtypes of NAFLD, one defined based on insulin resistance ('Metabolic NAFLD') and the other based on the PNPLA3 genotype at rs738409 ('PNPLA3 NAFLD', *vide infra*). Both subtypes of NAFLD had a similar increase in liver fat content and prevalence of NASH as compared to respective control groups. In addition, the subtypes were characterized by almost identical sample size, age, gender distribution and body mass index, thereby allowing study of effects of insulin resistance and those of the PNPLA3 I148M gene variant on the human liver lipidome independent of these confounders (**Table 1, Figure 5**).

In 'Metabolic NAFLD', the liver lipidome was enriched in saturated and monounsaturated TGs and free fatty acids (**Figure 7**). The liver in 'Metabolic NAFLD' was also characterized by a marked increase in insulin resistance-inducing DAGs and ceramides synthesized *via* the *de novo* ceramide synthetic pathway (**Figures 8 and 9**).

To investigate the effect of insulin resistance on the human liver lipidome in 'Metabolic NAFLD', the subjects were divided based on median HOMA-IR, a marker of insulin resistance. Median value was selected because of the lack of universally accepted cutoff threshold of HOMA-IR between insulin-sensitive and insulin-resistant subjects.

By definition, subjects in the 'High HOMA-IR' group were more insulin resistant than those in the 'Low HOMA-IR' group (**Table 1**). The 'High HOMA-IR' group was characterized by a 3-fold increase in liver fat content and a higher plasma triglyceride concentrations and lower plasma HDL cholesterol concentrations as compared to the 'Low HOMA-IR' (**Table 1, Figure 5**). These data are consistent with previous reports showing associations between insulin resistance, liver fat content, hypertriglyceridemia and low HDL cholesterol concentrations (Seppälä-Lindroos *et al.,* 2002; Kotronen *et al.,* 2007).

Although there are no previous reports regarding the human liver lipidome in NAFLD defined by insulin resistance, the enrichment in saturated and monounsaturated lipid species is consistent with a previous study with 18 subjects with NAFLD and 9 controls (Puri *et al.,* 2007). The liver biopsies were obtained after an overnight fast, when adipose tissue lipolysis and *de novo* lipogenesis are the major sources of fatty

acids for synthesis of IHTGs (Donnelly *et al.,* 2005). The majority of the fatty acids in adipose tissue TGs are saturated (approximately 25%) or monounsaturated (approximately 50%) (Hodson *et al.,* 2008). DNL produces exclusively saturated fatty acids from non-lipid substrates such as simple sugars and amino acids (Hellerstein *et al.,* 1996). These saturated fatty acids can be metabolized into monounsaturated fatty acids by stearoyl-CoA desaturase 1 (SCD-1) (Hellerstein *et al.,* 1996). Thus, the increase in free saturated and monounsaturated fatty acids in the 'High HOMA-IR' vs. the 'Low HOMA-IR' group could reflect increases in both lipolysis and DNL. These data are consistent with previous studies reporting impaired insulin-mediated suppression of adipose tissue lipolysis (Marchesini *et al.,* 2001; Seppälä-Lindroos *et al.,* 2002; Bugianesi *et al.,* 2005; Gastaldelli *et al.,* 2007; Kotronen *et al.,* 2008) and increased rates of hepatic DNL (Diraison *et al.,* 2003; Lambert *et al.,* 2014) in subjects with high liver fat content as compared to those with low liver fat content.

The concentrations of virtually all hepatic ceramide species were significantly increased in the 'High HOMA-IR' vs. the 'Low HOMA-IR' group (**Figure 8**). Previous human studies have failed to detect correlation between hepatic ceramide concentrations and insulin resistance. This may be due to small sample sizes in these studies, with 37 (Kumashiro *et al.,* 2011), 16 (Magkos *et al.,* 2012) and 29 (ter Horst *et al.,* 2017) subjects, *i.e.* much smaller than in the present study (N=125). Most importantly, the former two studies did not measure the concentrations of individual species of ceramides, of which only distinct ones have been associated with insulin resistance in mice (Hla *et al.,* 2014; Xia *et al.,*2015). Only one study in addition to the present study has examined the correlation of individual hepatic ceramide species and insulin resistance in humans (ter Horst *et al.,* 2017). In this study, both total hepatic ceramides and total hepatic DAGs tended to be higher in the insulin resistant as compared to insulin sensitive subjects, but statistical significance was not reached in either comparison, and no correlation was found between hepatic ceramide species and insulin resistance. The authors concluded that these conflicting results may be due to experimental techniques or limited sample size (ter Horst *et al.,* 2017).

The *de novo* ceramide synthetic pathway, as determined from increased hepatic concentrations of 4 out of 5 dihydroceramides, was increased in the 'High HOMA-IR' as compared to the 'Low HOMA-IR' group, while markers of the other pathways were unchanged (**Figure 9**). This is consistent with the increase in the availability of the first substrate in this pathway, i.e. free palmitate (C16:0). There are no previous reports on the distinct ceramide synthetic pathways in the human liver. In high-fat diet-fed mice, both whole-body and liver-specific knockout of *CerS6* decreases concentrations of hepatic C16:0-ceramides (i.e. ceramides with C16:0 fatty-acyl group) and increases fatty acid oxidation and glucose tolerance (Turpin *et al.,* 2014). Along the same lines, heterozygous *CerS2* knockout mice fed a high-fat diet have increased hepatic C16:0-ceramide concentrations, decreased lipid oxidation, decreased glucose tolerance and hepatic steatosis (Raichur *et al.,* 2014). In addition, knockdown of *CerS6* by anti-sense oligonucleotides in mice decreases *CerS6* expression by ~80% selectively in the liver and decreases hepatic C16:0-ceramide concentration by ~50% and increases glucose tolerance by ~50% as compared to control mice (Bielohuby *et al.,* 2017). The increase in the C16:0-dihydroceramides and C16:0-ceramides in the human liver in the 'High HOMA-IR' as compared to the 'Low HOMA-IR' group (**Figure 9**) is compatible with

these reports in mice.

Hepatic ceramide concentrations may also increase if their degradation is reduced. Adiponectin, an insulin-sensitizing adipokine (Scherer *et al.,* 1995), regulates ceramide metabolism *via* ceramidase activity (Holland *et al.,* 2011, Holland *et al.,* 2017) (**Figure 3**). Serum concentrations of adiponectin were lower in the 'High HOMA-IR' group as compared to the 'Low HOMA-IR' group (**Figure 5**), which could contribute to the differences in hepatic concentrations of ceramides in the groups. The present data are consistent with a recent study in mice, in which overexpression of acid ceramidase in the liver was characterized by reduced hepatic concentrations of C16:0-, C18:0- and C20:0-ceramides, decreased liver fat content and hepatic glucose production, and improved glucose tolerance as compared to control mice (Xia *et al.,* 2015).

The concentrations of 4 out of 5 hepatic DAG species (DAG(32:1), DAG(34:1), DAG(36:2) and DAG(36:3)) were increased in the 'High HOMA-IR' as compared to the 'Low HOMA-IR' group. Subjects with NAFLD have been previously shown to have increased hepatic DAG concentrations as compared to healthy controls (Kotronen *et al.,* 2009; Puri *et al.,* 2007). One study reported an increase in hepatic DAGs with 32 to 36 carbons and 0 to 3 double bonds in steatotic as compared to normal liver. These data are consistent with the present data, and also with previous smaller studies reporting correlation of hepatic DAG concentrations and insulin resistance in 37 (Kumashiro *et al.,* 2011), 16 (Magkos *et al.,* 2012) and 29 (ter Horst *et al.,* 2017) subjects. The latter study reported the correlation between 13 distinct cytosolic DAG species and insulin resistance, and found significant correlation in four: DAG(34:1), DAG(36:0), DAG(32:0) and DAG(36:2), two of which are the same as those reported in the present study (DAG(34:1) and DAG(36:2)).

A limitation in the present study, although representing the largest hitherto performed study on the human liver lipidome, is that the hepatic lipids were not measured in different subcellular compartments, in which they may confer differential metabolic effects. Also, some bioactive lipid species, such as eicosanoids, were not analysed in the present study. In addition, the majority of the subjects in the present study were women (66 %), which is not representative of epidemiologic studies, which report NAFLD to be more prevalent in men than in women (Lazo *et al.,* 2013). However, the gender distributions were similar between the subgroups (**Table 1**). Another limitation is that the subjects were bariatric surgery patients, and therefore morbidly obese, which is not representative of population. However, this can also be considered as strength since all subjects were very similar with respect to body mass index, thus allowing analyses independent of BMI.

In summary, the present data show that insulin resistance is associated with an excess of saturated and monounsaturated free fatty acids and triglycerides as well as ceramides and DAGs in the human liver. Ceramides originate especially from the *de novo* ceramide synthetic pathway. These data are consistent with previous reports in mice and with several known pathophysiological features of the human 'Metabolic NAFLD'.

6.2. 'GENETIC NAFLD'

6.2.1. 'PNPLA3 NAFLD'

In a contrast to 'Metabolic NAFLD', the liver in 'PNPLA3 NAFLD' was enriched with polyunsaturated TAGs with no changes in free fatty acids or ceramides (**Figures 7 and 8**).

To investigate the effect of the PNPLA3 I148M variant on the human liver lipidome in 'PNPLA3 NAFLD', the subjects were divided based on their PNPLA3 genotype at rs738409. Approximately 49 % of the study subjects carried the variant allele, in keeping with previous reports showing 20-50 % of all subjects carry this gene variant (Romeo *et al.,* 2008). The 'PNPLA3$^{148MM/MI}$' group (variant allele carriers) as compared to 'PNPLA3^{148II}' group (non-carriers), had a similarly 3-fold higher liver fat content as the 'High HOMA-IR' ('Metabolic NAFLD') compared to the 'Low HOMA-IR' group (**Table 1, Figure 5**). In contrast to the 'Metabolic NAFLD', there were no differences in insulin resistance as determined from HOMA-IR, Matsuda insulin sensitivity index and the glucose and insulin concentrations during the oral glucose tolerance test, or in concentrations of plasma lipids and serum adiponectin (**Table 1, Figure 5**). This is consistent with a recent systematic review of 14 studies showing that insulin sensitivity, as determined by HOMA-IR, the hyperinsulinemic-euglycemic clamp method, or fasting or post-glucose insulin or glucose concentrations, does not differ between carriers and non-carriers (Petäjä *et al.,* 2016). Regarding plasma triglycerides, the present study supports the majority of previous studies reporting unchanged total triglyceride concentrations in variant allele carriers (Petäjä *et al.,* 2016).

Livers of the variant allele carriers were markedly enriched with polyunsaturated TGs as compared to non-carriers (**Figure 7**). One previous study characterized relative fatty acid composition of hepatic TGs using thin layer chromatography between 19 carriers of the PNPLA3 I148M variant allele and 33 non-carriers undergoing liver surgery (Peter *et al.,* 2014). A decrease in the relative abundance of stearic acid was found in keeping with the present data. However, the subjects in this study were not characterized with respect to insulin resistance or hepatic ceramides and the hepatic TGs were not analyzed with respect to number of carbons and double bonds.

Concentrations of hepatic free fatty acids, which accounted for 80% of previously described free fatty acids and 87% of all free polyunsaturated fatty acids in the human liver (Puri *et al.,* 2007), were unchanged between the PNPLA3 groups. These data are consistent with a previous report showing unchanged adipose tissue insulin sensitivity in carriers as compared to non-carriers of the variant (Kotronen *et al.,* 2009), and supports the idea that the increase in polyunsaturated hepatic TGs in 'PNPLA3 NAFLD' is induced by mechanisms other than substrate availability.

One study suggested that PNPLA3 functions as a lysophosphatidic acid acyltransferase (LPAAT) converting lysophosphatidic acid into phosphatitidic acid with palmitoyl-, oleyl-, linoleyl- and arachidonyl-CoAs as the preferred substrates, and the I148M variant to increase this activity by two-fold (Kumari *et al.,* 2012). The increase in multiple hepatic polyunsaturated TGs and in one polyunsaturated DAG species (DAG(36:3)) in carriers as compared to non-carriers could be consistent with this study. However, subsequent studies have failed to replicate the LPAAT activity of PNPLA3 (Li *et al.,* 2012; BasuRay *et al.,* 2017).

In addition to LPAAT activity, PNPLA3 has been reported to hydrolyze TGs, DAGs, monoacylglycerols and oleyl-CoA, and the I148M to impair these functions (Huang *et al.,* 2011). Amongst distinct TG species, PNPLA3 hydrolysed TGs containing C14:0, C16:0, C18:1, C18:2 and C20:4, of which TGs containing C18:1 were the preferred substrates (Huang *et al.,* 2011). This mechanism could contribute to the hepatic TG profile seen

in carriers of the PNPLA3 I148M variant.

However, since neither the deletion nor the overexpression of the wild-type PNPLA3 results in hepatic steatosis, the effects of the PNPLA3 I148M variant may not be attributable simply to a loss or gain of the activity of the wild type PNPLA3 (Chen *et al.,* 2011; Basantani *et al.,* 2011; Li *et al.,* 2012). Recently, the I148M variant was suggested to disrupt proteosomal degradation of PNPLA3, leading to accumulation of the PNPLA3 protein in lipid droplets, and thereby to induce steatosis by impairing mobilization of TGs from lipid droplets (BasuRay *et al.,* 2017). The exact pathophysiological mechanism by which PNPLA3 I148M induces NAFLD in humans remains to be solved.

Etiology of liver injury. The subjects with 'Metabolic NAFLD' and 'PNPLA3 NAFLD' had an equal prevalence of NASH (**Table 1**) despite very different hepatic TG and bioactive lipid compositions (**Figures 7 and 8**). Thus, bioactive lipids such as ceramides and DAGs do not seem to be necessary for the development of NASH in carriers of the PNPLA3 I148M variant. Previous studies have established that the PNPLA3 gene variant predisposes to NASH independent of features insulin resistance (Sookoian *et al.,* 2011). Simple steatosis without hepatocellular injury has been shown in a paired-biopsy study to predict the development of NASH (McPherson *et al.,* 2015). In NASH, fat accumulates first in the perivenous area in Zone 3 (Brunt *et al.,* 1999), which is characterized by impaired microcirculation (Farrell *et al.,* 2008) and a lower oxygen concentration as compared to periportal areas (Jungermann *et al.,* 2000). Ballooning necrosis, the distinct feature of NASH, occurs amidst these fat-laden hepatocytes (Brunt *et al.,* 1999). The PNPLA3 gene variant could therefore increase the risk of NASH simply by increasing steatosis.

In summary, the human liver lipidome in 'PNPLA3 NAFLD' is enriched with polyunsaturated TGs. In contrast to the 'Metabolic NAFLD', the 'PNPLA3 NAFLD' is not enriched in bioactive lipids although both types of NAFLD similarly increase the prevalence of NASH, suggesting that these lipids are not required for the development of NASH.

6.2.2. 'MBOAT7 NAFLD'

In study II, the *MBOAT7* variant allele at rs641738 was associated with increased severity of NAFLD in 115 morbidly obese subjects. Histological characteristics that were significantly altered included steatosis, necroinflammation and fibrosis. Especially the prevalence of moderate or more severe liver fibrosis increased as a function of the number of variant alleles carried (**Figure 6**). The groups based on the MBOAT7 genotype were similar with respect to body mass index, waist circumference, and circulating concentrations of insulin, glucose and lipids. Regarding hepatic lipidome, the variant allele carriers had changes exclusively in polyunsaturated phosphatidylinositols. Concentrations of all other lipid classes in the liver were unchanged. Specifically, the hepatic concentrations of PI(36:4) and PI(38:3) were reduced, while that of PI(40:5) was increased in carriers of the variant allele as compared to non-carriers.

The findings are consistent with recent studies reporting increased severity of NAFLD in carriers of the MBOAT7 variant allele at rs641738 (Mancina *et al.,* 2016; Krawczyk *et al.,* 2017). The increase in the prevalence of moderate or more severe liver fibrosis is of particular concern, since fibrosis has been repeatedly shown to be the major determinant of overall and liver-related mortality in subjects with NAFLD (Dulai *et al.,* 2017; Hagström *et al.,* 2017).

The present data are also compatible with previous studies with up to 4,591 subjects reporting no differences in body composition, markers of insulin sensitivity or circulating lipids in carriers as compared to non-carriers of the MBOAT7 variant allele (Mancina *et al.,* 2016; Di Costanzo *et al.,* 2018). Despite an increased risk and severity of NAFLD, and in contrast to the 'Metabolic NAFLD', carriers of the variant allele have an unaltered risk of cardiovascular disease as compared to non-carriers (Simons *et al.,* 2017). This dissociation may in part be due to unaltered insulin sensitivity and circulating lipids, and lack of change in harmful bioactive lipids in the liver such as ceramides, which are associated with risk of cardiovascular disease (Summers, 2018).

In addition to replicating results from earlier studies, study II extends previous data by showing distinct alterations in polyunsaturated PIs in livers of carriers of the MBOAT7 variant allele. MBOAT7, also known as lysophosphatidylinositol acyltransferase 1 (LPIAT1), functions in the acyl-chain remodeling of PIs and incorporates a polyunsaturated arachidonic acid into a lyso-PI to form a polyunsaturated PI (Lee *et al.,* 2008). Carriers of the variant allele have lower expression of *MBOAT7* in the liver as compared to non-carriers, and therefore are hypothesized to have decreased activity of this enzyme (Mancina *et al.,* 2016).

In theory, decreased activity of an arachidonic acid-preferring lysophosphatidylinositol acyltransferase could increase the availability of free arachidonic acid (Robichaud *et al.,* 2015). Arachidonic acid activates collagen gene expression time- and dose-dependently in rat stellate cells overexpressing ethanol-inducible cytochrome P450 2E1 (Nieto *et al.,* 2000). In contrast, knockout of group IVA phospholipase A_2, which removes arachidonic acid from phospholipids, reduces the availability of free arachidonic acid and prevents stellate cell activation and hepatic macrophage infiltration in C57BL/6JJcl mice injected with carbon tetrachloride or fed a high-fat, high-cholesterol diet (Ishihara *et al.,* 2012). Arachidonic acid can be metabolized into bioactive lipid mediators such as eicosanoids, which concentrations are increased in the circulation of subjects with NASH (Puri *et al.,* 2009; Loomba *et al.,* 2015). Further studies are needed to determine whether the availability of free arachidonic acid or some other mechanism mediates the increased susceptibility to NAFLD and liver fibrosis due to altered hepatic phosphatidylinositol remodeling.

To summarize, study II confirms that the common variant in *MBOAT7* at rs641738 associates with histologically determined liver damage, particularly significant fibrosis. The study extends previous data by showing that altered polyunsaturated PI metabolism characterizes livers of carriers of the variant allele. These data are compatible with reports in plasma and a role for MBOAT7 in hepatic phosphatidylinositol remodeling (Mancina *et al.,* 2016).

6.2.3. 'TM6SF2 NAFLD'

Carriers of the TM6SF2 E167K variant allele had higher hepatic TGs and CEs but lower hepatic PCs due to a decrease in polyunsaturated PCs. In addition to PCs, polyunsaturated fatty acyl-groups were also deficient hepatic TGs, but relatively enriched amongst hepatic free fatty acids. Consistent with this *in vivo* finding, knockdown of *TM6SF2* in HuH-7 cells decreased incorporation of PUFAs into PCs and TGs *in vitro*. In the human liver, *TM6SF2* was downregulated in variant allele carriers and co-expressed with genes regulated by PUFAs. Thus, *TM6SF2* downregulation may impair hepatic lipid synthesis from PUFAs, thereby leading to a relative deficiency of polyunsaturated

PCs and a relative excess of free PUFAs, both of which may disrupt hepatic export of TGs and CEs and lead to their accumulation (Noga *et al.,* 2003; Pan *et al.,* 2004).

To investigate the effect of the TM6SF2 E167K variant on the human liver lipidome in 'TM6SF2 NAFLD', the subjects were divided based on their *TM6SF2* genotype at rs58542926 ('TM6SF2$^{EK/KK}$', variant allele carriers and 'TM6SF2^{EE}', non-carriers). Carriers of the variant variant allele had 2-fold higher liver fat content as compared to non-carriers (**Table 1**). In contrast to 'Metabolic NAFLD, the groups did not differ with respect to insulin sensitivity as determined by HOMA-IR or the Matsuda index (**Table 1**). Preserved insulin sensitivity is consistent with previous reports (Kozlitina *et al.,* 2014; Zhou *et al.,* 2015; Sookoian *et al.,* 2015; Goffredo *et al.,* 2016; Grandone *et al.,* 2016; Eslam *et al.,* 2016; Mancina *et al.,* 2016; Musso *et al.,* 2016; Dongiovanni *et al.,* 2015; Kim *et al.,* 2017; Petäjä *et al.,* 2016). The distribution of the PNPLA3 genotype was also similar between the groups.

Consistent with previous studies involving up to 400 subjects (Zhou *et al.,* 2015; Sookoian S *et al.,* 2015; Musso *et al.,* 2016; Goffredo *et al.,* 2016), fasting plasma triglyceride concentrations were similar in the *TM6SF2* genotype groups (**Table 1**). However, in larger studies, the variant allele has been associated with decreased concentrations of plasma triglycerides (Kozlitina *et al.,* 2014; Grandone *et al.,* 2016; Eslam *et al.,* 2016; Mancina *et al.,* 2016; Dongiovanni *et al.,* 2015; Kim *et al.,* 2017; O'Hare *et al.,* 2017; Liu *et al.,* 2017; Di Costanzo *et al.,* 2018). In the present study, variant allele carriers displayed relative deficiency of circulating polyunsaturated TGs and PCs as compared to non-carriers. This deficiency in the face of increased hepatic TG content suggests insufficient hepatic lipid export, consistent with previous studies (Kozlitina *et al.,* 2014; Mahdessian *et al.,* 2014; Musso *et al.,* 2016; Musso *et al.,* 2017; O'Hare *et al.,* 2017; Kim *et al.,* 2017).

Livers of TM6SF2 E167K variant carriers had a relative deficiency of polyunsaturated TG and PC species, while the relative abundance of free polyunsaturated fatty acid C20:4 was increased as compared to non-carriers (**Figure 10**). In *TM6SF2* silenced HuH-7 cells, the incorporation of PUFAs into both PCs and TGs were decreased (**Figure 10**). These data suggest that the TM6SF2 E167K variant may coordinate the channeling of PUFAs into PC and TG synthesis. In keeping with these findings *in vivo* in humans and *in vitro* in hepatoma cells, a deficiency in the relative abundance of polyunsaturated fatty acids C20:4 and C22:6 was found in total hepatic lipids in *TM6SF2* knockout mice (Smagris *et al.,* 2016).

This channeling starts by activation of a free polyunsaturated fatty acid into a fatty acyl-CoA by one of numerous *acyl-CoA synthetase* (ACS) enzymes (Cooper *et al.,* 2015). These isoenzymes have different substrate preferences and subcellular localisations, and thereby channel distinct fatty acids into different metabolic pathways (Ellis *et al.,* 2010; Cooper *et al.,* 2015). For example, knockdown of *acyl-CoA synthetase long-chain family member 3* (*ACSL3)*, which is expressed in the liver and intestine and localized in the endoplasmic reticulum similarly to *TM6SF2*, decreases incorporation of unsaturated fatty acids into PC, causes PC deficiency, and inhibits the secretion of apolipoprotein B, the major component of VLDL, in HuH-7 cells (Yao *et al.,* 2008).

In humans, large, lipid-rich $VLDL_1$ particles are markedly deficient in the circulation in the postprandial state in TM6SF2 E167K variant allele carriers compared to non-carriers (Musso *et al.,* 2016). Another study reported that

carriers of the variant have lower circulating concentration of apolipoprotein B100 as well as concentrations of triglycerides and cholesterol in liver-derived VLDL and LDL particles (Kim *et al.,* 2017). This deficiency could result from defects in the assembly, secretion, or pre-secretory degradation of VLDL particles. The assembly of VLDL has two major steps (Olofsson *et al.,* 2012). First, a nascent VLDL particle is synthesized in the ER, where it matures into a relatively lipid-poor small $VLDL_2$ particle (Olofsson *et al.,* 2012). This small particle is translocated to the Golgi complex and may be secreted as such, or undergo a second lipidation step in which more TGs and CEs are added to the particle to form a large, lipid-rich $VLDL_1$ particle (Olofsson *et al.,* 2012). VLDL particles can be degraded before being secreted *via* mechanisms such as post-endoplasmic reticulum pre-secretory proteolysis (Pan *et al.,* 2008).

A relative deficiency of PCs and a relative excess of free polyunsaturated fatty acids could interfere with VLDL metabolism. For example, in isolated mouse hepatocytes, decreased synthesis of PCs due to knockout of *PEMT* increases the post-ER pre-secretory degradation of VLDL particles, and decreases the secretion of especially highly-lipidated VLDL particles (Noga *et al.,* 2003). Similarly, excess polyunsaturated fatty acids induce post-ER pre-secretory degradation of VLDL particles in rat hepatoma or primary rodent hepatocytes by inducing lipid peroxidation and oxidative stress (Pan *et al.,* 2004). Thus, both PC deficiency and the relative excess in polyunsaturated FFA content in the liver in TM6SF2 variant carriers might lead to accumulation of TGs and CEs *via* degradation of lipid-rich VLDL particles, consistent with previous reports (Musso *et al.,* 2016; Kim *et al.,* 2017).
In the human liver, mRNA expression of *TM6SF2* was decreased in the E167K variant carriers, consistent with a previous report (Mahdessian *et al.,* 2014). The expression of genes related to lipogenesis such as *fatty acid synthase, acetyl-CoA carboxylase 2* were decreased, while that related to mitochondrial fatty acid oxidation, i.e. *carnitine palmitoyltransferase I*, was increased. These data are in keeping with a decrease in absolute concentrations of saturated and monounsaturated free fatty acids in the liver in carriers of the E167K variant in the present study. In addition, the expression of *apolipoprotein C-III*, which enhances the lipidation of VLDL particles and inhibits the lipoprotein remnant uptake by the liver, was decreased in variant carriers, providing another possible mechanism for the phenotype seen in E167K variant carriers (i.e. decreased plasma triglycerides in the face of increased liver triglycerides).

Interestingly, all of the observed changes in hepatic gene expression can be induced by polyunsaturated fatty acids (Sampath *et al.,* 2005), which are ligands for transcriptional factors such as peroxisome proliferator-activated receptor alpha (Forman *et al.,* 1997). Indeed, the hepatic expression of *peroxisome proliferator-activated receptor alpha* was increased in the variant carriers, who had excess relative abundance of polyunsaturated fatty acids in the liver.

Interestingly, silencing of *acyl-CoA synthetase long-chain family member 3* (*ACSL3)*, which is expressed in the liver and intestine and localized in the endoplasmic reticulum similarly to *TM6SF2*, decreases incorporation of unsaturated fatty acids into PCs, causes PC deficiency and a relative excess of free unsaturated fatty acids, and inhibits secretion of apolipoprotein B in HuH-7 cells (Yao *et al.,* 2008). Silencing of this gene in rat hepatocytes decrease lipogenic gene expression and *de novo* lipogenesis (Bu *et al.,* 2009). Together, these data

support the idea that differences in hepatic gene expression in carriers of the TM6SF2 E167K variant allele may have been driven by excess polyunsaturated fatty acids secondary to their impaired incorporation into complex lipids.

Consistently with previous studies (Liu *et al.,* 2014; O'Hare *et al.,* 2017), carriers of the TM6SF2 E167K variant allele tended to have increased liver fibrosis as compared to non-carriers (60 vs 31 %, p=0.09). The relative deficiency of PC and the relative excess of arachidonic acid found in the present study could contribute to the development of NASH and fibrosis by several mechanisms. Deficiency of hepatic PCs induced by a methionine-choline-deficient diet induces lipid peroxidation, stellate cell activation and fibrosis in rats (George *et al.,* 2003). As already discussed in **section 6.2.2.**, excess arachidonic acid can stimulate fibrogenesis by regulating stellate cell activation.

Arachidonic acid can be metabolized into proinflammatory eicosanoids (Cooper *et al.,* 2015), which circulating concentrations are increased in subjects with NASH (Puri *et al.,* 2007; Loomba *et al.,* 2015). Expression of *arachidonate 5-lipoxygenase* was increased in the TM6SF2 variant allele carriers in the present study. Interestingly, the corresponding enzyme produces arachidonic acid-derived proinflammatory eicosanoids such as 5-hydroxyeicosatetraenoic acid, which appear increased in NASH (Puri *et al.,* 2007; Loomba *et al.,* 2015).

As a limitation, even though representing the largest study on the human liver lipidome, the number of variant allele carriers was low given the variant allele frequency of 7%. Thus, the observed differences may underestimate true differences between carriers and non-carriers of the *TM6SF2* E167K gene variant.

To summarize, incorporation of polyunsaturated fatty acids into complex lipids is impaired in the livers of the TM6SF2 E167K gene variant carriers and leads to a relative deficiency of polyunsaturated PCs and a relative excess of polyunsaturated FFA in the human liver. These changes, based on a large body of experimental evidence, could impair VLDL lipidation *via* increased degradation, and explain the phenotype characterizing the carriers of the TM6SF2 E167K variant, i.e. hepatic steatosis, lack of circulating hypertriglyceridemia and an increased risk of NASH.

6.3. METABOLIC EFFECTS OF DIFFERENT OVERFEEDING DIETS

Even though obesity is the main acquired risk factor of NAFLD, it does not develop in all overweight subjects (Browning *et al.,* 2004; Rosqvist *et al.,* 2014). In study IV, the aim was to examine whether overfeeding-induced pathways of hepatic fatty acid supply and insulin resistance depend on the macronutrient composition of the diet. Consumption of a hypercaloric diet enriched either with saturated (SAT) or unsaturated fat (UNSAT), or simple sugars (CARB) for 3 weeks increased IHTG content. The macronutrient composition of the diet had a distinct effect on pathways contributing to hepatic fatty acids. Only the CARB diet induced *de novo* lipogenesis, while only the SAT diet stimulated adipose tissue lipolysis (**Figure 12**), which may explain why this diet increased IHTG content more than the UNSAT diet in the face of similar energy excess. The SAT diet was also the only diet to induce insulin resistance, endotoxemia and an increase in plasma ceramides (**Figure 12**) during the 3-week overfeeding period. The diets had also markedly different effects on the adipose tissue transcriptome (**Figure 13**).

The fatty acid composition of VLDL-TGs secreted from the liver after an overnight fast is similar to hepatic TGs and reflects the composition of their sources (Donnelly *et al.,* 2005). In study IV, the fatty acid composition of VLDL-TGs was used as a biomarker of compliance and of the fatty acid composition of hepatic TGs. The SAT diet increased the relative abundance of saturated fatty acids and decreased that of polyunsaturated fatty acids while the UNSAT diet had an opposite effect (**Figure 11**). Similarly to the SAT diet, the CARB diet increased the relative abundance of saturated fatty acids, which are the exclusive products of DNL (Sevastianova *et al.,* 2012), and decreased that of polyunsaturated fatty acids in VLDL-TG. These data demonstrate that subjects were compliant, and are novel in showing that diets with different macronutrient composition have distinct effects on the fatty acid composition of hepatic TGs as determined from that in VLDL-TG. Moreover, compliance was also confirmed by analysis of dietary records.

6.3.1 Effects on sources of hepatic fatty acids

It is well established that overfeeding increases IHTG content (Kechagias *et al.,* 2008; van der Meer *et al.,* 2008; Bortolotti *et al.,* 2009; Sobrecases *et al.,* 2010; Sevastianova *et al.,* 2012; Rosqvist *et al.,* 2014; Fabbrini *et al.,* 2016). Study IV extends previous findings by showing that the magnitude and mechanisms by which overfeeding influences IHTG content depends on the composition of the diet.

In the present study, the SAT diet increased IHTG content significantly more than the UNSAT diet in the face of similar hypercaloric energy intakes and changes in body weight. This greater increase in IHTG in the SAT group as compared to the UNSAT group is in line with a previous report that overfeeding a diet enriched with saturated as compared to polyunsaturated fat induces a greater increase in IHTG (Rosqvist *et al.,* 2014). In an isocaloric study comparing high-saturated fat/low-polyunsaturated fat diet to low-saturated fat/high-polyunsaturated fat, the former increased liver fat content as compared to the latter (Bjermo *et al.,* 2012). Cross-sectionally, higher intakes of saturated fatty acids and cholesterol and lower intakes of fiber, protein and polyunsaturated fatty acids characterize subjects with NASH as compared to age-, gender-, and body mass index-matched controls (Musso *et al.,* 2003). Together these studies suggest that the macronutrient composition of the diet influences the magnitude of ectopic fat deposition in the liver, and that saturated fat induces a greater accumulation of IHTG than unsaturated fat.

Regarding the mechanisms underlying the increased deposition of fatty acids into IHTGs during overfeeding, the fatty acid sources contributing to IHTG need to be considered. Direct measurements using stable isotopes in humans have shown that the majority of the fatty acids in IHTGs in subjects with NAFLD originate from lipolysis (59%) and DNL (26%) (Donnelly *et al.,* 2005).

In the present study, adipose tissue lipolysis increased in response to the SAT diet. There are no previous overfeeding studies measuring lipolysis in humans, but in mice high-fat feeding stimulates lipolysis (Perry *et al.,* 2015). A saturated fat-enriched diet has been reported to increase the expression of inflammation-related genes as compared to a diet enriched with monounsaturated fat in a parallel controlled-feeding trial with 20 abdominally obese subjects (van Dijk *et al.,* 2009). In keeping with these data, the SAT diet induced upregulation in multiple inflammation-related pathways, such as 'pathogenic E. coli infection', 'natural killer cell mediated cytotoxicity', 'NOD

like receptor signaling pathway' and 'leukocyte transendothelial migration' in the adipose tissue. The ability of the SAT but not UNSAT or CARB diet to stimulate lipolysis, the major contributor of fatty acids in IHTG, could explain why the SAT diet increased IHTG to a greater extent than the two other diets.

Overfeeding of simple sugars has been shown to increase DNL and IHTGs (Sevastianova *et al.,* 2012). DNL produces exclusively saturated fatty acids (Hellerstein *et al.,* 1996). Consistent with these data, the CARB diet increased hepatic DNL (**Figure 12**) and the relative abundance of saturated fatty acids in VLDL-TG (**Figure 11**). However, the stimulation of DNL was not able to increase IHTG content to the same extent as the SAT diet, which stimulated adipose tissue lipolysis. These results are consistent with isocaloric studies showing that high-fat, low-carbohydrate diets increase IHTG more than low-fat, high-carbohydrate diets (Westerbacka *et al.,* 2005; van Herpen *et al.,* 2011; Utzschneider *et al.,* 2013) in humans. The carbohydrates consumed in the present study were simple sugars, which may confer different metabolic effects as compared to complex carbohydrates. Therefore the data may not be generalizable to all carbohydrates.

The UNSAT diet did not change the rate of DNL, but surprisingly and in contrast to the other diets, decreased lipolysis during hyperinsulinemia (**Figure 12**). These results and the predominant increase in the abundance of polyunsaturated C18:2 (**Figure 11**), which cannot be synthesized endogenously, in VLDL-TG, suggest that the increase in IHTG during the UNSAT diet was mainly derived from dietary fatty acids. The UNSAT diet induced upregulation in distinct pathways in adipose tissue, such as 'oxidative phosphorylation' (**Figure 13**). This pathway has previously been reported to be downregulated in omental adipose tissue in three obese subjects as compared to three gender-matched controls (Walewski *et al.,* 2010), and upregulated in subcutaneous adipose tissue of 47 healthy men in response to a 6-month exercise intervention (Rönn *et al.,* 2014), implying that it might be a metabolically beneficial pathway. Polyunsaturated fatty acids suppress adipose tissue lipolysis *via* activation of GPR120 receptors in mice (Wang *et al.,* 2017), but the exact mechanism in humans is not known.

6.3.2 Effects on insulin resistance

During the 3-week overfeeding period, the SAT diet induced insulin resistance. Cross-sectionally, high intakes of saturated fat have been shown to associate with insulin resistance in subjects with NASH as compared to age-, gender-, and body mass index-matched controls (Musso *et al.,* 2003). In addition, isocaloric substitution of saturated for monounsaturated fat (Vessby *et al.,* 2001; Pérez-Jiménez *et al.,* 2001), carbohydrates (Vessby *et al.,* 2001), or polyunsaturated fat (Summers *et al.,* 2002) ameliorates insulin resistance. Recently, a large prospective study reported intake of foods enriched in saturated fat, such as butter and cheese, to increase the risk of type 2 diabetes (Guasch-Ferré *et al.,* 2017). Even a single saturated fat-enriched meal compared to water is sufficient to induce insulin resistance in mice and humans (Hernández *et al.,* 2017).

Intrahepatic TGs by themselves are metabolically inert and do not confer insulin resistance (Amaro *et al.,* 2010; Sun *et al.,* 2013; Cohen *et al.,* 2011). In the present study, the SAT diet-induced insulin resistance was associated with a marked increase in circulating ceramides (**Figure 12**). In mice, ceramides mediate saturated fat-induced insulin resistance (Chavez *et al.,* 2012; Xie *et al.,* 2017;

Holland *et al.,* 2011; Holland *et al.,* 2007; Raichur *et al.,* 2014; Turpin *et al.,* 2014; Xia *et al.,* 2015). In keeping with these data, insulin resistance was associated with a marked increases in saturated fatty acids, dihydroceramides (markers of *de novo* ceramide synthesis) and ceramides in the human liver in study I.

In addition to availability of the substrate, i.e. palmitoyl-CoA, the *de novo* ceramide synthetic pathway is upregulated by inflammatory ligands of TLR-4 such as endotoxin, a component of gram-negative bacteria (Holland *et al.,* 2007; Holland *et al.,* 2011). In the present study, the SAT diet induced endotoxemia, as determined from the LBP-to-sCD14 ratio in serum. This is consistent with previous studies demonstrating that endotoxemia occurs in humans in response to a single high-fat meal enriched in butter (Erridge *et al.,* 2007) or cream (Deopurkar *et al.,* 2010) but not after consuming equicaloric amount of orange juice or a dose of water (Deopurkar *et al.,* 2010). Endotoxemia is also induced by a 4-week saturated fat-enriched diet in humans (Pendyala *et al.,* 2012). The upregulation of inflammatory gene expression pathways in adipose tissue during the SAT diet (**Figure 13**) could be a consequence of endotoxemia. In mice, high-fat feeding increases the proportion of endotoxin-containing bacteria in the gut and plasma concentrations of endotoxin, and induces insulin resistance (Cani *et al.,* 2007). Another study in mice reported that saturated but not polyunsaturated fat feeding increases the abundance of gram-negative gut bacteria, and induces endotoxemia, and Toll-like receptor activation and inflammation in the adipose tissue (Caesar *et al.,* 2015). These data suggest that *de novo* synthesis of ceramides induced by increased availability of saturated fatty acids and endotoxin could contribute to SAT diet-induced insulin resistance. The present data showing that the SAT diet stimulates adipose tissue lipolysis and increases HOMA-IR are also consistent with data showing hepatic gluconeogenesis to be indirectly regulated by hepatic acetyl-CoA originating from adipose tissue lipolysis (Perry *et al.,* 2015).

NAFLD increases the risk of cardiovascular disease (Anstee *et al.,* 2013), which is the most common cause of death in subjects with NAFLD (Ekstedt *et al.* 2006). Plasma ceramides have been recently reported in five prospective studies to predict cardiovascular events and death, even independent of LDL cholesterol concentrations (Tarasov *et al.,* 2014; Cheng *et al.,* 2015; Laaksonen *et al.,* 2016; Havulinna *et al.,* 2016; Wang *et al.,* 2017). Increased intake of saturated fat could therefore be harmful to cardiovascular health by increasing both LDL cholesterol and plasma ceramides. This is consistent with the advisory of the American Heart Association, which concluded that reducing the intake of saturated fat by replacing it with unsaturated fat decreases the incidence of cardiovascular disease (Sacks *et al.,* 2017).

In conclusion, overfeeding diets enriched with saturated or unsaturated fat or simple sugars for 3 weeks increases IHTG content, but the magnitude and the associated metabolic changes depend on the macronutrient composition of the diet. Saturated fat induced the highest increase in IHTG by stimulating adipose tissue lipolysis, the major source of FAs in IHTG. Moreover, saturated fat induced IR and increased circulating concentrations of ceramides. In contrast to saturated fat, overfeeding of unsaturated fat led to a smaller increase in IHTG, decreased lipolysis, and no change in ceramides. Simple sugars increased IHTG by stimulating DNL. Consistent with current dietary recommendations (US Department of Health and Human Services *et al.,* 2015), study IV demonstrates that saturated fat seems harmful not just in terms of the risk of

diabetes and cardiovascular disease but also in terms of the liver.

6.4. 'DOUBLE TROUBLE' AND 'TRIPLE TROUBLE'

'Double trouble'. Given the high prevalence of both metabolic and genetic risk factors for NAFLD, they can co-exist in an individual. Indeed, when the cohort in study I was divided into four groups of subjects who had both insulin resistance and carried the I148M variant allele ('double trouble'), either ('single trouble'), or neither risk factor, the effects of insulin resistance and the variant allele seemed to be additive with respect to increases in liver fat content and the prevalence of NASH (**Figure 14**).

Very recently, a study in multiple large cohorts demonstrated that the effect of the PNPLA3 I148M variant allele on IHTG content is amplified by increasing adiposity (Stender *et al.,* 2017). In normal weight subjects (BMI < 25 kg/m^2), the average IHTG content among homozygous variant carriers and non-carriers was 2.8% and 1.8%, respectively. In subjects with BMI > 35 kg/m^2, the average IHTG content was threefold higher in homozygous variant carriers (14.2%) as compared to non-carriers (4.7%). Adiposity also intensified the effect of the PNPLA3 variant allele on serum ALT and the prevalence of liver cirrhosis. The same study demonstrated that the effect of the TM6SF2 E167K on IHTG content is also magnified by obesity (Stender *et al.,* 2017).

In addition to possible co-existence of metabolic risk factors with a single genetic risk allele, it is possible that several risk alleles are present in an individual. Mancina *et al.* demonstrated in a cohort of 2,736 subjects from the Dallas Heart Study, that the IHTG content determined by ^{1}H-MRS increased additively as a function of the total number of PNPLA3, MBOAT7 and TM6SF2 risk variants (Mancina *et al.,* 2016). In this study, the average IHTG content increased from less than 5 % in subjects without any risk allele to over 15 % in subjects with a total of 5 risk alleles (Mancina *et al.,* 2016). Another study comprising 416 biopsy-proven NAFLD patients and 109 controls found that the PNPLA3 and TM6SF2 risk variants increased the risk of NASH and significant fibrosis in an additive fashion, even in subjects with low insulin resistance (Koo *et al.,* 2017). Moreover, it was shown in a cohort of 765 Italian NAFLD patients that also the risk of hepatocellular carcinoma increases in a step-wise fashion as a function of the total number of PNPLA3, MBOAT7 and TM6SF2 risk variants (Donati *et al.,* 2017). The risk of hepatocellular carcinoma was over 9-fold higher (OR 9.25, 95% CI 3.83-22.8) in subjects carrying 5 risk alleles as compared to those carrying none (Donati *et al.,* 2017).

'Triple trouble'. In addition to the metabolic and genetic risk factors of fatty liver disease, a third common risk factor exists: alcohol. According to a recent review, alcohol consumption and metabolic risk factors have synergistic effects in the development of advanced liver disease and hepatocellular carcinoma (Boyle *et al.,* 2018). This was elegantly demonstrated in a population-based longitudinal study with 6,732 participants, in which both the features of insulin resistance and the average alcohol intake independently predicted liver-related events, such as hospitalization, death or diagnosis of liver cancer (Åberg *et al.,* 2017). Of note, alcohol intake predicted these events within the current thresholds of alcohol intake defining NAFLD (Åberg *et al.,* 2017).

Alcoholic liver disease (ALD), similarly to NAFLD, is a spectrum of disease ranging from steatosis to steatohepatitis and cirrhosis (Greuter *et al.,* 2017). It also

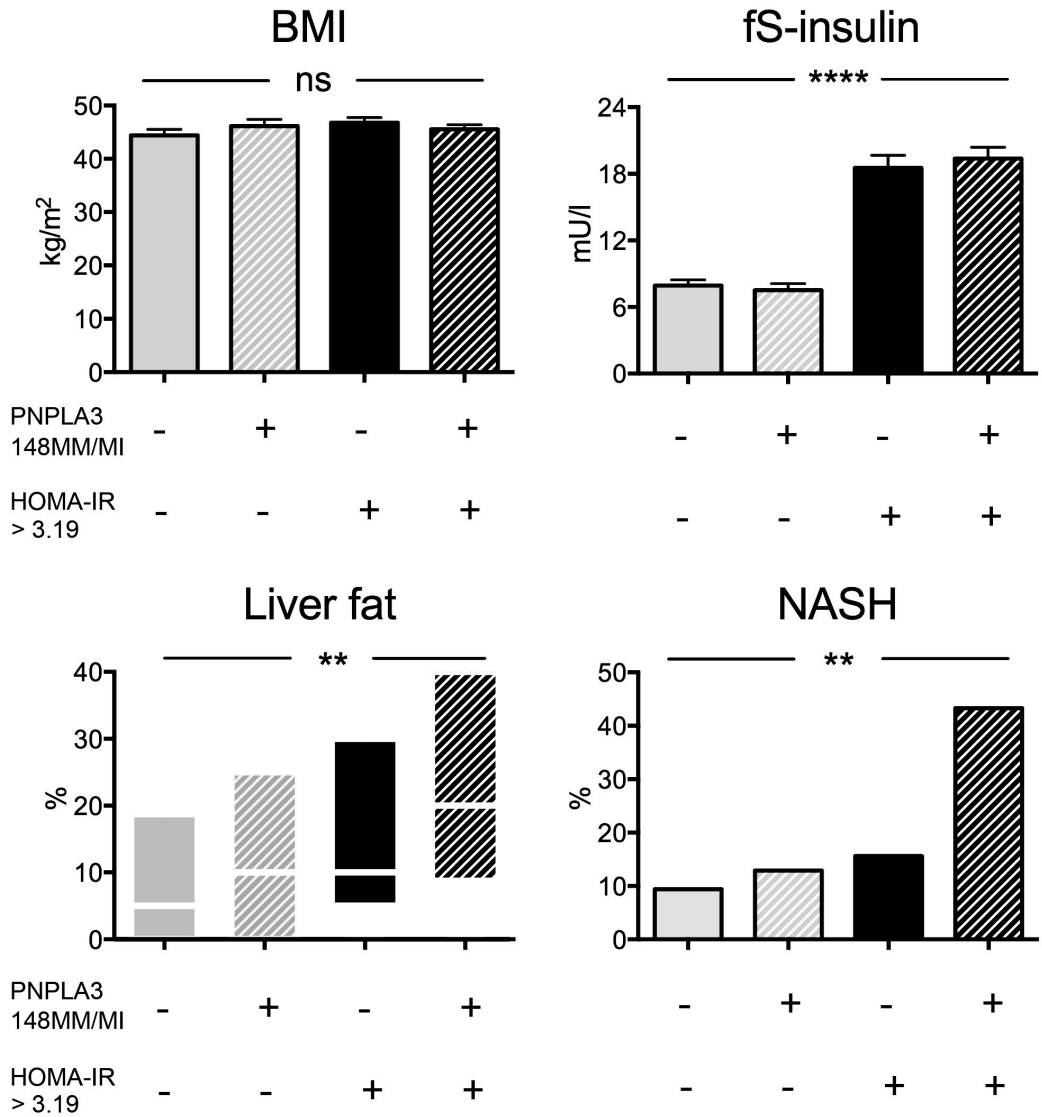

Figure 14. The additive effect of the PNPLA3 I148M gene variant and insulin resistance on liver fat content and the prevalence of NASH. The upper left panel shows body mass index, the upper right panel fasting serum insulin, the lower left panel liver fat content and the lower right panel the prevalence of NASH in non-overlapping groups of subjects either carrying (+) or not carrying (-) the PNPLA3 I148M gene variant and having HOMA-IR value above (+) or below (-) 3.19. Adapted from Luukkonen PK *et al., Journal of Hepatology*. 2016; 64:1167-75 and reproduced with the permission of Elsevier.

increases the risk of hepatocellular carcinoma (Boyle *et al.,* 2018). Histologically, NAFLD and ALD are characterized by similar features such as macrovesicular steatosis; and in steatohepatitis, hepatocellular ballooning, immune cell infiltration and fibrosis (Greuter *et al.,* 2017) Moreover, these diseases share a common genetic background, as the PNPLA3, MBOAT7

and TM6SF2 variants predispose not only to NAFLD but also to ALD (Buch *et al.,* 2015). These data suggest that, contrary to current dogma, NAFLD and ALD may represent two extremes of a single fatty liver disease (Boyle *et al.,* 2018).

Taken together, the metabolic and genetic risk factors, and a high intake of alcohol exhibit additive effects in the pathogenesis of NAFLD, and these features may characterize the subjects who are at the highest risk of advanced liver disease and the associated mortality.

7. SUMMARY AND CONCLUSIONS

The present series of studies aimed to characterize heterogeneity of human NAFLD, with a special emphasis on the regulation of hepatic lipid metabolism by genetic and nutritional factors.

In study I, we determined whether the human liver lipidome differs between 'Metabolic NAFLD' and 'PNPLA3 NAFLD'. The insulin-resistant human liver in 'Metabolic NAFLD' was enriched in saturated and monounsaturated free fatty acids and TGs as well as insulin resistance-inducing lipids i.e. ceramides and DAGs. The increase in hepatic ceramides appeared to be due to an increase in the *de novo* ceramide synthetic pathway, which produces ceramides from saturated fatty acids. In contrast to 'Metabolic NAFLD', the human liver lipidome in the insulin-sensitive 'PNPLA3 NAFLD' lacked all of the aforementioned features and was characterized by increased concentrations of polyunsaturated TGs. These data are novel and document that the lipid composition of the human liver is markedly dependent upon the etiology of NAFLD.

In study II, we studied the human liver histology and lipidome in the 'MBOAT7 NAFLD'. Histologically, carriers of the MBOAT7 gene variant had more liver fibrosis than non-carriers. With respect to liver lipidome, concentrations of several polyunsaturated phosphatidylinositols, but not other lipids, were significantly altered. Thus, 'MBOAT7 NAFLD' is also associated with distinct alterations in the human liver lipidome.

In study III, we investigated the human liver and serum lipidome and hepatic gene expression in 'TM6SF2 NAFLD'. In addition, the incorporation of different fatty acids into complex lipids was determined in TM6SF2 knockdown cells *in vitro*. A relative deficiency of polyunsaturated triglycerides and phosphatidylcholines, and a relative excess of polyunsaturated free fatty acids characterized the liver lipidome. The hepatic gene expression profile in the 'TM6SF2 NAFLD' was characterized by alterations in genes regulated by PUFAs. The incorporation of polyunsaturated fatty acids into complex lipids was decreased in TM6SF2 knockdown cells. Together these data suggest that hepatic lipid synthesis from polyunsaturated fatty acids is impaired in carriers of the TM6SF2 E167K variant.

In study IV, we demonstrated in healthy overweight humans that 3 weeks of overfeeding diets enriched either in saturated or unsaturated fat or simple sugars increases IHTG content, but the magnitude and the associated metabolic changes depend on macronutrient composition of the diet.

Saturated fat induced a higher increase in IHTG than unsaturated fat. The former diet stimulated while the latter decreased adipose tissue lipolysis, the major source of FAs in IHTG, which may explain the differential changes in IHTG in the face of similar energy excess. All diets had distinct effects on adipose tissue transcriptome, and particularly saturated fat induced multiple inflammation-related pathways. Moreover, saturated fat induced IR, endotoxemia and an increase in circulating concentrations of harmful ceramides. Simple sugar-enriched diet increased IHTG content by stimulating DNL.

Despite strikingly different liver lipidomes, all phenotypes of NAFLD in the present study were characterized by histological liver damage. Macrovesicular steatosis was a unifying characteristic in all phenotypes, and may be an obligate driver for intrahepatic damage. In addition, alterations in the metabolism of

polyunsaturated fatty acids emerged as a common characteristic of the genetic NAFLDs (i.e. the 'PNPLA3 NAFLD', 'MBOAT7 NAFLD' and 'TM6SF2 NAFLD'). These two characteristics may provide targets for treatment of intrahepatic damage in NAFLD.

The insulin-resistant 'Metabolic NAFLD', but not the genetic NAFLDs, confer an increased risk of diabetes and cardiovascular disease. 'Metabolic NAFLD' was characterized by increases in triglycerides, especially insulin resistance-inducing ceramides. Consistent with these data, overconsumption of saturated fat for 3 weeks induced a highly saturated, ceramide-enriched lipidome, insulin resistance, and a marked increase in IHTG content. Thus, consistent with the current dietary recommendations, avoidance of foods rich in saturated fats and replacing them with unsaturated fat may be beneficial for the liver.

The phenotypes of NAFLD in the present study are not mutually exclusive. A subject may carry none, one, or several of these risk factors (insulin resistance and genetic risk alleles). Those with several risk factors may be at the highest risk of NAFLD-related morbidity and mortality.

In conclusion, genetic and nutritional factors have a marked effect on the hepatic lipid metabolism and the resulting phenotype.

8. ACKNOWLEDGEMENTS

The work of this thesis was carried out in the Department of Medicine, University of Helsinki and Helsinki University Hospital, and in the Minerva Foundation Institute of Medical Research during the years 2014-2018.

I would like to express my sincere thanks to all those who have contributed to the work of this thesis and helped me during these years. In particular, I wish to thank the following:

First, I wish to express my deepest gratitude to professor Hannele Yki-Järvinen for her fantastic mentorship. It is safe to say that the privilege to work in your laboratory has been among the best things that has happened in my life. I have sincerely enjoyed every aspect of these years, and greatly appreciate all that you have done for me. I admire your world-class scientific expertise, intellectual curiosity and innovativeness.

I am honoured to have professor Rosalind Coleman from the University of North Carolina, Chapel Hill, North Carolina, USA, as my opponent.

I sincerely thank professor emeritus Tapani Rönnemaa, University of Turku, and adjunct professor Fredrik Åberg, Helsinki University Hospital, for their constructive comments and stimulating discussions during the review of this thesis.

I would also like to thank my steering committee members professor Petri Kovanen and adjunct professor Matti Jauhiainen for valuable comments and advice.

I wish to express my gratitude to all co-authors of the articles of this thesis. Thank you Linda Ahonen, Ashfaq Ali, Quentin Anstee, Johanna Arola, Karine Clément, Om Dwivedi, Melania Gaggini, Amalia Gastaldelli, Leif Groop, Helena Gylling, Antti Hakkarainen, Nidhina Haridas, Leanne Hodson, Tuulia Hyötyläinen, Ching Jian, Anne Juuti, Brandon Kayser, Marja Leivonen, Nina Lundbom, Vesa Olkkonen, Matej Orešič, Marju Orho-Melander, Jeremy Palmer, Véronique Pelloux, Aila Rissanen, Anne Salonen, Emma Scott, Taru Tukiainen and Petter Vikman for the excellent collaboration.

I wish to thank Anne Salo, Aila Karioja-Kallio, Päivi Ihamuotila, Mia Urjansson, Pentti Pölönen, Erja Juvonen, Leena Kaipiainen and Raisa Harjula for their superb technical assistance, as well as Cia Olsson and Carita Estlander-Kortman for their support.

I sincerely thank all the members of our research group, especially You Zhou for the great teamwork and invaluable expertise in statistics, as well as Sanja Sädevirta, Elina Isokuortti, Susanna Lallukka and Jenni Hyysalo for sharing the path to doctorate with me.

I wish to thank all the volunteers who have participated in the studies.

I am thankful for the University of Helsinki and Helsinki University Hospital for granting me the joint doctoral candidate position for 2016-2017, and for the University of Helsinki for granting me the doctoral candidate position for 2018. I would also like to thank the Yrjö Jahnsson Foundation, the Finnish Medical Foundation, the Emil Aaltonen Foundation, the Maud Kuistila Memorial Foundation, the Finnish Diabetes Research Foundation and the Medical Society of Helsinki for the financial

support of this thesis.

In addition, I am thankful for the Elucidating Pathways of Steatohepatitis (EPoS) consortium funded by the Horizon 2020 Framework Program of the European Union, the EU/EFPIA Innovative Medicines Initiative Joint Undertaking (EMIF), the EVO funding of the Helsinki University Hospital, the Academy of Finland, the Sigrid Juselius Foundation and the Novo Nordisk Foundation for financially supporting the research group.

I also wish to thank the University of Helsinki, the European Association for the Study of the Liver, the European Association for the Study of Diabetes, the EPoS consortium, the Finnish Society of Diabetes Research and Diabetologists, Novo Nordisk and the Finnish Society of Gastroenterology for supporting my participation in educational events and congresses in places such as Vienna, Newcastle, Stockholm, Copenhagen, Oxford, Munich, Turin, Gothenburg, San Diego, London, St. Louis, New Haven, Dallas, Nashville, Keystone, Örebro, Paris and Amsterdam.

My special thanks go to all my friends for helping me to forget about research every once in a while.

Above all, I wish to thank my mother Pirjo, father Pekka as well as Riitta, Pasi, Marianne and Hanna-Kaisa for their love and support in all my endeavors.

Finally, I wish to express my deepest thanks to my lovely wife, Siiri. In addition to the figures in this book, you have made my life beautiful. Thank you for your never-ending patience, support and love.

Helsinki, July 2018

Panu Luukkonen

9. REFERENCES

Adiels M, Westerbacka J, Soro-Paavonen A, Häkkinen AM, Vehkavaara S, Caslake MJ, Packard C, Olofsson SO, Yki-Järvinen H, Taskinen MR, Borén J. Acute suppression of VLDL1 secretion rate by insulin is associated with hepatic fat content and insulin resistance. Diabetologia. 2007 Nov;50(11):2356-65.

Amaro A, Fabbrini E, Kars M, Yue P, Schechtman K, Schonfeld G, Klein S. Dissociation between intrahepatic triglyceride content and insulin resistance in familial hypobetalipoproteinemia. Gastroenterology. 2010 Jul;139(1):149-53.

Anderson KE, Kielkowska A, Durrant TN, Juvin V, Clark J, Stephens LR, Hawkins PT. Lysophosphatidylinositol-acyltransferase-1 (LPIAT1) is required to maintain physiological levels of PtdIns and PtdInsP(2) in the mouse. PLoS One. 2013;8(3):e58425.

Anstee QM, Targher G, Day CP. Progression of NAFLD to diabetes mellitus, cardiovascular disease or cirrhosis. Nat Rev Gastroenterol Hepatol. 2013;10(6):330-44.

Arita Y, Kihara S, Ouchi N, Takahashi M, Maeda K, Miyagawa J, Hotta K, Shimomura I, Nakamura T, Miyaoka K, Kuriyama H, Nishida M, Yamashita S, Okubo K, Matsubara K, Muraguchi M, Ohmoto Y, Funahashi T, Matsuzawa Y.P aradoxical decrease of an adipose-specific protein, adiponectin, in obesity. 1999. Biochem Biophys Res Commun. 2012 Aug 31;425(3):560-4.

Basantani MK, Sitnick MT, Cai L, Brenner DS, Gardner NP, Li JZ, Schoiswohl G, Yang K, Kumari M, Gross RW, Zechner R, Kershaw EE. Pnpla3/Adiponutrin deficiency in mice does not contribute to fatty liver disease or metabolic syndrome. J Lipid Res. 2011 Feb;52(2):318-29.

BasuRay S, Smagris E, Cohen JC, Hobbs HH. The PNPLA3 variant associated with fatty liver disease (I148M) accumulates on lipid droplets by evading ubiquitylation. Hepatology. 2017 Oct;66(4):1111-1124.

Bedossa P, Poitou C, Veyrie N, Bouillot JL, Basdevant A, Paradis V, Tordjman J, Clement K. Histopathological algorithm and scoring system for evaluation of liver lesions in morbidly obese patients. Hepatology. 2012 Nov;56(5):1751-9.

Bergman BC, Brozinick JT, Strauss A, Bacon S, Kerege A, Bui HH, Sanders P, Siddall P, Kuo MS, Perreault L. Serum sphingolipids: relationships to insulin sensitivity and changes with exercise in humans. Am J Physiol Endocrinol Metab. 2015 Aug 15;309(4):E398-408.

Bès-Houtmann S, Roche R, Hoareau L, Gonthier MP, Festy F, Caillens H, Gasque P, Lefebvre d'Hellencourt C, Cesari M. Presence of functional TLR2 and TLR4 on human adipocytes. Histochem Cell Biol. 2007 Feb;127(2):131-7.

Bielohuby M, Prakash S, Brunner B, Pfenninger A, Werner U, Turpin-Nolan S, Brüning J, Tennagels N. Ceramide synthase 6 inhibition as a novel therapeutic approach for obesity and type 2 diabetes. Endocrine Abstracts 2017;49:GP105 doi:10.1530/endoabs.49.GP105

Bjermo H, Iggman D, Kullberg J, Dahlman I, Johansson L, Persson L, Berglund J, Pulkki K, Basu S, Uusitupa M, Rudling M, Arner P, Cederholm T, Ahlström H, Risérus U. Effects of n-6 PUFAs compared with SFAs on liver fat, lipoproteins, and inflammation in abdominal obesity: a randomized controlled trial. Am J Clin Nutr. 2012 May;95(5):1003-12.

Bortolotti M, Kreis R, Debard C, Cariou B, Faeh D, Chetiveaux M, Ith M, Vermathen P, Stefanoni N, Lê KA, Schneiter P, Krempf M, Vidal H, Boesch C, Tappy L. High protein intake reduces intrahepatocellular lipid deposition in humans. Am J Clin Nutr. 2009 Oct;90(4):1002-10.

Boyle M, Masson S, Anstee QM. The bidirectional impacts of alcohol consumption and the metabolic syndrome: Cofactors for progressive fatty liver disease. J Hepatol. 2018 Feb;68(2):251-267.

Browning JD, Baker JA, Rogers T, Davis J, Satapati S, Burgess SC. Short-term weight loss and hepatic triglyceride reduction: evidence of a metabolic advantage with dietary carbohydrate restriction. Am J Clin Nutr. 2011 May;93(5):1048-52.

Browning JD, Szczepaniak LS, Dobbins R, Nuremberg P, Horton JD, Cohen JC, Grundy SM, Hobbs HH. Prevalence of hepatic steatosis in an urban population in the United States: impact of ethnicity. Hepatology. 2004 Dec;40(6):1387-95.

Brunt EM, Janney CG, Di Bisceglie AM, Neuschwander-Tetri BA, Bacon BR. Nonalcoholic steatohepatitis: a proposal for grading and staging the histological lesions. Am J Gastroenterol. 1999 Sep;94(9):2467-74.

Bruschi FV, Claudel T, Tardelli M, Caligiuri A, Stulnig TM, Marra F, Trauner M. The PNPLA3 I148M variant modulates the fibrogenic phenotype of human hepatic stellate cells. Hepatology. 2017 Jun;65(6):1875-1890.

Bu SY, Mashek MT, Mashek DG. Suppression of long chain acyl-CoA synthetase 3 decreases hepatic de novo fatty acid synthesis through decreased transcriptional activity. J Biol Chem. 2009 Oct 30;284(44):30474-83.

Bugianesi E, Gastaldelli A, Vanni E, Gambino R, Cassader M, Baldi S, Ponti V, Pagano G, Ferrannini E, Rizzetto M. Insulin resistance in non-diabetic patients with non-alcoholic fatty liver disease: sites and mechanisms. Diabetologia. 2005 Apr;48(4):634-42.

Buch S, Stickel F, Trépo E, Way M, Herrmann A, Nischalke HD, Brosch M, Rosendahl J, Berg T, Ridinger M, Rietschel M, McQuillin A, Frank J, Kiefer F, Schreiber S, Lieb W, Soyka M, Semmo N, Aigner E, Datz C, Schmelz R, Brückner S, Zeissig S, Stephan AM, Wodarz N, Devière J, Clumeck N, Sarrazin C, Lammert F, Gustot T, Deltenre P, Völzke H, Lerch MM, Mayerle J, Eyer F, Schafmayer C, Cichon S, Nöthen MM, Nothnagel M, Ellinghaus D, Huse K, Franke A, Zopf S, Hellerbrand C, Moreno C, Franchimont D, Morgan MY, Hampe J. A genome-wide association study confirms PNPLA3 and identifies TM6SF2 and MBOAT7 as risk loci for alcohol-related cirrhosis. Nat Genet. 2015 Dec;47(12):1443-8.

Caesar R, Tremaroli V, Kovatcheva-Datchary P, Cani PD, Bäckhed F. Crosstalk between Gut Microbiota and Dietary Lipids Aggravates WAT Inflammation through TLR Signaling. Cell Metab. 2015 Oct 6;22(4):658-68.

Cani PD, Amar J, Iglesias MA, Poggi M, Knauf C, Bastelica D, Neyrinck AM, Fava F, Tuohy KM, Chabo C, Waget A, Delmée E, Cousin B, Sulpice T, Chamontin B, Ferrières J, Tanti JF, Gibson GR, Casteilla L, Delzenne NM, Alessi MC, Burcelin R. Metabolic endotoxemia initiates obesity and insulin resistance. Diabetes. 2007 Jul;56(7):1761-72.

Cannito S, Paternostro C, Busletta C, Bocca C, Colombatto S, Miglietta A, Novo E, Parola M. Hypoxia, hypoxia-inducible factors and fibrogenesis in chronic liver diseases. Histol Histopathol. 2014 Jan;29(1):33-44.

Caussy C, Soni M, Cui J, Bettencourt R, Schork N, Chen CH, Ikhwan MA, Bassirian S, Cepin S, Gonzalez MP, Mendler M, Kono Y, Vodkin I, Mekeel K, Haldorson J, Hemming A, Andrews B, Salotti J, Richards L, Brenner DA, Sirlin CB, Loomba R; Familial NAFLD Cirrhosis Research Consortium. Nonalcoholic fatty liver disease with cirrhosis increases familial risk for advanced fibrosis. J Clin Invest. 2017 Jun 30;127(7):2697-2704.

Chaurasia B, Summers SA. Ceramides - Lipotoxic Inducers of Metabolic Disorders. Trends Endocrinol Metab. 2015;26(10):538-550.

Chavez JA, Summers SA. A ceramide-centric view of insulin resistance. Cell Metab. 2012;15:585–594.

Chen Q, Galleano M, Cederbaum AI. Cytotoxicity and apoptosis produced by arachidonic acid in Hep G2 cells overexpressing human cytochrome P4502E1. J Biol Chem. 1997 Jun 6;272(23):14532-41.

Chen W, Chang B, Li L, Chan L. Patatin-like phospholipase domain-containing 3/adiponutrin deficiency in mice is not associated with fatty liver disease. Hepatology. 2010 Sep;52(3):1134-42.

Cheng JM, Suoniemi M, Kardys I, Vihervaara T, de Boer SP, Akkerhuis KM, Sysi-Aho M, Ekroos K, Garcia-Garcia HM, Oemrawsingh RM, Regar E, Koenig W, Serruys PW, van Geuns RJ, Boersma E, Laaksonen R. Plasma concentrations of molecular lipid species in relation to coronary plaque characteristics and cardiovascular outcome: Results of the ATHEROREMO-IVUS study. Atherosclerosis. 2015 Dec;243(2):560-6.

Chow JC, Young DW, Golenbock DT, Christ WJ, Gusovsky F. Toll-like receptor-4 mediates lipopolysaccharide-induced signal transduction. J Biol Chem. 1999 Apr 16;274(16):10689-92.

Cohen JC, Horton JD, Hobbs HH. Human fatty liver disease: old questions and new insights. Science. 2011 Jun 24;332(6037):1519-23.

Cole LK, Vance JE, Vance DE. Phosphatidylcholine biosynthesis and lipoprotein metabolism. Biochim Biophys Acta. 2012 May;1821(5):754-61.

Cooper DE, Young PA, Klett EL, Coleman RA. Physiological Consequences of Compartmentalized Acyl-CoA Metabolism. J Biol Chem. 2015 Aug 14;290(33):20023-31.

DeFronzo RA, Matsuda M. Reduced time points to calculate the composite index. Diabetes Care. 2010 Jul;33(7):e93.

DeFronzo RA, Tobin JD, Andres R. Glucose clamp technique: a method for quantifying insulin secretion and resistance. Am J Physiol. 1979 Sep;237(3):E214-23.

Del Ben M, Polimeni L, Brancorsini M, Di Costanzo A, D'Erasmo L, Baratta F, Loffredo L, Pastori D, Pignatelli P, Violi F, Arca M, Angelico F. Non-alcoholic fatty liver disease, metabolic syndrome and patatin-like phospholipase domain-containing protein3 gene variants. Eur J Intern Med. 2014 Jul;25(6):566-70.

de Mello VD, Lankinen M, Schwab U, Kolehmainen M, Lehto S, Seppänen-Laakso T, Oresic M, Pulkkinen L, Uusitupa M, Erkkilä AT. Link between plasma ceramides, inflammation and insulin resistance: association with serum IL-6 concentration in patients with coronary heart disease. Diabetologia. 2009 Dec;52(12):2612-5.

Deopurkar R, Ghanim H, Friedman J, Abuaysheh S, Sia CL, Mohanty P, Viswanathan P, Chaudhuri A, Dandona P. Differential effects of cream, glucose, and orange juice on inflammation, endotoxin, and the expression of Toll-like receptor-4

and suppressor of cytokine signaling-3. Diabetes Care. 2010 May;33(5):991-7.

Di Costanzo A, Belardinilli F, Bailetti D, Sponziello M, D'Erasmo L, Polimeni L, Baratta F, Pastori D, Ceci F, Montali A, Girelli G, De Masi B, Angeloni A, Giannini G, Del Ben M, Angelico F, Arca M. Evaluation of Polygenic Determinants of Non-Alcoholic Fatty Liver Disease (NAFLD) By a Candidate Genes Resequencing Strategy. Sci Rep. 2018 Feb 27;8(1):3702.

Diehl AM, Day C. Nonalcoholic Steatohepatitis. N Engl J Med. 2018 Feb 22;378(8):781.

Diraison F, Moulin P, Beylot M. Contribution of hepatic de novo lipogenesis and reesterification of plasma non esterified fatty acids to plasma triglyceride synthesis during non-alcoholic fatty liver disease. Diabetes Metab. 2003 Nov;29(5):478-85.

Diraison F, Yankah V, Letexier D, Dusserre E, Jones P, Beylot M. Differences in the regulation of adipose tissue and liver lipogenesis by carbohydrates in humans. J Lipid Res. 2003 Apr;44(4):846-53.

Dobin A, Davis CA, Schlesinger F, Drenkow J, Zaleski C, Jha S, *et al.* STAR: ultrafast universal RNA-seq aligner. Bioinformatics. 2013 Jan 1;29(1):15-21.

Donati B, Dongiovanni P, Romeo S, Meroni M, McCain M, Miele L, Petta S, Maier S, Rosso C, De Luca L, Vanni E, Grimaudo S, Romagnoli R, Colli F, Ferri F, Mancina RM, Iruzubieta P, Craxi A, Fracanzani AL, Grieco A, Corradini SG, Aghemo A, Colombo M, Soardo G, Bugianesi E, Reeves H, Anstee QM, Fargion S, Valenti L. MBOAT7 rs641738 variant and hepatocellular carcinoma in non-cirrhotic individuals. Sci Rep. 2017 Jul 3;7(1):4492.

Dongiovanni P, Petta S, Maglio C, Fracanzani AL, Pipitone R, Mozzi E, Motta BM, Kaminska D, Rametta R, Grimaudo S, Pelusi S, Montalcini T, Alisi A, Maggioni M, Kärjä V, Borén J, Käkelä P, Di Marco V, Xing C, Nobili V, Dallapiccola B, Craxi A, Pihlajamäki J, Fargion S, Sjöström L, Carlsson LM, Romeo S, Valenti L. Transmembrane 6 superfamily member 2 gene variant disentangles nonalcoholic steatohepatitis from cardiovascular disease. Hepatology. 2015 Feb;61(2):506-14

Donnelly KL, Smith CI, Schwarzenberg SJ, Jessurun J, Boldt MD, Parks EJ. Sources of fatty acids stored in liver and secreted via lipoproteins in patients with nonalcoholic fatty liver disease. J Clin Invest 2005;115:1343–51.

Doycheva I, Cui J, Nguyen P, Costa EA, Hooker J, Hofflich H, Bettencourt R, Brouha S, Sirlin CB, Loomba R. Non-invasive screening of diabetics in primary care for NAFLD and advanced fibrosis by MRI and MRE. Aliment Pharmacol Ther. 2016 Jan;43(1):83-95.

D'Souza K, Epand RM. Enrichment of phosphatidylinositols with specific acyl chains. Biochim Biophys Acta. 2014 Jun;1838(6):1501-8.

Dulai PS, Singh S, Patel J, Soni M, Prokop LJ, Younossi Z, Sebastiani G, Ekstedt M, Hagstrom H, Nasr P, Stal P, Wong VW, Kechagias S, Hultcrantz R, Loomba R. Increased risk of mortality by fibrosis stage in nonalcoholic fatty liver disease: Systematic review and meta-analysis. Hepatology. 2017 May;65(5):1557-1565.

Dyson J, Jaques B, Chattopadyhay D, Lochan R, Graham J, Das D, Aslam T, Patanwala I, Gaggar S, Cole M, Sumpter K, Stewart S, Rose J, Hudson M, Manas D, Reeves HL. Hepatocellular cancer: the impact of obesity, type 2 diabetes and a multidisciplinary team. J Hepatol. 2014 Jan;60(1):110-7.

Edgar RC. Search and clustering orders of magnitude faster than BLAST. Bioinformatics. 2010;26(19):2460-1.

Ehrhardt N, Doche ME, Chen S, Mao HZ, Walsh MT, Bedoya C, Guindi M, Xiong W, Ignatius Irudayam J, Iqbal J, Fuchs S, French SW, Mahmood Hussain M, Arditi M, Arumugaswami V, Péterfy M. Hepatic Tm6sf2 overexpression affects cellular ApoB-trafficking, plasma lipid levels, hepatic steatosis and atherosclerosis. Hum Mol Genet. 2017 Jul 15;26(14):2719-2731.

Ekstedt M, Franzén LE, Mathiesen UL, Thorelius L, Holmqvist M, Bodemar G, Kechagias S. Long-term follow-up of patients with NAFLD and elevated liver enzymes. Hepatology. 2006 Oct;44(4):865-73.

Ekstedt M, Hagström H, Nasr P, Fredrikson M, Stål P, Kechagias S, Hultcrantz R. Fibrosis stage is the strongest predictor for disease-specific mortality in NAFLD after up to 33 years of follow-up. Hepatology. 2015 May;61(5):1547-54.

Ellis JM, Frahm JL, Li LO, Coleman RA. Acyl-coenzyme A synthetases in metabolic control. Curr Opin Lipidol. 2010 Jun;21(3):212-7.

Erridge C, Attina T, Spickett CM, Webb DJ. A high-fat meal induces low-grade endotoxemia: evidence of a novel mechanism of postprandial inflammation. Am J Clin Nutr. 2007 Nov;86(5):1286-92.

Eslam M, Mangia A, Berg T, Chan HL, Irving WL, Dore GJ, Abate ML, Bugianesi E, Adams LA, Najim MA, Miele L, Weltman M, Mollison L, Cheng W, Riordan S, Fischer J, Romero-Gomez M, Spengler U, Nattermann J, Rahme A, Sheridan D, Booth DR, McLeod D, Powell E, Liddle C, Douglas MW, van der Poorten D, George J; International Liver Disease Genetics Consortium. Diverse impacts of the rs58542926 E167K variant in TM6SF2 on viral and metabolic liver disease phenotypes. Hepatology. 2016 Jul;64(1):34-46.

European Association for the Study of the Liver (EASL); European Association for the Study of Diabetes (EASD); European Association for the Study of Obesity (EASO). EASL-EASD-EASO Clinical Practice Guidelines for the management of non-alcoholic fatty liver disease. J Hepatol. 2016 Jun;64(6):1388-402.

Fabbrini E, Sullivan S, Klein S. Obesity and nonalcoholic fatty liver disease: biochemical, metabolic, and clinical implications. Hepatology. 2010 Feb;51(2):679-89.

Fabbrini E, Tiemann Luecking C, Love-Gregory L, Okunade AL, Yoshino M, Fraterrigo G, Patterson BW, Klein S. Physiological Mechanisms of Weight Gain-Induced Steatosis in People With Obesity. Gastroenterology. 2016 Jan;150(1):79-81.e2.

Fabregat A, Sidiropoulos K, Garapati P, Gillespie M, Hausmann K, Haw R, *et al.* The Reactome pathway Knowledgebase. Nucleic Acids Res. 2014 Jan;42(Database issue):D472-7.

Falleti E, Cussigh A, Cmet S, Fabris C, Toniutto P. PNPLA3 rs738409 and TM6SF2 rs58542926 variants increase the risk of hepatocellular carcinoma in alcoholic cirrhosis. Dig Liver Dis. 2016 Jan;48(1):69-75.

Farrell GC, Teoh NC, McCuskey RS. Hepatic microcirculation in fatty liver disease. Anat Rec (Hoboken). 2008 Jun;291(6):684-92.

Ferrannini E .The theoretical bases of indirect calorimetry: a review. Metabolism. 1988 Mar;37(3):287-301.

Folch J, Lees M, Sloane Stanley GH. A simple method for the isolation and purification of total lipides from animal tissues. J Biol Chem. 1957;226(1): 497-509.

Forman BM, Chen J, Evans RM. Hypolipidemic drugs, polyunsaturated fatty acids, and eicosanoids are ligands for peroxisome proliferator-activated receptors alpha and delta. Proc Natl Acad Sci U S A. 1997 Apr 29;94(9):4312-7.

Fernández-Real JM, Broch M, Richart C, Vendrell J, López-Bermejo A, Ricart W. CD14 monocyte receptor, involved in the inflammatory cascade, and insulin sensitivity. J Clin Endocrinol Metab. 2003 Apr;88(4):1780-4.

Frayn KN, Arner P, Yki-Järvinen H. Fatty acid metabolism in adipose tissue, muscle and liver in health and disease. Essays Biochem. 2006;42:89-103.

Gastaldelli A, Coggan AR, Wolfe RR. Assessment of methods for improving tracer estimation of non-steady-state rate of appearance. J Appl Physiol (1985). 1999 Nov;87(5):1813-22.

Gastaldelli A, Cusi K, Pettiti M, Hardies J, Miyazaki Y, Berria R, Buzzigoli E, Sironi AM, Cersosimo E, Ferrannini E, Defronzo RA. Relationship between hepatic/visceral fat and hepatic insulin resistance in nondiabetic and type 2 diabetic subjects. Gastroenterology. 2007 Aug;133(2):496-506.

George J, Pera N, Phung N, Leclercq I, Yun Hou J, Farrell G. Lipid peroxidation, stellate cell activation and hepatic fibrogenesis in a rat model of chronic steatohepatitis. J Hepatol. 2003 Nov;39(5):756-64.

Gerber L, Otgonsuren M, Mishra A, Escheik C, Birerdinc A, Stepanova M, Younossi ZM. Non-alcoholic fatty liver disease (NAFLD) is associated with low level of physical activity: a population-based study. Aliment Pharmacol Ther. 2012 Oct;36(8):772-81.

Gijón MA, Riekhof WR, Zarini S, Murphy RC, Voelker DR. Lysophospholipid acyltransferases and arachidonate recycling in human neutrophils. J Biol Chem. 2008 Oct 31;283(44):30235-45.

Goffredo M, Caprio S, Feldstein AE, D'Adamo E, Shaw MM, Pierpont B, Savoye M, Zhao H, Bale AE, Santoro N. Role of TM6SF2 rs58542926 in the pathogenesis of nonalcoholic pediatric fatty liver disease: A multiethnic study. Hepatology. 2016 Jan;63(1):117-25.

Gorden DL, Ivanova PT, Myers DS, McIntyre JO, VanSaun MN, Wright JK, Matrisian LM, Brown HA. Increased diacylglycerols characterize hepatic lipid changes in progression of human nonalcoholic fatty liver disease; comparison to a murine model. PLoS One. 2011;6(8):e22775.

Grandone A, Cozzolino D, Marzuillo P, Cirillo G, Di Sessa A, Ruggiero L, Di Palma MR, Perrone L, Miraglia Del Giudice E. TM6SF2 Glu167Lys polymorphism is associated with low levels of LDL-cholesterol and increased liver injury in obese children. Pediatr Obes. 2016 Apr;11(2):115-9.

Greuter T, Malhi H, Gores GJ, Shah VH. Therapeutic opportunities for alcoholic steatohepatitis and nonalcoholic steatohepatitis: exploiting similarities and differences in pathogenesis. JCI Insight. 2017 Sep 7;2(17). pii: 95354.

Grevengoed TJ, Klett EL, Coleman RA. Acyl-CoA metabolism and partitioning. Annu Rev Nutr. 2014;34:1-30.

Guasch-Ferré M, Becerra-Tomás N, Ruiz-Canela M, Corella D, Schröder H, Estruch R, Ros E, Arós F, Gómez-Gracia E, Fiol M, Serra-Majem L, Lapetra J, Basora J,

Martín-Calvo N, Portoles O, Fitó M, Hu FB, Forga L, Salas-Salvadó J. Total and subtypes of dietary fat intake and risk of type 2 diabetes mellitus in the Prevención con Dieta Mediterránea (PREDIMED) study. Am J Clin Nutr. 2017;105(3):723-735.

Hajduch E, Turban S, Le Liepvre X, Le Lay S, Lipina C, Dimopoulos N, Dugail I, Hundal HS. Targeting of PKCzeta and PKB to caveolin-enriched microdomains represents a crucial step underpinning the disruption in PKB-directed signalling by ceramide. Biochem J. 2008 Mar 1;410(2):369-79.

Hagström H, Nasr P, Ekstedt M, Hammar U, Stål P, Hultcrantz R, Kechagias S. Fibrosis stage but not NASH predicts mortality and time to development of severe liver disease in biopsy-proven NAFLD. J Hepatol. 2017 Dec;67(6):1265-1273.

Haufe S, Engeli S, Kast P, Böhnke J, Utz W, Haas V, Hermsdorf M, Mähler A, Wiesner S, Birkenfeld AL, Sell H, Otto C, Mehling H, Luft FC, Eckel J, Schulz-Menger J, Boschmann M, Jordan J. Randomized comparison of reduced fat and reduced carbohydrate hypocaloric diets on intrahepatic fat in overweight and obese human subjects. Hepatology. 2011 May;53(5):1504-14.

Haus JM, Kashyap SR, Kasumov T, Zhang R, Kelly KR, Defronzo RA, Kirwan JP. Plasma ceramides are elevated in obese subjects with type 2 diabetes and correlate with the severity of insulin resistance. Diabetes. 2009 Feb;58(2):337-43.

Havel RJ, Eder HA, Bragdon JH. The distribution and chemical composition of ultracentrifugally separated lipoproteins in human serum. J Clin Invest. 1955 Sep;34(9):1345-53.

Havulinna AS, Sysi-Aho M, Hilvo M, Kauhanen D, Hurme R, Ekroos K, Salomaa V, Laaksonen R. Circulating Ceramides Predict Cardiovascular Outcomes in the Population-Based FINRISK 2002 Cohort. Arterioscler Thromb Vasc Biol. 2016 Dec;36(12):2424-2430.

Heath RB, Karpe F, Milne RW, Burdge GC, Wootton SA, Frayn KN. Selective partitioning of dietary fatty acids into the VLDL TG pool in the early postprandial period. J Lipid Res. 2003 Nov;44(11):2065-72.

Hellerstein MK, Schwarz JM, Neese RA. Regulation of hepatic de novo lipogenesis in humans. Annu Rev Nutr. 1996;16:523-57.

Hernández EÁ, Kahl S, Seelig A, Begovatz P, Irmler M, Kupriyanova Y, Nowotny B, Nowotny P, Herder C, Barosa C, Carvalho F, Rozman J, Neschen S, Jones JG, Beckers J, de Angelis MH, Roden M. Acute dietary fat intake initiates alterations in energy metabolism and insulin resistance. J Clin Invest. 2017;127(2):695-708.

Hla T, Kolesnick R. C16:0-ceramide signals insulin resistance. Cell Metab. 2014;20(5):703-5.

Hochberg Y, Benjamini Y. More powerful procedures for multiple significance testing. Statistics in Medicine. 1990;9:811–818.

Hodson L, Skeaff CM, Fielding BA. Fatty acid composition of adipose tissue and blood in humans and its use as a biomarker of dietary intake. Prog Lipid Res. 2008 Sep;47(5):348-80.

Holland WL, Brozinick JT, Wang LP, Hawkins ED, Sargent KM, Liu Y, Narra K, Hoehn KL, Knotts TA, Siesky A, Nelson DH, Karathanasis SK, Fontenot GK, Birnbaum MJ, Summers SA. Inhibition of

ceramide synthesis ameliorates glucocorticoid-, saturated-fat-, and obesity-induced insulin resistance. Cell Metab. 2007;5(3):167-79.

Holland WL, Miller RA, Wang ZV, Sun K, Barth BM, Bui HH, Davis KE, Bikman BT, Halberg N, Rutkowski JM, Wade MR, Tenorio VM, Kuo MS, Brozinick JT, Zhang BB, Birnbaum MJ, Summers SA, Scherer PE. Receptor-mediated activation of ceramidase activity initiates the pleiotropic actions of adiponectin. Nat Med. 2011 Jan;17(1):55-63.

Holland WL, Xia JY, Johnson JA, Sun K, Pearson MJ, Sharma AX, Quittner-Strom E, Tippetts TS, Gordillo R, Scherer PE. Inducible overexpression of adiponectin receptors highlight the roles of adiponectin-induced ceramidase signaling in lipid and glucose homeostasis. Mol Metab. 2017 Jan 12;6(3):267-275.

Holmen OL, Zhang H, Fan Y, Hovelson DH, Schmidt EM, Zhou W, Guo Y, Zhang J, Langhammer A, Løchen ML, Ganesh SK, Vatten L, Skorpen F, Dalen H, Zhang J, Pennathur S, Chen J, Platou C, Mathiesen EB, Wilsgaard T, Njølstad I, Boehnke M, Chen YE, Abecasis GR, Hveem K, Willer CJ. Systematic evaluation of coding variation identifies a candidate causal variant in TM6SF2 influencing total cholesterol and myocardial infarction risk. Nat Genet. 2014 Apr;46(4):345-51.

Hotamisligil GS. Inflammation and metabolic disorders. Nature. 2006 Dec 14;444(7121):860-7.

He S, McPhaul C, Li JZ, Garuti R, Kinch L, Grishin NV, Cohen JC, Hobbs HH. A sequence variation (I148M) in PNPLA3 associated with nonalcoholic fatty liver disease disrupts triglyceride hydrolysis. J Biol Chem. 2010 Feb 26;285(9):6706-15.

Hu W, Ross J, Geng T, Brice SE, Cowart LA. Differential regulation of dihydroceramide desaturase by palmitate versus monounsaturated fatty acids: implications for insulin resistance. J Biol Chem. 2011 May 13;286(19):16596-605.

Huang H, Kasumov T, Gatmaitan P, Heneghan HM, Kashyap SR, Schauer PR, Brethauer SA, Kirwan JP. Gastric bypass surgery reduces plasma ceramide subspecies and improves insulin sensitivity in severely obese patients. Obesity (Silver Spring). 2011 Nov;19(11):2235-40.

Huang Y, Cohen JC, Hobbs HH. Expression and characterization of a PNPLA3 protein isoform (I148M) associated with nonalcoholic fatty liver disease. J. Biol. Chem. 2011;286:37085–37093.

Huang Y, He S, Li JZ, Seo YK, Osborne TF, Cohen JC, Hobbs HH. A feed-forward loop amplifies nutritional regulation of PNPLA3. Proc Natl Acad Sci U S A. 2010 Apr 27;107(17):7892-7.

Hyysalo J, Gopalacharyulu P, Bian H, Hyötyläinen T, Leivonen M, Jaser N, Juuti A, Honka MJ, Nuutila P, Olkkonen VM, Oresic M, Yki-Järvinen H. Circulating triacylglycerol signatures in nonalcoholic fatty liver disease associated with the I148M variant in PNPLA3 and with obesity. Diabetes. 2014 Jan;63(1):312-22.

Hyysalo J, Männistö VT, Zhou Y, Arola J, Kärjä V, Leivonen M, Juuti A, Jaser N, Lallukka S, Käkelä P, Venesmaa S, Simonen M, Saltevo J, Moilanen L, Korpi-Hyövalti E, Keinänen-Kiukaanniemi S, Oksa H, Orho-Melander M, Valenti L, Fargion S, Pihlajamäki J, Peltonen M, Yki-Järvinen H. A population-based study on the prevalence of NASH using scores validated against liver histology. J Hepatol. 2014 Apr;60(4):839-46.

Ishihara K, Miyazaki A, Nabe T, Fushimi H, Iriyama N, Kanai S, Sato T, Uozumi N, Shimizu T, Akiba S. Group IVA phospholipase A2 participates in the progression of hepatic fibrosis. FASEB J. 2012 Oct;26(10):4111-21.

Jungermann K, Kietzmann T. Oxygen: modulator of metabolic zonation and disease of the liver. Hepatology. 2000 Feb;31(2):255-60.

Kechagias S, Ernersson A, Dahlqvist O, Lundberg P, Lindström T, Nystrom FH; Fast Food Study Group. Fast-food-based hyper-alimentation can induce rapid and profound elevation of serum alanine aminotransferase in healthy subjects. Gut. 2008 May;57(5):649-54.

Kim DS, Jackson AU, Li YK, Stringham HM; FinMetSeq Investigators, Kuusisto J, Kangas AJ, Soininen P, Ala-Korpela M, Burant CF, Salomaa V, Boehnke M, Laakso M, Speliotes EK. Novel association of TM6SF2 rs58542926 genotype with increased serum tyrosine levels and decreased apoB-100 particles in Finns. J Lipid Res. 2017 Jul;58(7):1471-1481.

Kirk E, Reeds DN, Finck BN, Mayurranjan SM, Patterson BW, Klein S. Dietary fat and carbohydrates differentially alter insulin sensitivity during caloric restriction. Gastroenterology. 2009 May;136(5):1552-60. doi: 10.1053/j.gastro.2009.01.048.

Kolak M, Westerbacka J, Velagapudi VR, Wågsäter D, Yetukuri L, Makkonen J, Rissanen A, Häkkinen AM, Lindell M, Bergholm R, Hamsten A, Eriksson P, Fisher RM, Oresic M, Yki-Järvinen H. Adipose tissue inflammation and increased ceramide content characterize subjects with high liver fat content independent of obesity. Diabetes. 2007 Aug;56(8):1960-8.

Koo BK, Joo SK, Kim D, Bae JM, Park JH, Kim JH, Kim W. Additive effects of PNPLA3 and TM6SF2 on the histological severity of non-alcoholic fatty liver disease. J Gastroenterol Hepatol. 2017 Nov 29. doi: 10.1111/jgh.14056.

Korenblat KM, Fabbrini E, Mohammed BS, Klein S. Liver, muscle, and adipose tissue insulin action is directly related to intrahepatic triglyceride content in obese subjects. Gastroenterology. 2008 May;134(5):1369-75.

Korpela K. mare: Microbiota Analysis in R Easily. R package version 10" 23-Apr-2016

Kotronen A, Johansson LE, Johansson LM, Roos C, Westerbacka J, Hamsten A, Bergholm R, Arkkila P, Arola J, Kiviluoto T, Fisher RM, Ehrenborg E, Orho-Melander M, Ridderstråle M, Groop L, Yki-Järvinen H. A common variant in PNPLA3, which encodes adiponutrin, is associated with liver fat content in humans. Diabetologia. 2009 Jun;52(6):1056-60.

Kotronen A, Seppälä-Lindroos A, Vehkavaara S, Bergholm R, Frayn KN, Fielding BA, Yki-Järvinen H. Liver fat and lipid oxidation in humans. Liver Int. 2009 Oct;29(9):1439-46.

Kotronen A, Seppänen-Laakso T, Westerbacka J, Kiviluoto T, Arola J, Ruskeepää AL, Oresic M, Yki-Järvinen H. Hepatic stearoyl-CoA desaturase (SCD)-1 activity and diacylglycerol but not ceramide concentrations are increased in the nonalcoholic human fatty liver. Diabetes. 2009 Jan;58(1):203-8.

Kotronen A, Joutsi-Korhonen L, Sevastianova K, Bergholm R, Hakkarainen A, Pietiläinen KH, Lundbom N, Rissanen A, Lassila R, Yki-Järvinen H. Increased coagulation factor VIII, IX, XI and XII activities in non-alcoholic fatty

liver disease. Liver Int. 2011 Feb;31(2):176-83.

Kotronen A, Juurinen L, Tiikkainen M, Vehkavaara S, Yki-Järvinen H. Increased liver fat, impaired insulin clearance, and hepatic and adipose tissue insulin resistance in type 2 diabetes. Gastroenterology. 2008 Jul;135(1):122-30.

Kotronen A, Velagapudi VR, Yetukuri L, Westerbacka J, Bergholm R, Ekroos K, Makkonen J, Taskinen MR, Oresic M, Yki-Järvinen H. Serum saturated fatty acids containing triacylglycerols are better markers of insulin resistance than total serum triacylglycerol concentrations. Diabetologia. 2009 Apr;52(4):684-90.

Kotronen A, Westerbacka J, Bergholm R, Pietiläinen KH, Yki-Järvinen H. Liver fat in the metabolic syndrome. J Clin Endocrinol Metab. 2007 Sep;92(9):3490-7.

Kozich JJ, Westcott SL, Baxter NT, Highlander SK, Schloss PD. Development of a dual-index sequencing strategy and curation pipeline for analyzing amplicon sequence data on the MiSeq Illumina sequencing platform. Appl Environ Microbiol. 2013;79(17):5112-20.

Kozlitina J, Smagris E, Stender S, Nordestgaard BG, Zhou HH, Tybjærg-Hansen A, *et al.* Exome-wide association study identifies a TM6SF2 variant that confers susceptibility to nonalcoholic fatty liver disease. Nat Genet 2014;46:352–6.

Krawczyk M, Rau M, Schattenberg JM, Bantel H, Pathil A, Demir M, Kluwe J, Boettler T, Lammert F, Geier A; NAFLD Clinical Study Group. Combined effects of the PNPLA3 rs738409, TM6SF2 rs58542926, and MBOAT7 rs641738 variants on NAFLD severity: a multicenter biopsy-based study. J Lipid Res. 2017 Jan;58(1):247-255.

Kumari M, Schoiswohl G, Chitraju C, Paar M, Cornaciu I, Rangrez AY, Wongsiriroj N, Nagy HM, Ivanova PT, Scott SA, Knittelfelder O, Rechberger GN, Birner-Gruenberger R, Eder S, Brown HA, Haemmerle G, Oberer M, Lass A, Kershaw EE, Zimmermann R, Zechner R. Adiponutrin functions as a nutritionally regulated lysophosphatidic acid acyltransferase. Cell Metab. 2012 May 2;15(5):691-702.

Kumashiro N, Erion DM, Zhang D, Kahn M, Beddow SA, Chu X, *et al.* Cellular mechanism of insulin resistance in nonalcoholic fatty liver disease. Proc. Natl. Acad. Sci. U.S.A. 2011;108:16381–16385.

Kursawe R, Dixit VD, Scherer PE, Santoro N, Narayan D, Gordillo R, Giannini C, Lopez X, Pierpont B, Nouws J, Shulman GI, Caprio S. A Role of the Inflammasome in the Low Storage Capacity of the Abdominal Subcutaneous Adipose Tissue in Obese Adolescents. Diabetes. 2016 Mar;65(3):610-8.

Laaksonen R, Ekroos K, Sysi-Aho M, Hilvo M, Vihervaara T, Kauhanen D, Suoniemi M, Hurme R, März W, Scharnagl H, Stojakovic T, Vlachopoulou E, Lokki ML, Nieminen MS, Klingenberg R, Matter CM, Hornemann T, Jüni P, Rodondi N, Räber L, Windecker S, Gencer B, Pedersen ER, Tell GS, Nygård O, Mach F, Sinisalo J, Lüscher TF. Plasma ceramides predict cardiovascular death in patients with stable coronary artery disease and acute coronary syndromes beyond LDL-cholesterol. Eur Heart J. 2016 Jul 1;37(25):1967-76.

Lallukka S, Luukkonen PK, Zhou Y, Isokuortti E, Leivonen M, Juuti A, Hakkarainen A, Orho-Melander M, Lundbom N, Olkkonen VM, Lassila R, Yki-Järvinen H. Obesity/insulin

resistance rather than liver fat increases coagulation factor activities and expression in humans. Thromb Haemost. 2017 Jan 26;117(2):286-294.

Lallukka S, Sevastianova K, Perttilä J, Hakkarainen A, Orho-Melander M, Lundbom N, Olkkonen VM, Yki-Järvinen H. Adipose tissue is inflamed in NAFLD due to obesity but not in NAFLD due to genetic variation in PNPLA3. Diabetologia. 2013 Apr;56(4):886-92.

Lallukka S, Yki-Järvinen H. Non-alcoholic fatty liver disease and risk of type 2 diabetes. Best Pract Res Clin Endocrinol Metab. 2016 Jun;30(3):385-95.

Lambert JE, Ramos-Roman MA, Browning JD, Parks EJ. Increased de novo lipogenesis is a distinct characteristic of individuals with nonalcoholic fatty liver disease. Gastroenterology 2014;146:726–35.

Langin D. Adipose tissue lipolysis as a metabolic pathway to define pharmacological strategies against obesity and the metabolic syndrome. Pharmacol Res. 2006 Jun;53(6):482-91.

Larson-Meyer DE, Heilbronn LK, Redman LM, Newcomer BR, Frisard MI, Anton S, Smith SR, Alfonso A, Ravussin E. Effect of calorie restriction with or without exercise on insulin sensitivity, beta-cell function, fat cell size, and ectopic lipid in overweight subjects. Diabetes Care. 2006 Jun;29(6):1337-44

Lassenius MI, Pietiläinen KH, Kaartinen K, Pussinen PJ, Syrjänen J, Forsblom C, Pörsti I, Rissanen A, Kaprio J, Mustonen J, Groop PH, Lehto M; FinnDiane Study Group. Bacterial endotoxin activity in human serum is associated with dyslipidemia, insulin resistance, obesity, and chronic inflammation. Diabetes Care. 2011 Aug;34(8):1809-15.

Lazo M, Hernaez R, Eberhardt MS, Bonekamp S, Kamel I, Guallar E, Koteish A, Brancati FL, Clark JM. Prevalence of nonalcoholic fatty liver disease in the United States: the Third National Health and Nutrition Examination Survey, 1988-1994. Am J Epidemiol. 2013 Jul 1;178(1):38-45.

Lee HC, Inoue T, Imae R, Kono N, Shirae S, Matsuda S, Gengyo-Ando K, Mitani S, Arai H. Caenorhabditis elegans mboa-7, a member of the MBOAT family, is required for selective incorporation of polyunsaturated fatty acids into phosphatidylinositol. Mol Biol Cell. 2008 Mar;19(3):1174-84.

Ley RE, Peterson DA, Gordon JI. Ecological and evolutionary forces shaping microbial diversity in the human intestine. Cell. 2006 Feb 24;124(4):837-48.

Li JZ, Huang Y, Karaman R, Ivanova PT, Brown HA, Roddy T, Castro-Perez J, Cohen JC, Hobbs HH. Chronic overexpression of PNPLA3I148M in mouse liver causes hepatic steatosis. J Clin Invest. 2012 Nov;122(11):4130-44.

Liao Y, Smyth GK, Shi W. featureCounts: an efficient general purpose program for assigning sequence reads to genomic features. Bioinformatics. 2014 Apr 1;30(7):923-30.

Liu DJ, Peloso GM, Yu H, Butterworth AS, Wang X, Mahajan A, Saleheen D, Emdin C, Alam D, Alves AC, Amouyel P, Di Angelantonio E, Arveiler D, Assimes TL, Auer PL, Baber U, Ballantyne CM, Bang LE, Benn M, Bis JC, Boehnke M, Boerwinkle E, Bork-Jensen J, Bottinger EP, Brandslund I, Brown M, Busonero F, Caulfield MJ, Chambers JC, Chasman DI, Chen YE, Chen YI, Chowdhury R, Christensen C, Chu AY, Connell JM, Cucca F, Cupples LA, Damrauer SM, Davies G, Deary IJ, Dedoussis G, Denny JC, Dominiczak A, Dubé MP, Ebeling T,

Eiriksdottir G, Esko T, Farmaki AE, Feitosa MF, Ferrario M, Ferrieres J, Ford I, Fornage M, Franks PW, Frayling TM, Frikke-Schmidt R, Fritsche LG, Frossard P, Fuster V, Ganesh SK, Gao W, Garcia ME, Gieger C, Giulianini F, Goodarzi MO, Grallert H, Grarup N, Groop L, Grove ML, Gudnason V, Hansen T, Harris TB, Hayward C, Hirschhorn JN, Holmen OL, Huffman J, Huo Y, Hveem K, Jabeen S, Jackson AU, Jakobsdottir J, Jarvelin MR, Jensen GB, Jørgensen ME, Jukema JW, Justesen JM, Kamstrup PR, Kanoni S, Karpe F, Kee F, Khera AV, Klarin D, Koistinen HA, Kooner JS, Kooperberg C, Kuulasmaa K, Kuusisto J, Laakso M, Lakka T, Langenberg C, Langsted A, Launer LJ, Lauritzen T, Liewald DCM, Lin LA, Linneberg A, Loos RJF, Lu Y, Lu X, Mägi R, Malarstig A, Manichaikul A, Manning AK, Mäntyselkä P, Marouli E, Masca NGD, Maschio A, Meigs JB, Melander O, Metspalu A, Morris AP, Morrison AC, Mulas A, Müller-Nurasyid M, Munroe PB, Neville MJ, Nielsen JB, Nielsen SF, Nordestgaard BG, Ordovas JM, Mehran R, O'Donnell CJ, Orho-Melander M, Molony CM, Muntendam P, Padmanabhan S, Palmer CNA, Pasko D, Patel AP, Pedersen O, Perola M, Peters A, Pisinger C, Pistis G, Polasek O, Poulter N, Psaty BM, Rader DJ, Rasheed A, Rauramaa R, Reilly DF, Reiner AP, Renström F, Rich SS, Ridker PM, Rioux JD, Robertson NR, Roden DM, Rotter JI, Rudan I, Salomaa V, Samani NJ, Sanna S, Sattar N, Schmidt EM, Scott RA, Sever P, Sevilla RS, Shaffer CM, Sim X, Sivapalaratnam S, Small KS, Smith AV, Smith BH, Somayajula S, Southam L, Spector TD, Speliotes EK, Starr JM, Stirrups KE, Stitziel N, Strauch K, Stringham HM, Surendran P, Tada H, Tall AR, Tang H, Tardif JC, Taylor KD, Trompet S, Tsao PS, Tuomilehto J, Tybjaerg-Hansen A, van Zuydam NR, Varbo A, Varga TV, Virtamo J, Waldenberger M, Wang N, Wareham NJ, Warren HR, Weeke PE, Weinstock J, Wessel J, Wilson JG, Wilson PWF, Xu M, Yaghootkar H, Young R, Zeggini E, Zhang H, Zheng NS, Zhang W, Zhang Y, Zhou W, Zhou Y, Zoledziewska M; Charge Diabetes Working Group; EPIC-InterAct Consortium; EPIC-CVD Consortium; GOLD Consortium; VA Million Veteran Program, Howson JMM, Danesh J, McCarthy MI, Cowan CA, Abecasis G, Deloukas P, Musunuru K, Willer CJ, Kathiresan S. Exome-wide association study of plasma lipids in >300,000 individuals. Nat Genet. 2017 Dec;49(12):1758-1766.

Liu YL, Reeves HL, Burt AD, Tiniakos D, McPherson S, Leathart JB, Allison ME, Alexander GJ, Piguet AC, Anty R, Donaldson P, Aithal GP, Francque S, Van Gaal L, Clement K, Ratziu V, Dufour JF, Day CP, Daly AK, Anstee QM. TM6SF2 rs58542926 influences hepatic fibrosis progression in patients with non-alcoholic fatty liver disease. Nat Commun. 2014 Jun 30;5:4309.

Liu Z, Que S, Zhou L, Zheng S, Romeo S, Mardinoglu A, Valenti L. The effect of the TM6SF2 E167K variant on liver steatosis and fibrosis in patients with chronic hepatitis C: a meta-analysis. Sci Rep. 2017 Aug 24;7(1):9273.

Longo R, Pollesello P, Ricci C, *et al.* Proton MR spectroscopy in quantitative in vivo determination of fat content in human liver steatosis. J Magn Reson Imaging 1995;5:281–285.

Loomba R, Abraham M, Unalp A, Wilson L, Lavine J, Doo E, Bass NM; Nonalcoholic Steatohepatitis Clinical Research Network. Association between diabetes, family history of diabetes, and risk of nonalcoholic steatohepatitis and fibrosis. Hepatology. 2012 Sep;56(3):943-51.

Loomba R, Quehenberger O, Armando A, Dennis EA. Polyunsaturated fatty acid metabolites as novel lipidomic biomarkers for noninvasive diagnosis of

nonalcoholic steatohepatitis. J Lipid Res. 2015 Jan;56(1):185-92.

Mahdessian H, Taxiarchis A, Popov S, Silveira A, Franco-Cereceda A, Hamsten A, *et al.* TM6SF2 is a regulator of liver fat metabolism influencing triglyceride secretion and hepatic lipid droplet content. Proc Natl Acad Sci USA 2014;111:8913–8.

Magkos F, Su X, Bradley D, Fabbrini E, Conte C, Eagon JC, *et al.* Intrahepatic Diacylglycerol Content Is Associated With Hepatic Insulin Resistance in Obese Subjects. Gastroenterology. 2012;142:1444–1446.

Mancina RM, Dongiovanni P, Petta S, Pingitore P, Meroni M, Rametta R, Borén J, Montalcini T, Pujia A, Wiklund O, Hindy G, Spagnuolo R, Motta BM, Pipitone RM, Craxì A, Fargion S, Nobili V, Käkelä P, Kärjä V, Männistö V, Pihlajamäki J, Reilly DF, Castro-Perez J, Kozlitina J, Valenti L, Romeo S. The MBOAT7-TMC4 Variant rs641738 Increases Risk of Nonalcoholic Fatty Liver Disease in Individuals of European Descent. Gastroenterology. 2016;150(5):1219-1230.e6.

Mancina RM, Matikainen N, Maglio C, Söderlund S, Lundbom N, Hakkarainen A, Rametta R, Mozzi E, Fargion S, Valenti L, Romeo S, Taskinen MR, Borén J. Paradoxical dissociation between hepatic fat content and de novo lipogenesis due to PNPLA3 sequence variant. J Clin Endocrinol Metab. 2015 May;100(5):E821-5.

Mancina RM, Sentinelli F, Incani M, Bertoccini L, Russo C, Romeo S, Baroni MG. Transmembrane-6 superfamily member 2 (TM6SF2) E167K variant increases susceptibility to hepatic steatosis in obese children. Dig Liver Dis. 2016 Jan;48(1):100-1. b

Marchesini G, Brizi M, Bianchi G, Tomassetti S, Bugianesi E, Lenzi M, McCullough AJ, Natale S, Forlani G, Melchionda N. Nonalcoholic fatty liver disease: a feature of the metabolic syndrome. Diabetes. 2001 Aug;50(8):1844-50.

Matthews DR, Hosker JP, Rudenski AS, Naylor BA, Treacher DF, Turner RC. Homeostasis model assessment: insulin resistance and beta-cell function from fasting plasma glucose and insulin concentrations in man. Diabetologia 1985;28:412–9.

McPherson S, Hardy T, Henderson E, Burt AD, Day CP, Anstee QM. Evidence of NAFLD progression from steatosis to fibrosing-steatohepatitis using paired biopsies: implications for prognosis and clinical management. J Hepatol. 2015 May;62(5):1148-55.

Mederacke I, Hsu CC, Troeger JS, Huebener P, Mu X, Dapito DH, Pradere JP, Schwabe RF. Fate tracing reveals hepatic stellate cells as dominant contributors to liver fibrosis independent of its aetiology. Nat Commun. 2013;4:2823.

Mehta NN, McGillicuddy FC, Anderson PD, Hinkle CC, Shah R, Pruscino L, Tabita-Martinez J, Sellers KF, Rickels MR, Reilly MP. Experimental endotoxemia induces adipose inflammation and insulin resistance in humans. Diabetes. 2010 Jan;59(1):172-81.

Milacic M, Haw R, Rothfels K, Wu G, Croft D, Hermjakob H, *et al.* Annotating cancer variants and anti-cancer therapeutics in reactome. Cancers (Basel). 2012 Nov 8;4(4):1180-211.

Mouzaki M, Comelli EM, Arendt BM, Bonengel J, Fung SK, Fischer SE, McGilvray ID, Allard JP. Intestinal microbiota in patients with nonalcoholic

fatty liver disease. Hepatology. 2013 Jul;58(1):120-7.

Mozaffarian D, Hao T, Rimm EB, Willett WC, Hu FB. Changes in diet and lifestyle and long-term weight gain in women and men. N Engl J Med. 2011 Jun 23;364(25):2392-404.

Munukka E, Pekkala S, Wiklund P, Rasool O, Borra R, Kong L, Ojanen X, Cheng SM, Roos C, Tuomela S, Alen M, Lahesmaa R, Cheng S. Gut-adipose tissue axis in hepatic fat accumulation in humans. J Hepatol. 2014 Jul;61(1):132-8.

Musso G, Cassader M, Paschetta E, Gambino R. TM6SF2 may drive postprandial lipoprotein cholesterol toxicity away from the vessel walls to the liver in NAFLD. J Hepatol. 2016 Apr;64(4):979-81.

Musso G, Gambino R, De Michieli F, Cassader M, Rizzetto M, Durazzo M, Fagà E, Silli B, Pagano G. Dietary habits and their relations to insulin resistance and postprandial lipemia in nonalcoholic steatohepatitis. Hepatology. 2003 Apr;37(4):909-16.

Männistö VT, Simonen M, Hyysalo J, Soininen P, Kangas AJ, Kaminska D, Matte AK, Venesmaa S, Käkelä P, Kärjä V, Arola J, Gylling H, Cederberg H, Kuusisto J, Laakso M, Yki-Järvinen H, Ala-Korpela M, Pihlajamäki J. Ketone body production is differentially altered in steatosis and non-alcoholic steatohepatitis in obese humans. Liver Int. 2015 Jul;35(7):1853-61.

Nasr P, Ignatova S, Kechagias S, Ekstedt M. Natural history of nonalcoholic fatty liver disease: A prospective follow-up study with serial biopsies. Hepatol Commun. 2017 Dec 27;2(2):199-210

Neuschwander-Tetri BA. Hepatic lipotoxicity and the pathogenesis of nonalcoholic steatohepatitis: the central role of nontriglyceride fatty acid metabolites. Hepatology. 2010 Aug;52(2):774-88.

Nielsen TS, Jessen N, Jørgensen JO, Møller N, Lund S.Dissecting adipose tissue lipolysis: molecular regulation and implications for metabolic disease. J Mol Endocrinol. 2014 Jun;52(3):R199-222

Nieto N, Greenwel P, Friedman SL, Zhang F, Dannenberg AJ, Cederbaum AI. Ethanol and arachidonic acid increase alpha 2(I) collagen expression in rat hepatic stellate cells overexpressing cytochrome P450 2E1. Role of H2O2 and cyclooxygenase-2. J Biol Chem. 2000 Jun 30;275(26):20136-45.

Noga AA, Zhao Y, Vance DE. An unexpected requirement for phosphatidylethanolamine N-methyltransferase in the secretion of very low density lipoproteins. J Biol Chem. 2002 Nov 1;277(44):42358-65.

Nurjhan N, Campbell PJ, Kennedy FP, Miles JM, Gerich JE. Insulin dose-response characteristics for suppression of glycerol release and conversion to glucose in humans. Diabetes. 1986 Dec;35(12):1326-31.

O'Hare EA, Yang R, Yerges-Armstrong LM, Sreenivasan U, McFarland R, Leitch CC, Wilson MH, Narina S, Gorden A, Ryan KA, Shuldiner AR, Farber SA, Wood GC, Still CD, Gerhard GS, Robishaw JD, Sztalryd C, Zaghloul NA. TM6SF2 rs58542926 impacts lipid processing in liver and small intestine. Hepatology. 2017 May;65(5):1526-1542.

Oh DY, Talukdar S, Bae EJ, Imamura T, Morinaga H, Fan W, Li P, Lu WJ, Watkins SM, Olefsky JM. GPR120 is an omega-3 fatty acid receptor mediating potent anti-inflammatory and insulin-sensitizing effects. Cell. 2010 Sep 3;142(5):687-98.

Oksanen JFGB, R. Kindt, P. Legendre, P.R. Minchin, R.B. O'Hara, G.L. Simpson, P. Solymos, M.H.H. Stevens, H.Wagner. Package 'vegan' version 2.0-2. 2011

Olofsson SO, Borén J. Apolipoprotein B secretory regulation by degradation. Arterioscler Thromb Vasc Biol. 2012 Jun;32(6):1334-8.

Pais R, Charlotte F, Fedchuk L, Bedossa P, Lebray P, Poynard T, Ratziu V; LIDO Study Group. A systematic review of follow-up biopsies reveals disease progression in patients with non-alcoholic fatty liver. J Hepatol. 2013 Sep;59(3):550-6.

Pan M, Cederbaum AI, Zhang YL, Ginsberg HN, Williams KJ, Fisher EA. Lipid peroxidation and oxidant stress regulate hepatic apolipoprotein B degradation and VLDL production. J Clin Invest. 2004 May;113(9):1277-87.

Pan M, Maitin V, Parathath S, Andreo U, Lin SX, St Germain C, Yao Z, Maxfield FR, Williams KJ, Fisher EA. Presecretory oxidation, aggregation, and autophagic destruction of apoprotein-B: a pathway for late-stage quality control. Proc Natl Acad Sci U S A. 2008 Apr 15;105(15):5862-7.

Pang J, Xu W, Zhang X, Wong GL, Chan AW, Chan HY, Tse CH, Shu SS, Choi PC, Chan HL, Yu J, Wong VW. Significant positive association of endotoxemia with histological severity in 237 patients with non-alcoholic fatty liver disease. Aliment Pharmacol Ther. 2017 Jul;46(2):175-182.

Pendyala S, Walker JM, Holt PR. A high-fat diet is associated with endotoxemia that originates from the gut. Gastroenterology. 2012 May;142(5):1100-1101.e2.

Perry RJ, Camporez JP, Kursawe R, Titchenell PM, Zhang D, Perry CJ, Jurczak MJ, Abudukadier A, Han MS, Zhang XM, Ruan HB, Yang X, Caprio S, Kaech SM, Sul HS, Birnbaum MJ, Davis RJ, Cline GW, Petersen KF, Shulman GI. Hepatic acetyl CoA links adipose tissue inflammation to hepatic insulin resistance and type 2 diabetes. Cell. 2015 Feb 12;160(4):745-58.

Peter A, Kovarova M, Nadalin S, Cermak T, Königsrainer A, Machicao F, Stefan N, Häring HU, Schleicher E. PNPLA3 variant I148M is associated with altered hepatic lipid composition in humans. Diabetologia. 2014 Oct;57(10):2103-7.

Petersen KF, Befroy DE, Dufour S, Rothman DL, Shulman GI. Assessment of Hepatic Mitochondrial Oxidation and Pyruvate Cycling in NAFLD by (13)C Magnetic Resonance Spectroscopy. Cell Metab. 2016 Jul 12;24(1):167-71.

Petersen KF, Dufour S, Befroy D, Lehrke M, Hendler RE, Shulman GI. Reversal of nonalcoholic hepatic steatosis, hepatic insulin resistance, and hyperglycemia by moderate weight reduction in patients with type 2 diabetes. Diabetes. 2005 Mar;54(3):603-8.

Petersen MC, Madiraju AK, Gassaway BM, Marcel M, Nasiri AR, Butrico G, Marcucci MJ, Zhang D, Abulizi A, Zhang XM, Philbrick W, Hubbard SR, Jurczak MJ, Samuel VT, Rinehart J, Shulman GI. Insulin receptor Thr1160 phosphorylation mediates lipid-induced hepatic insulin resistance. J Clin Invest. 2016 Nov 1;126(11):4361-4371.

Petersen MC, Shulman GI. Roles of Diacylglycerols and Ceramides in Hepatic Insulin Resistance. Trends Pharmacol Sci. 2017;38(7):649-665.

Petäjä EM, Yki-Järvinen H. Definitions of Normal Liver Fat and the Association of Insulin Sensitivity with Acquired and Genetic NAFLD-A Systematic Review. Int J Mol Sci. 2016 Apr 27;17(5).

Pirazzi C, Adiels M, Burza MA, Mancina RM, Levin M, Ståhlman M, Taskinen MR, Orho-Melander M, Perman J, Pujia A, Andersson L, Maglio C, Montalcini T, Wiklund O, Borén J, Romeo S. Patatin-like phospholipase domain-containing 3 (PNPLA3) I148M (rs738409) affects hepatic VLDL secretion in humans and in vitro. J Hepatol. 2012 Dec;57(6):1276-82.

Pirazzi C, Valenti L, Motta BM, Pingitore P, Hedfalk K, Mancina RM, Burza MA, Indiveri C, Ferro Y, Montalcini T, Maglio C, Dongiovanni P, Fargion S, Rametta R, Pujia A, Andersson L, Ghosal S, Levin M, Wiklund O, Iacovino M, Borén J, Romeo S. PNPLA3 has retinyl-palmitate lipase activity in human hepatic stellate cells. Hum Mol Genet. 2014 Aug 1;23(15):4077-85.

Polyzos SA, Mantzoros CS. Adiponectin as a target for the treatment of nonalcoholic steatohepatitis with thiazolidinediones: A systematic review. Metabolism. 2016 Sep;65(9):1297-306.

Postic C, Girard J. Contribution of de novo fatty acid synthesis to hepatic steatosis and insulin resistance: lessons from genetically engineered mice. J Clin Invest. 2008 Mar;118(3):829-38.

Puri P, Baillie RA, Wiest MM, Mirshahi F, Choudhury J, Cheung O, Sargeant C, Contos MJ, Sanyal AJ. A lipidomic analysis of nonalcoholic fatty liver disease. Hepatology. 2007 Oct;46(4):1081-90.

Puri P, Wiest MM, Cheung O, Mirshahi F, Sargeant C, Min HK, Contos MJ, Sterling RK, Fuchs M, Zhou H, Watkins SM, Sanyal AJ. The plasma lipidomic signature of nonalcoholic steatohepatitis. Hepatology. 2009 Dec;50(6):1827-38.

Pussinen PJ, Havulinna AS, Lehto M, Sundvall J, Salomaa V. Endotoxemia is associated with an increased risk of incident diabetes. Diabetes Care. 2011 Feb;34(2):392-7.

Quast C, Pruesse E, Yilmaz P, Gerken J, Schweer T, Yarza P, *et al.* The SILVA ribosomal RNA gene database project: improved data processing and web-based tools. Nucleic Acids Res. 2012;gks1219.

Rabøl R, Petersen KF, Dufour S, Flannery C, Shulman GI. Reversal of muscle insulin resistance with exercise reduces postprandial hepatic de novo lipogenesis in insulin resistant individuals. Proc Natl Acad Sci U S A. 2011 Aug 16;108(33):13705-9.

Raddatz K, Turner N, Frangioudakis G, Liao BM, Pedersen DJ, Cantley J, Wilks D, Preston E, Hegarty BD, Leitges M, Raftery MJ, Biden TJ, Schmitz-Peiffer C. Time-dependent effects of Prkce deletion on glucose homeostasis and hepatic lipid metabolism on dietary lipid oversupply in mice. Diabetologia. 2011 Jun;54(6):1447-56.

Raichur S, Wang ST, Chan PW, Li Y, Ching J, Chaurasia B, Dogra S, Öhman MK, Takeda K, Sugii S, Pewzner-Jung Y, Futerman AH, Summers SA. CerS2 haploinsufficiency inhibits β-oxidation and confers susceptibility to diet-induced steatohepatitis and insulin resistance. Cell Metab. 2014;20:687–695.

Rinella ME, Green RM. The methionine-choline deficient dietary model of steatohepatitis does not exhibit insulin resistance. J Hepatol. 2004 Jan;40(1):47-51.

Robichaud PP, Surette ME. Polyunsaturated fatty acid-phospholipid remodeling and inflammation. Curr Opin Endocrinol Diabetes Obes. 2015 Apr;22(2):112-8.

Romeo S, Kozlitina J, Xing C, Pertsemlidis A, Cox D, Pennacchio LA, *et al.* Genetic variation in PNPLA3 confers

susceptibility to nonalcoholic fatty liver disease. Nat Genet 2008;40:1461–5.

Rong X, Wang B, Dunham MM, Hedde PN, Wong JS, Gratton E, Young SG, Ford DA, Tontonoz P. Lpcat3-dependent production of arachidonoyl phospholipids is a key determinant of triglyceride secretion. Elife. 2015;25:4.

Rosqvist F, Iggman D, Kullberg J, Cedernaes J, Johansson HE, Larsson A, Johansson L, Ahlström H, Arner P, Dahlman I, Risérus U. Overfeeding polyunsaturated and saturated fat causes distinct effects on liver and visceral fat accumulation in humans. Diabetes. 2014 Jul;63(7):2356-68.

Ryysy L, Häkkinen AM, Goto T, Vehkavaara S, Westerbacka J, Halavaara J, Yki-Järvinen H. Hepatic fat content and insulin action on free fatty acids and glucose metabolism rather than insulin absorption are associated with insulin requirements during insulin therapy in type 2 diabetic patients. Diabetes. 2000 May;49(5):749-58.

Rönn T, Volkov P, Tornberg A, Elgzyri T, Hansson O, Eriksson KF, Groop L, Ling C. Extensive changes in the transcriptional profile of human adipose tissue including genes involved in oxidative phosphorylation after a 6-month exercise intervention. Acta Physiol (Oxf). 2014 May;211(1):188-200.

Sacks FM, Lichtenstein AH, Wu JHY, Appel LJ, Creager MA, Kris-Etherton PM, Miller M, Rimm EB, Rudel LL, Robinson JG, Stone NJ, Van Horn LV; American Heart Association. Dietary Fats and Cardiovascular Disease: A Presidential Advisory From the American Heart Association. Circulation. 2017 Jul 18;136(3):e1-e23.

Sampath H, Ntambi JM. Polyunsaturated fatty acid regulation of genes of lipid metabolism. Annu Rev Nutr. 2005;25:317-40.

Santoro N, Caprio S, Pierpont B, Van Name M, Savoye M, Parks EJ. Hepatic De Novo Lipogenesis in Obese Youth Is Modulated by a Common Variant in the GCKR Gene. J Clin Endocrinol Metab. 2015 Aug;100(8):E1125-32.

Sanyal AJ, Campbell-Sargent C, Mirshahi F, Rizzo WB, Contos MJ, Sterling RK, Luketic VA, Shiffman ML, Clore JN. Nonalcoholic steatohepatitis: association of insulin resistance and mitochondrial abnormalities. Gastroenterology. 2001 Apr;120(5):1183-92.

Sanyal A, Poklepovic A, Moyneur E, Barghout V. Population-based risk factors and resource utilization for HCC: US perspective. Curr Med Res Opin. 2010 Sep;26(9):2183-91.

Samuel VT, Liu ZX, Qu X, Elder BD, Bilz S, Befroy D, Romanelli AJ, Shulman GI. Mechanism of hepatic insulin resistance in non-alcoholic fatty liver disease. J Biol Chem. 2004 Jul 30;279(31):32345-53.

Samuel VT, Liu ZX, Wang A, Beddow SA, Geisler JG, Kahn M, Zhang XM, Monia BP, Bhanot S, Shulman GI. Inhibition of protein kinase Cepsilon prevents hepatic insulin resistance in nonalcoholic fatty liver disease. J Clin Invest. 2007 Mar;117(3):739-45.

Samuel VT, Shulman GI. Nonalcoholic Fatty Liver Disease as a Nexus of Metabolic and Hepatic Diseases. Cell Metab. 2018 Jan 9;27(1):22-41.

Samuel VT, Shulman GI. The pathogenesis of insulin resistance: integrating signaling pathways and substrate flux. J Clin Invest. 2016 Jan;126(1):12-22.

Satapati S, Qian Y, Wu MS, Petrov A, Dai G, Wang SP, Zhu Y, Shen X, Muise ES,

Chen Y, Zycband E, Weinglass A, Di Salvo J, Debenham JS, Cox JM, Lan P, Shah V, Previs SF, Erion M, Kelley DE, Wang L, Howard AD, Shang J. GPR120 suppresses adipose tissue lipolysis and synergizes with GPR40 in antidiabetic efficacy. J Lipid Res. 2017 Aug;58(8):1561-1578.

Scherer PE, Williams S, Fogliano M, Baldini G, Lodish HF. A novel serum protein similar to C1q, produced exclusively in adipocytes. J Biol Chem. 1995 Nov 10;270(45):26746-9.

Schwarz JM, Neese RA, Turner S, Dare D, Hellerstein MK. Short-term alterations in carbohydrate energy intake in humans. Striking effects on hepatic glucose production, de novo lipogenesis, lipolysis, and whole-body fuel selection. J Clin Invest. 1995;96(6):2735-43.

Semple RK, Sleigh A, Murgatroyd PR, Adams CA, Bluck L, Jackson S, Vottero A, Kanabar D, Charlton-Menys V, Durrington P, Soos MA, Carpenter TA, Lomas DJ, Cochran EK, Gorden P, O'Rahilly S, Savage DB. Postreceptor insulin resistance contributes to human dyslipidemia and hepatic steatosis. J Clin Invest. 2009 Feb;119(2):315-22.

Seppälä-Lindroos A, Vehkavaara S, Häkkinen AM, Goto T, Westerbacka J, Sovijärvi A, Halavaara J, Yki-Järvinen H. Fat accumulation in the liver is associated with defects in insulin suppression of glucose production and serum free fatty acids independent of obesity in normal men. J Clin Endocrinol Metab. 2002 Jul;87(7):3023-8.

Sevastianova K, Kotronen A, Gastaldelli A, Perttilä J, Hakkarainen A, Lundbom J, Suojanen L, Orho-Melander M, Lundbom N, Ferrannini E, Rissanen A, Olkkonen VM, Yki-Järvinen H. Genetic variation in PNPLA3 (adiponutrin) confers sensitivity to weight loss-induced decrease in liver fat in humans. Am J Clin Nutr. 2011 Jul;94(1):104-11.

Sevastianova K, Santos A, Kotronen A, Hakkarainen A, Makkonen J, Silander K, Peltonen M, Romeo S, Lundbom J, Lundbom N, Olkkonen VM, Gylling H, Fielding BA, Rissanen A, Yki-Järvinen H. Effect of short-term carbohydrate overfeeding and long-term weight loss on liver fat in overweight humans. Am J Clin Nutr. 2012 Oct;96(4):727-34.

Shah K, Stufflebam A, Hilton TN, Sinacore DR, Klein S, Villareal DT. Diet and exercise interventions reduce intrahepatic fat content and improve insulin sensitivity in obese older adults. Obesity (Silver Spring). 2009 Dec;17(12):2162-8.

Shen JH, Li YL, Li D, Wang NN, Jing L, Huang YH. The rs738409 (I148M) variant of the PNPLA3 gene and cirrhosis: a meta-analysis. J Lipid Res. 2015 Jan;56(1):167-75.

Sharifnia T, Antoun J, Verriere TG, Suarez G, Wattacheril J, Wilson KT, Peek RM Jr, Abumrad NN, Flynn CR. Hepatic TLR4 signaling in obese NAFLD. Am J Physiol Gastrointest Liver Physiol. 2015 Aug 15;309(4):G270-8.

Shoelson SE, Lee J, Goldfine AB. Inflammation and insulin resistance. J Clin Invest. 2006 Jul;116(7):1793-801.

Shindou H, Shimizu T. Acyl-CoA:lysophospholipid acyltransferases. J Biol Chem. 2009 Jan 2;284(1):1-5.

Simons N, Isaacs A, Koek GH, Kuč S, Schaper NC, Brouwers MCGJ. PNPLA3, TM6SF2, and MBOAT7 Genotypes and Coronary Artery Disease. Gastroenterology. 2017 Mar;152(4):912-913.

Singal AG, Manjunath H, Yopp AC, Beg MS, Marrero JA, Gopal P, Waljee AK. The effect of PNPLA3 on fibrosis progression and development of hepatocellular

carcinoma: a meta-analysis. Am J Gastroenterol. 2014 Mar;109(3):325-34.

Singh S, Allen AM, Wang Z, Prokop LJ, Murad MH, Loomba R. Fibrosis progression in nonalcoholic fatty liver vs nonalcoholic steatohepatitis: a systematic review and meta-analysis of paired-biopsy studies. Clin Gastroenterol Hepatol. 2015 Apr;13(4):643-54.e1-9

Smagris E, BasuRay S, Li J, Huang Y, Lai KM, Gromada J, Cohen JC, Hobbs HH. Pnpla3I148M knockin mice accumulate PNPLA3 on lipid droplets and develop hepatic steatosis. Hepatology. 2015 Jan;61(1):108-18.

Smagris E, Gilyard S, BasuRay S, Cohen JC, Hobbs HH. Inactivation of Tm6sf2, a Gene Defective in Fatty Liver Disease, Impairs Lipidation but Not Secretion of Very Low Density Lipoproteins. J Biol Chem. 2016 May 13;291(20):10659-76.

Sobrecases H, Lê KA, Bortolotti M, Schneiter P, Ith M, Kreis R, Boesch C, Tappy L. Effects of short-term overfeeding with fructose, fat and fructose plus fat on plasma and hepatic lipids in healthy men. Diabetes Metab. 2010 Jun;36(3):244-6.

Sookoian S, Castaño GO, Burgueño AL, Gianotti TF, Rosselli MS, Pirola CJ. A nonsynonymous gene variant in the adiponutrin gene is associated with nonalcoholic fatty liver disease severity. J Lipid Res. 2009 Oct;50(10):2111-6.

Sookoian S, Castaño GO, Scian R, Mallardi P, Fernández Gianotti T, Burgueño AL, San Martino J, Pirola CJ. Genetic variation in transmembrane 6 superfamily member 2 and the risk of nonalcoholic fatty liver disease and histological disease severity. Hepatology. 2015 Feb;61(2):515-25.

Sookoian S, Pirola CJ. Genetic predisposition in nonalcoholic fatty liver disease. Clin Mol Hepatol. 2017 Mar;23(1):1-12.

Sookoian S, Pirola CJ. Meta-analysis of the influence of I148M variant of patatin-like phospholipase domain containing 3 gene (PNPLA3) on the susceptibility and histological severity of nonalcoholic fatty liver disease. Hepatology. 2011 Jun;53(6):1883-94.

Soronen J, Laurila PP, Naukkarinen J, Surakka I, Ripatti S, Jauhiainen M, Olkkonen VM, Yki-Järvinen H. Adipose tissue gene expression analysis reveals changes in inflammatory, mitochondrial respiratory and lipid metabolic pathways in obese insulin-resistant subjects. BMC Med Genomics. 2012;5:9.

Stefan D, Di Cesare F, Andrasescu A, *et al.* Quantitation of magnetic resonance spectroscopy signals: the jMRUI software package. Measurement Science and Technology 2009;20(10):104035.

Stender S, Kozlitina J, Nordestgaard BG, Tybjærg-Hansen A, Hobbs HH, Cohen JC. Adiposity amplifies the genetic risk of fatty liver disease conferred by multiple loci. Nat Genet. 2017 Jun;49(6):842-847.

Stienstra R, van Diepen JA, Tack CJ, Zaki MH, van de Veerdonk FL, Perera D, Neale GA, Hooiveld GJ, Hijmans A, Vroegrijk I, van den Berg S, Romijn J, Rensen PC, Joosten LA, Netea MG, Kanneganti TD. Inflammasome is a central player in the induction of obesity and insulin resistance. Proc Natl Acad Sci U S A. 2011 Sep 13;108(37):15324-9.

Stratford S, Hoehn KL, Liu F, Summers SA. Regulation of insulin action by ceramide: dual mechanisms linking ceramide accumulation to the inhibition of Akt/protein kinase B. J Biol Chem. 2004 Aug 27;279(35):36608-15.

Summers SA. Could Ceramides Become the New Cholesterol? Cell Metab. 2018 Feb 6;27(2):276-280.

Sun Z, Lazar MA. Dissociating fatty liver and diabetes. Trends Endocrinol Metab. 2013 Jan;24(1):4-12.

Sunny NE, Bril F, Cusi K. Mitochondrial Adaptation in Nonalcoholic Fatty Liver Disease: Novel Mechanisms and Treatment Strategies. Trends Endocrinol Metab. 2017 Apr;28(4):250-260.

Suomela E, Oikonen M, Pitkänen N, Ahola-Olli A, Virtanen J, Parkkola R, Jokinen E, Laitinen T, Hutri-Kähönen N, Kähönen M, Lehtimäki T, Taittonen L, Tossavainen P, Jula A, Loo BM, Mikkilä V, Telama R, Viikari JSA, Juonala M, Raitakari OT. Childhood predictors of adult fatty liver. The Cardiovascular Risk in Young Finns Study. J Hepatol. 2016 Oct;65(4):784-790.

Szczepaniak LS, Babcock EE, Schick F, *et al.* Measurement of intracellular triglyceride stores by H spectroscopy: validation in vivo. Am J Physiol 1999;276:E977–E989

Szczepaniak LS, Nurenberg P, Leonard D, Browning JD, Reingold JS, Grundy S, Hobbs HH, Dobbins RL. Magnetic resonance spectroscopy to measure hepatic triglyceride content: prevalence of hepatic steatosis in the general population. Am J Physiol Endocrinol Metab. 2005 Feb;288(2):E462-8.

Tamura Y, Tanaka Y, Sato F, Choi JB, Watada H, Niwa M, Kinoshita J, Ooka A, Kumashiro N, Igarashi Y, Kyogoku S, Maehara T, Kawasumi M, Hirose T, Kawamori R. Effects of diet and exercise on muscle and liver intracellular lipid contents and insulin sensitivity in type 2 diabetic patients. J Clin Endocrinol Metab. 2005 Jun;90(6):3191-6.

Tarasov K, Ekroos K, Suoniemi M, Kauhanen D, Sylvänne T, Hurme R, Gouni-Berthold I, Berthold HK, Kleber ME, Laaksonen R, März W. Molecular lipids identify cardiovascular risk and are efficiently lowered by simvastatin and PCSK9 deficiency. J Clin Endocrinol Metab. 2014 Jan;99(1):E45-52.

Ter Horst KW, Gilijamse PW, Versteeg RI, Ackermans MT, Nederveen AJ, la Fleur SE, Romijn JA, Nieuwdorp M, Zhang D, Samuel VT, Vatner DF, Petersen KF, Shulman GI, Serlie MJ. Hepatic Diacylglycerol-Associated Protein Kinase Cε Translocation Links Hepatic Steatosis to Hepatic Insulin Resistance in Humans. Cell Rep. 2017 Jun 6;19(10):1997-2004.

Thabet K, Asimakopoulos A, Shojaei M, Romero-Gomez M, Mangia A, Irving WL, Berg T, Dore GJ, Grønbæk H, Sheridan D, Abate ML, Bugianesi E, Weltman M, Mollison L, Cheng W, Riordan S, Fischer J, Spengler U, Nattermann J, Wahid A, Rojas A, White R, Douglas MW, McLeod D, Powell E, Liddle C, van der Poorten D, George J, Eslam M; International Liver Disease Genetics Consortium. MBOAT7 rs641738 increases risk of liver inflammation and transition to fibrosis in chronic hepatitis C. Nat Commun. 2016 Sep 15;7:12757.

Thabet K, Chan HLY, Petta S, Mangia A, Berg T, Boonstra A, Brouwer WP, Abate ML, Wong VW, Nazmy M, Fischer J, Liddle C, George J, Eslam M. The membrane-bound O-acyltransferase domain-containing 7 variant rs641738 increases inflammation and fibrosis in chronic hepatitis B. Hepatology. 2017 Jun;65(6):1840-1850.

Thoma C, Day CP, Trenell MI. Lifestyle interventions for the treatment of non-alcoholic fatty liver disease in adults: a systematic review. J Hepatol. 2012 Jan;56(1):255-66.

Tian C, Stokowski RP, Kershenobich D, Ballinger DG, Hinds DA. Variant in PNPLA3 is associated with alcoholic liver disease. Nat Genet. 2010 Jan;42(1):21-3.

Tiikkainen M, Bergholm R, Vehkavaara S, Rissanen A, Häkkinen AM, Tamminen M, Teramo K, Yki-Järvinen H. Effects of identical weight loss on body composition and features of insulin resistance in obese women with high and low liver fat content. Diabetes. 2003 Mar;52(3):701-7.

Topping DL, Mayes PA. Insulin and non-esterified fatty acids. Acute regulators of lipogenesis in perfused rat liver. Biochem J. 1982 May 15;204(2):433-9

Trépo E, Gustot T, Degré D, Lemmers A, Verset L, Demetter P, Ouziel R, Quertinmont E, Vercruysse V, Amininejad L, Deltenre P, Le Moine O, Devière J, Franchimont D, Moreno C. Common polymorphism in the PNPLA3/adiponutrin gene confers higher risk of cirrhosis and liver damage in alcoholic liver disease. J Hepatol. 2011 Oct;55(4):906-12.

Trépo E, Nahon P, Bontempi G, Valenti L, Falleti E, Nischalke HD, Hamza S, Corradini SG, Burza MA, Guyot E, Donati B, Spengler U, Hillon P, Toniutto P, Henrion J, Franchimont D, Devière J, Mathurin P, Moreno C, Romeo S, Deltenre P. Association between the PNPLA3 (rs738409 C>G) variant and hepatocellular carcinoma: Evidence from a meta-analysis of individual participant data. Hepatology. 2014 Jun;59(6):2170-7.

Tripodi A, Mannucci PM. The coagulopathy of chronic liver disease. N Engl J Med. 2011 Jul 14;365(2):147-56.

Tsuchida T, Friedman SL. Mechanisms of hepatic stellate cell activation. Nat Rev Gastroenterol Hepatol. 2017 Jul;14(7):397-411.

Turer AT, Browning JD, Ayers CR, Das SR, Khera A, Vega GL, Grundy SM, Scherer PE. Adiponectin as an independent predictor of the presence and degree of hepatic steatosis in the Dallas Heart Study. J Clin Endocrinol Metab. 2012 Jun;97(6):E982-6.

Turpin SM, Nicholls HT, Willmes DM, Mourier A, Brodesser S, Wunderlich CM, Mauer J, Xu E, Hammerschmidt P, Brönneke HS, Trifunovic A, LoSasso G, Wunderlich FT, Kornfeld JW, Blüher M, Krönke M, Brüning JC. Obesity-induced CerS6-dependent C16:0 ceramide production promotes weight gain and glucose intolerance. Cell Metab. 2014;20:678–686.

US Department of Health and Human Services; US Department of Agriculture. *2015-2020 Dietary Guidelines for Americans*. 8th ed. Washington, DC: US Dept of Health and Human Services; December 2015. http://www.health.gov/DietaryGuidelines. Accessed March 16, 2018

Utzschneider KM, Bayer-Carter JL, Arbuckle MD, Tidwell JM, Richards TL, Craft S. Beneficial effect of a weight-stable, low-fat/low-saturated fat/low-glycaemic index diet to reduce liver fat in older subjects. Br J Nutr. 2013 Mar 28;109(6):1096-104.

Valenti L, Al-Serri A, Daly AK, Galmozzi E, Rametta R, Dongiovanni P, Nobili V, Mozzi E, Roviaro G, Vanni E, Bugianesi E, Maggioni M, Fracanzani AL, Fargion S, Day CP. Homozygosity for the patatin-like phospholipase-3/adiponutrin I148M polymorphism influences liver fibrosis in patients with nonalcoholic fatty liver disease. Hepatology. 2010 Apr;51(4):1209-17.

Vandanmagsar B, Youm YH, Ravussin A, Galgani JE, Stadler K, Mynatt RL, Ravussin E, Stephens JM, Dixit VD. The NLRP3 inflammasome instigates obesity-

induced inflammation and insulin resistance. Nat Med. 2011 Feb;17(2):179-88.

van der Meer RW, Hammer S, Lamb HJ, Frölich M, Diamant M, Rijzewijk LJ, de Roos A, Romijn JA, Smit JW. Effects of short-term high-fat, high-energy diet on hepatic and myocardial triglyceride content in healthy men. J Clin Endocrinol Metab. 2008 Jul;93(7):2702-8.

van Dijk SJ, Feskens EJ, Bos MB, Hoelen DW, Heijligenberg R, Bromhaar MG, de Groot LC, de Vries JH, Müller M, Afman LA. A saturated fatty acid-rich diet induces an obesity-linked proinflammatory gene expression profile in adipose tissue of subjects at risk of metabolic syndrome. Am J Clin Nutr. 2009 Dec;90(6):1656-64.

Vanhamme L, van den Boogaart A, Van Huffel S. Improved method for accurate and efficient quantification of MRS data with use of prior knowledge. J Magn Reson 1997;129:35– 43.

van Herpen NA, Schrauwen-Hinderling VB, Schaart G, Mensink RP, Schrauwen P. Three weeks on a high-fat diet increases intrahepatic lipid accumulation and decreases metabolic flexibility in healthy overweight men. J Clin Endocrinol Metab. 2011 Apr;96(4):E691-5.

van Meer G, Voelker DR, Feigenson GW. Membrane lipids: where they are and how they behave. Nat Rev Mol Cell Biol. 2008 Feb;9(2):112-24.

Verrijken A, Francque S, Mertens I, Prawitt J, Caron S, Hubens G, Van Marck E, Staels B, Michielsen P, Van Gaal L. Prothrombotic factors in histologically proven nonalcoholic fatty liver disease and nonalcoholic steatohepatitis. Hepatology. 2014 Jan;59(1):121-9.

Vilar-Gomez E, Martinez-Perez Y, Calzadilla-Bertot L, Torres-Gonzalez A, Gra-Oramas B, Gonzalez-Fabian L, Friedman SL, Diago M, Romero-Gomez M. Weight Loss Through Lifestyle Modification Significantly Reduces Features of Nonalcoholic Steatohepatitis. Gastroenterology. 2015 Aug;149(2):367-78.e5

Walewski JL, Ge F, Gagner M, Inabnet WB, Pomp A, Branch AD, Berk PD. Adipocyte accumulation of long-chain fatty acids in obesity is multifactorial, resulting from increased fatty acid uptake and decreased activity of genes involved in fat utilization. Obes Surg. 2010 Jan;20(1):93-107.

Wang DD, Toledo E, Hruby A, Rosner BA, Willett WC, Sun Q, Razquin C, Zheng Y, Ruiz-Canela M, Guasch-Ferré M, Corella D, Gómez-Gracia E, Fiol M, Estruch R, Ros E, Lapetra J, Fito M, Aros F, Serra-Majem L, Lee CH, Clish CB, Liang L, Salas-Salvadó J, Martínez-González MA, Hu FB. Plasma Ceramides, Mediterranean Diet, and Incident Cardiovascular Disease in the PREDIMED Trial (Prevención con Dieta Mediterránea). Circulation. 2017 May 23;135(21):2028-2040.

Wang M, Zhang X, Ma LJ, Feng RB, Yan C, Su H, He C, Kang JX, Liu B, Wan JB. Omega-3 polyunsaturated fatty acids ameliorate ethanol-induced adipose hyperlipolysis: A mechanism for hepatoprotective effect against alcoholic liver disease. Biochim Biophys Acta. 2017 Dec;1863(12):3190-3201.

Warshauer JT, Lopez X, Gordillo R, Hicks J, Holland WL, Anuwe E, Blankfard MB, Scherer PE, Lingvay I. Effect of pioglitazone on plasma ceramides in adults with metabolic syndrome. Diabetes Metab Res Rev. 2015 Oct;31(7):734-44.

Weisberg SP, McCann D, Desai M, Rosenbaum M, Leibel RL, Ferrante AW Jr. Obesity is associated with macrophage

accumulation in adipose tissue. J Clin Invest. 2003 Dec;112(12):1796-808.

Westerbacka J, Kotronen A, Fielding BA, Wahren J, Hodson L, Perttilä J, Seppänen-Laakso T, Suortti T, Arola J, Hultcrantz R, Castillo S, Olkkonen VM, Frayn KN, Orešič M, Yki-Järvinen H. Splanchnic balance of free fatty acids, endocannabinoids, and lipids in subjects with nonalcoholic fatty liver disease. Gastroenterology. 2010 Dec;139(6):1961-1971.e1.

Westerbacka J, Lammi K, Häkkinen AM, Rissanen A, Salminen I, Aro A, Yki-Järvinen H. Dietary fat content modifies liver fat in overweight nondiabetic subjects. J Clin Endocrinol Metab. 2005 May;90(5):2804-9.

Wong RJ, Aguilar M, Cheung R, Perumpail RB, Harrison SA, Younossi ZM, Ahmed A. Nonalcoholic steatohepatitis is the second leading etiology of liver disease among adults awaiting liver transplantation in the United States. Gastroenterology. 2015 Mar;148(3):547-55.

Wong VW, Tse CH, Lam TT, Wong GL, Chim AM, Chu WC, Yeung DK, Law PT, Kwan HS, Yu J, Sung JJ, Chan HL. Molecular characterization of the fecal microbiota in patients with nonalcoholic steatohepatitis--a longitudinal study. PLoS One. 2013 Apr 25;8(4):e62885.

Wong VW, Wong GL, Choi PC, Chan AW, Li MK, Chan HY, Chim AM, Yu J, Sung JJ, Chan HL. Disease progression of non-alcoholic fatty liver disease: a prospective study with paired liver biopsies at 3 years. Gut. 2010 Jul;59(7):969-74.

Xia JY, Holland WL, Kusminski CM, Sun K, Sharma AX, Pearson MJ, Sifuentes AJ, McDonald JG, Gordillo R, Scherer PE. Targeted Induction of Ceramide Degradation Leads to Improved Systemic Metabolism and Reduced Hepatic Steatosis. Cell Metab. 2015 Aug 4;22(2):266-278.

Xie C, Jiang C, Shi J, Gao X, Sun D, Sun L, Wang T, Takahashi S, Anitha M, Krausz KW, Patterson AD, Gonzalez FJ. An Intestinal Farnesoid X Receptor-Ceramide Signaling Axis Modulates Hepatic Gluconeogenesis in Mice. Diabetes. 2017 Mar;66(3):613-626.

Yilmaz M, Claiborn KC, Hotamisligil GS. De Novo Lipogenesis Products and Endogenous Lipokines. Diabetes. 2016 Jul;65(7):1800-7.

Yki-Järvinen H. Action of insulin on glucose metabolism in vivo. Baillieres Clin Endocrinol Metab. 1993 Oct;7(4):903-27.

Yki-Järvinen H. Non-alcoholic fatty liver disease as a cause and a consequence of metabolic syndrome. Lancet Diabetes Endocrinol. 2014;2(11):901-10.

Yki-Järvinen H. Nutritional Modulation of Non-Alcoholic Fatty Liver Disease and Insulin Resistance. Nutrients. 2015 Nov 5;7(11):9127-38.

Yki-Järvinen H, Puhakainen I, Saloranta C, Groop L, Taskinen MR. Demonstration of a novel feedback mechanism between FFA oxidation from intracellular and intravascular sources. Am J Physiol. 1991 May;260(5 Pt 1):E680-9.

Yki-Järvinen H, Young AA, Lamkin C, Foley JE. Kinetics of glucose disposal in whole body and across the forearm in man. J Clin Invest. 1987 Jun;79(6):1713-9.

Yao H, Ye J. Long chain acyl-CoA synthetase 3-mediated phosphatidylcholine synthesis is required for assembly of very low density lipoproteins in human hepatoma Huh7 cells. J Biol Chem. 2008 Jan 11;283(2):849-54.

Younossi Z, Anstee QM, Marietti M, Hardy T, Henry L, Eslam M, George J, Bugianesi E. Global burden of NAFLD and NASH: trends, predictions, risk factors and prevention. Nat Rev Gastroenterol Hepatol. 2018 Jan;15(1):11-20.

Younossi ZM, Koenig AB, Abdelatif D, Fazel Y, Henry L, Wymer M. Global epidemiology of nonalcoholic fatty liver disease-Meta-analytic assessment of prevalence, incidence, and outcomes. Hepatology. 2016;64(1):73-84.

Zelber-Sagi S, Nitzan-Kaluski D, Goldsmith R, Webb M, Blendis L, Halpern Z, Oren R. Long term nutritional intake and the risk for non-alcoholic fatty liver disease (NAFLD): a population based study. J Hepatol. 2007 Nov;47(5):711-7.

Zhou Y, Llauradó G, Orešič M, Hyötyläinen T, Orho-Melander M, Yki-Järvinen H. Circulating triacylglycerol signatures and insulin sensitivity in NAFLD associated with the E167K variant in TM6SF2. J Hepatol. 2015 Mar;62(3):657-63.

Zhu L, Baker SS, Gill C, Liu W, Alkhouri R, Baker RD, Gill SR. Characterization of gut microbiomes in nonalcoholic steatohepatitis (NASH) patients: a connection between endogenous alcohol and NASH. Hepatology. 2013 Feb;57(2):601-9.

Zu L, He J, Jiang H, Xu C, Pu S, Xu G. Bacterial endotoxin stimulates adipose lipolysis via toll-like receptor 4 and extracellular signal-regulated kinase pathway. J Biol Chem. 2009 Feb 27;284(9):5915-26.

Åberg F, Helenius-Hietala J, Puukka P, Färkkilä M, Jula A. Interaction between alcohol consumption and metabolic syndrome in predicting severe liver disease in the general population. Hepatology. 2017 Nov 22. doi: 10.1002/hep.29631.

Recent Publications in this Series

27/2018 Katariina Maaninka
Atheroinflammatory Properties of LDL and HDL Particles Modified by Human Mast Cell Neutral Proteases
28/2018 Sonja Paetau
Neuronal ICAM-5 Regulates Synaptic Maturation and Microglia Functions
29/2018 Niina Kaartinen
Carbohydrates in the Diet of Finnish Adults - Focus on Intake Assessment and Associations with Other Dietary Components and Obesity
30/2018 Tuija Jääskeläinen
Public Health Importance of Vitamin D: Results from the Population-based Health 2000/2011 Survey
31/2018 Tiina Lipiäinen
Stability and Analysis of Solid-State Forms in Pharmaceutical Powders
32/2018 Johanna Ruohoalho
Complications and Their Registration in Otorhinolaryngology – Head and Neck Surgery: Special Emphasis in Tonsil Surgery Quality Registration
33/2018 Alok Jaiswal
Integrative Bioinformatics of Functional and Genomic Profiles for Cancer Systems Medicine
34/2018 Riikka Uotila
Let's Get Cracking —Nut Allergy Diagnostics and Peanut Oral Immunotherapy
35/2018 Solomon Olusegun Nwhator
Association between a-MMP-8 Chairside Test for Chronic Periodontitis and Selected Reproductive Health Parameters
36/2018 Anna-Kaisa Rimpelä
Ocular Pharmacokinetic Effects of Drug Binding to Melanin Pigment and the Vitreous Humor
37/2018 Henna Vepsäläinen
Food Environment and Whole-Diet in Children – Studies on Parental Role Modelling and Food Availability
38/2018 Eeva-Liisa Tuovinen
Weight Concerns and Abdominal Obesity among Ever-Smokers: A Population-Based Study of Finnish Adults
39/2018 Maheswary Muniandy
Molecular Effects of Obesity and Related Metabolic Risk Factors – A Transcriptomics and Metabolomics Approach
40/2018 Cristian Capasso
Development of Novel Vaccine Platforms for the Treatment of Cancer
41/2018 Ainoleena Turku
Discovery of OX1 and OX2 Orexin Receptor Ligands
42/2018 Johanna Pekkala
Occupational Class Differences in Sickness Absence – Changes Over Time and Diagnostic Causes
43/2018 Heli Paukkonen
Nanofibrillar Cellulose for Encapsulation and Release of Pharmaceuticals
44/2018 Teppo Leino
Synthesis of Azulene-Based Compounds for Targeting Orexin Receptors
45/2018 Jonni Hirvonen
Systems-Level Neural Mechanisms of Conscious Perception in Health and Schizophrenia

Helsinki 2018 **ISSN 2342-3161** **ISBN 978-951-51-4372-3**